Digital Soil Mapping
Available Water Content
in the Lower Macquarie Valley, NSW

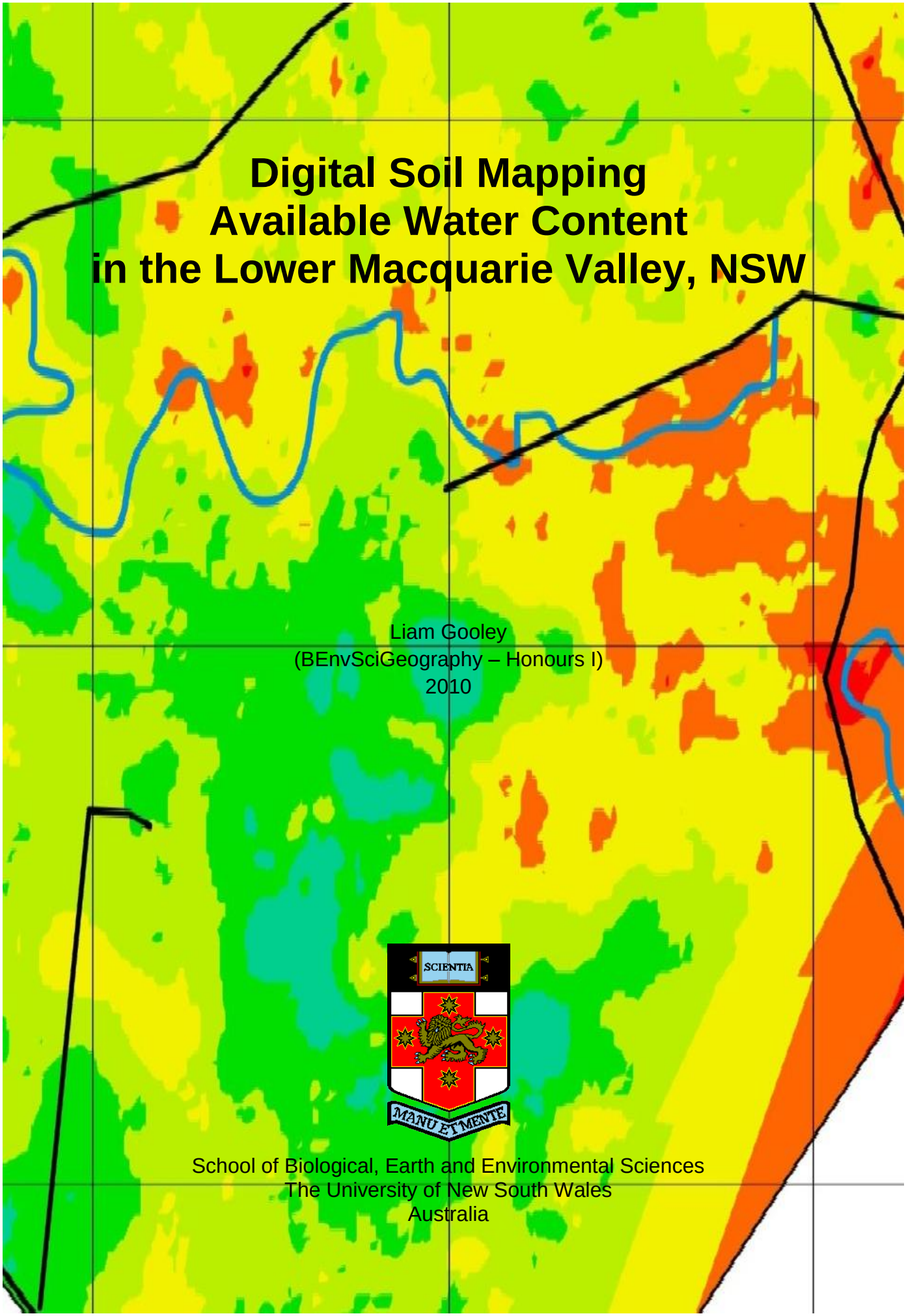

Liam Gooley
(BEnvSciGeography – Honours I)
2010

School of Biological, Earth and Environmental Sciences
The University of New South Wales
Australia

Acknowledgements

First and foremost, this thesis would not have been possible without my supervisor, Dr John Triantafilis. His support, guidance, encouragement, patience, and occasional motivational speech right from the beginning to the very end have been a vital component of this project. I appreciate the immense amount of time and effort he has invested in this research and cannot thank him enough.

I would also like to thank the Cotton, Catchment and Communities Cooperative Research Centre for funding my summer scholarship (CRC-5.10.03.25).

Special Thanks also goes to Jess Roe who showed me the ropes early on in the year and taught me how to survive honours. Thank you so much for the proof reading and thoughtful comments.

I also thank those who started my journey at UNSW with me, in particular Jess C, Alice and Simon. And to those who are finishing the journey with me, especially Jak, who has been a huge inspiration. Thanks to all of you.

Lastly, my family, who have put up with my odd hours and given me a place to rest and reflect on all my work. I wouldn't be here without all of you; Mum, Dad, Sean, and Caitlin, thanks.

Abstract

Two thirds of all irrigated agriculture in Australia is undertaken within the Murray-Darling Basin. However climate change predictions for this region suggest rainfall will decrease. In addition, environmental concerns and new industries are competing for water resources. In order to maintain profitability, more will need to be done by irrigators with less water. In this regard, irrigators need to be aware of the spatial distribution of the available water content (AWC) in the root-zone (i.e. 0.0-0.90 m). Owing to the expense of traditional soil survey methods, digital soil mapping techniques are being used with increasing frequency to map soil properties. This includes, soil properties related to AWC such as clay content and mineralogy. This thesis aims to create a digital soil map of the AWC at the district scale. This is achieved by determining AWC by the difference between the permanent wilting point (PWP) and Field Capacity (FC) which were measured in the laboratory using a pressure plate apparatus. The PWP and FC was coupled with ancillary information including gamma ray spectrometry (i.e. dose rate, Potassium (K %), Uranium (eU ppm), Thorium (eTh ppm)), electromagnetic induction data (i.e. EM38 and EM34) and two trend surface parameters using various multiple linear regression models (e.g. stepwise). This information is used as the basis of developing a hierarchical spatial regression (HSR) model to predict AWC in the irrigation areas of Warren and Trangie. The reliability of the models were compared using prediction precision (RMSE – root mean square error) and bias (ME–mean error). It was found that using EM38-v, EM34-10, eU, and eTh provided the best results (r^2=0.55). The DSM maps are consistent with the known pedoderms and soil types and provide a basis for irrigation management and future research.

Digital Soil Mapping of
Available Water Content
in the Lower Macquarie Valley, NSW.

List of Figures

List of Tables

List of Abbreviations

AWC	Available Water Content
EC_a	apparent soil electrical conductivity
EM	electromagnetic (EM) induction
EM34-10	EM34 signal reading at 10m coil spacing in the horizontal dipole mode
EM34-20	EM34 signal reading at 20m coil spacing in the horizontal dipole mode
EM34-40	EM34 signal reading at 40m coil spacing in the horizontal dipole mode
EM38-v	EM38 signal reading in the vertical dipole mode
EM38-h	EM38 signal reading in the horizontal dipole mode
K	potassium (%)
eU	Uranium (ppm)
eTh	Thorium (ppm)
DR	Dose rate???
HSR	Hierachical Spatial Regression
MLR	Multiple Linear Regression
FC	Field Capacity
PWP	Permanent Wilting Point
P	Precipitation
I	Irrigation
DD	Deep drainage
DS	Change is soil moisture
Et	Evapotranspiration
θ	volumetric water content (cm^3/cm^3)
ρ	bulk density of the soil (g/cm^3)
w	soil wetness (g/g)
RMSE	root mean square error
ME	mean error

1. Introduction

The Murray-Darling Basin (MDB) is Australia's food bowl and covers 1.65 million ha, comprising 65% of the total irrigated land in Australia (ABS, 2008). Of this, cotton production comprises 20% of water used for irrigation (ABS, 2008). However, it is forecast that climate change will see reduced rainfall and hence less water available for irrigation (Kothavala, 1999). Added to this is the increasing demand for environmental flows (Gawne et al., 2010), gold production (e.g. Cadia Mine Orange, NSW Gov, 2010), and the expansion of coal mining (NSW DPI, 2005). In order to sustain irrigated agriculture there is an urgent need to improve water use efficiency (Green et al., 2006). This requires irrigators to maximize the various components of the water balance equation: Precipitation (P) + Irrigation (I) = Runoff (R) + Evapotranspiration (Et) + Deep Drainage (DD) + change in soil moisture (ΔS).

Previous research in irrigated cotton systems has focused on: improving the rate (Hedley and Yule, 2009, Kim et al., 2008) and frequency (Hulugalle et al., 2010) of I; identifying DD risk (Triantafilis et al., 2004), implementing alternative irrigation practices (Bethune, 2004); and maximizing Et (Sankaranarayanan et al., 2010). There is however a lack of work on ΔS, which the amount of water available (AWC) in the soil (i.e. difference between Field Capacity (FC) and Permanent Wilting Point (PWP). The AWC is also important because it varies with soil texture (McCutcheon et al., 2006, Wiatrak et al., 2009). Whilst field measurement of AWC can be collected quickly [i.e. neutron (Al-Ain et al., 2009) and capacitance probes (Chanzy et al., 1998) and time domain reflectometry (Robinson et al., 2003)] the information is not readily transferable to district levels. Conversely, laboratory determination of AWC by filter paper (Leong et al.,

2002), vapour equilibration (Nam et al., 2010) and pressure plate is time consuming and costly (Cresswell et al., 2008, Jones and Graham, 1993).

In order to map the spatial variation of AWC at the district scale, and using laboratory determined AWC, an integrated approach using ancillary data is required (Nelson and Odeh, 2009, Schmugge et al., 1980). Ancillary data is secondary soil information which can be directly related to a soil property being investigated. This is in essence the process of Digital Soil Mapping (DSM). Using ancillary data such as the apparent soil electrical conductivity (EC_a) and gamma radiometrics, it has been shown that soil properties such as clay content (Mertens et al., 2008, Friedman, 2005), cation exchange capacity (Triantafilis et al., 2009b) and the volumetric water content (θ) (Bierworth, 1996, Reedy and Scanlon, 2003) can be mapped. To combine laboratory and ancillary data, it is recognised a robust statistical methods need to be developed (Contador et al., 2006). Such approaches include artificial neural networks (Cockx et al., 2009, Jiang and Cotton, 2004), linear regression (Kachanoski et al., 1988, Sheets and Hendrickx, 1995), and multiple linear regression (Hedley et al., 2004, Kuhn et al., 2009).

The aim of this study is to demonstrate how a DSM of PWP and FC can be generated to estimate AWC within the root-zone (0-0.90 m) and at the district level. In the first instance PWP and FC are determined using a pressure plate apparatus. A MLR is developed between this data and ancillary data consisting of EC_a from an EM34 and EM38, combined with Potassium, Uranium, and Thorium gamma spectrometry data. This information is used as the basis of developing a hierarchical spatial regression (HSR) model. The DSM maps are compared with the known pedoderms and soil types in the two study areas.

2. Material and Methods

2.1. Materials

2.1.1. Study Area

The study area is located in the Lower Macquarie Valley in the central west of New South Wales. Specifically, two areas which are predominantly irrigated will be studied: Trangie and Warren (Fig. 2) in western NSW. 20-60m of recent alluvium has been deposited since the late Pleistocene from an extensive river network. The source of this alluvium is sediment weathered from the slopes and tablelands of the Macquarie Valley and other tributaries of the Macquarie River. A major tributary of the Macquarie River upstream is dominated by the Bathurst batholith. The Bathurst batholith is a series of large plutons which are characterised by a number of granitic units. The main granite units of the Bathurst batholiths are the Icely, Dunkeld, and Bathurst granites. Granites are characterized by various primary minerals including quartz, orthoclase (K-feldspar), muscovite and/or biotite (micas), and plagioclase. When granite weathers, the primary minerals weather to produce sand, silt and clay sized particles produced. These are characterized by quartz, micas and kaolin and/or illite, respectively. These products are then deposited downstream in alluvial clay plains landscapes which characterise the irrigated areas of Trangie and Warren.

These soils developed in a paleoclimate of alternating cold, dry periods and warm, moist periods. The recent climate has been relatively stable with low rainfall and warm temperatures enabling pedological development. Land uses have change significantly over the last 100 years, shifting from native vegetation to dryland agriculture to the present irrigated agriculture.

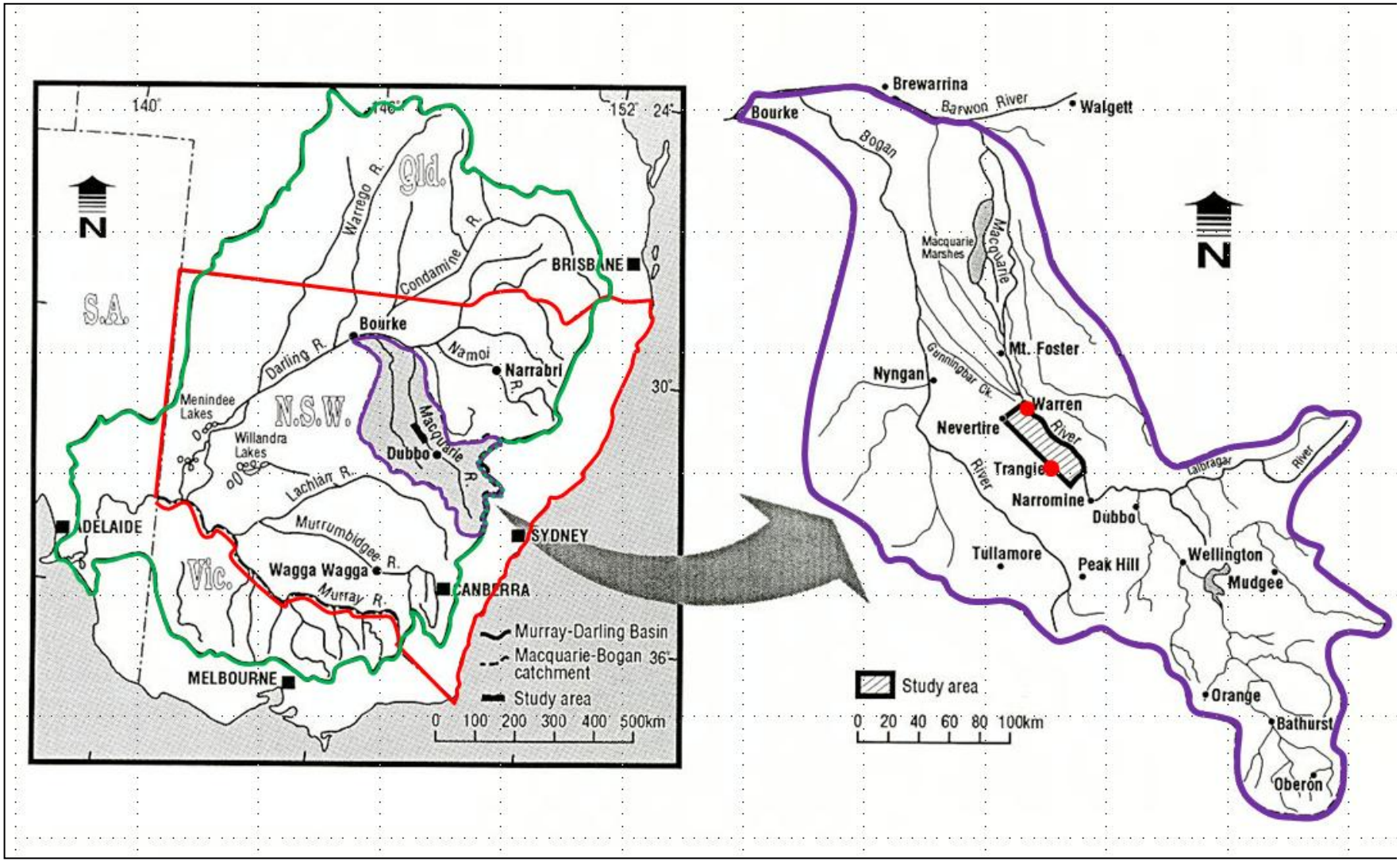

Fig. 1. Location of Trangie and Warren relative to New South Wales (red), the Lower Macquarie Valley (purple), and the Murray-Darling Basin (green). Adapted from McKenzie, 1992

2.1.2. Soil

An extensive soil survey of the study area was carried out by McKenzie (1992) whereby he sampled the soils and characterised 224 soil profiles along five transects of the Lower Macquarie Valley. He then used aerial photos and his profile descriptions to develop a soil map of the region ultimately identifying five pedoderms. Where a pedoderm is a mappable unit of soil which has physical properties, as well as a stratigraphic relationship within the landscape (Brewer et al., 1970). As shown in Fig. 2 these pedoderms include: the Old Alluvium; Gin Gin Hills; Macquarie Alluvium; Trangie Cowal; and the Contemporary Macquarie.

In the two study areas, McKenzie (1992) mapped six main components of these pedoderms. These are: (1) the Meander Plain and (2) Backplain of the Old Alluvium; (3) Gin Gin Hills pedoderm, which is made up of hills and crests; (4) the Macquarie Alluvium Backplain Complex, which contains a series of backplain deposits; (5) the Trangie Cowal Alluvial Plain, which has depressions as a minor component; and (6) the Contemporary Macquarie, which is a single stratigraphic unit. The Gin Gin Hills pedoderm is local to Trangie, and the Macquarie Alluvium Backplain Complex and Contemporary Macquarie are local to the Warren study area (Fig. 2). The Meander Plain and Backplain of the Old Alluvium and the Trangie Cowal Alluvial Plain are common to both study areas.

The Old Alluvium pedoderm is the oldest soil unit and is located furthest from the Macquarie River. It was deposited between 130,000 – 25,000 years ago in an extended period of alluvial deposition. The Meander Plain component was deposited in a higher energy environment and as such is characterised by a strong texture contrast,

dominated by coarse sands (~25%) with a low silt content (< 10%) with low activity kaolin clay at depth (Table 1). The Backplain component soils were deposited in a low energy environment and as such are dominated by smectite clays (with kaolin and illite subdominant) (~50%), which has resulted in cracking clay soils with a uniform profile texture (Table 1).

The Gin Gin Hills pedoderm is thought to have formed around the same time as the Old Alluvium pedoderm but by aeolian accession. It is similar to the Old Alluvium pedoderm in that there is clay at depth, however the clays here are predominantly kaolin. The soils are also strongly red (2.5YR) with a sandy texture (Table 3).

The Macquarie Alluvium Backplain Complex (Table 2) was deposited between 130,000 to 15,000 years ago. This unit was deposited by fluvial sediments from the Macquarie River and occurs parallel to the river. The soils are similar to the Old Alluvium pedoderm, but the mineral composition of the cracking clays is higher in smecite, and slightly more active.

The Trangie Cowal pedoderm has been recently deposited between 25,000 to 15,000 years ago. It has formed from the deposition of fine suspended sediment along the Trangie Cowal and is typically silty red-brown earths. The lower hue of these soils indicates they are less weathered, as does the large silt content (~30%) (Table 1).

The most recent soil unit is the Contemporary Macquarie pedoderm which has been deposited from 15,000 years ago to the present. This soil unit has been deposited by the Macquarie River and consists of fine sandy to silty clay sediments (Table 2), and as a result of their young age exhibit minimal development. There has been extensive

deposition of this unit in unison with changing land practices in the region, namely the clearing of trees along the Macquarie River since European settlement.

In addition to the detailed soil survey performed by McKenzie (1992), the landscape has been mapped repeatedly by the Australian Geological Society of Australia. The Trangie study site is located in the most northern part of the Narromine mapsheet (Sherwin, 1996) where the different soil units are identified but the focus is on geological formations. The Trangie study area is characterised as eroded red silt alluvium. This is consistent with McKenzie's (1992) description of the Trangie Cowal pedoderm.

The Warren study area is located in the southern section of the Nyngan map sheet (Watkins and Meakin, 1996). This AGSO map is different to the Narromine map in that it identifies different soil formations across the landscape as well as the underlying lithology. The three main formations identified across the study areas from this map are Trangie, Bugwah, and Marra Creek. The Trangie formation is comprised of channel, meander, and backplain facies, with the associated soils being dark brown to grey silts and clays. This formation is the oldest and is most likely equivalent to the Old Alluvium pedoderm (McKenzie, 1992). The Bugwah formation is comprised of a meander plain facies characterised by orange brown to grey silt/silty clay with fine sand. This formation was deposited after the Trangie formation and is equivalent to the Trangie Cowal pedoderm. The Marra Creek formation is comprised of meander plain and back plain facies characterised by mid grey to brown silts and clays with light grey sandy lenses and cracking. This formation is the most recent and is most likely the equivalent of the Macquarie Alluvium pedoderm.

Table 1 Summary of the pedoderms present and the Warren and Trangie study areas (adapted from McKenzie, 1992)

Pedoderm	Soil Class	Depth (m)	Colour	Texture	Particle Size (%)			Moisture (cm^3/cm^3)		
					sand	silt	clay	PWP	FC	AWC
Old Alluvium	Mitchell	0.1	5YR 4/4 (reddish brown)	sandy clay loam without coarse fragments	64	15	21	0.07	0.12	0.08
Meander		0.3	2.5YR 4/7 (red)	medium clay without coarse fragments				0.09	0.13	0.06
Plain		0.7	2.5YR 4/7 (red)	medium clay without coarse fragments	42	9	49	0.14	0.19	0.08
Old Alluvium	Mullah	0.1	10YR 4/2 (dark greyish brown)	medium heavy clay	38	12	50	0.20	0.27	0.10
Backplain	(grey)	0.3	10YR 4/1 (dark grey)	heavy clay				0.21	0.28	0.10
		0.7	7.5YR 4/3 (medium brown)	heavy clay	36	17	47	0.23	0.33	0.14
	Buddah	0.1	7.5YR 3/3 (dark brown)	medium clay	38	14	48	0.16	0.26	0.15
		0.3	5YR 3/4 (dark reddish brown)	medium heavy clay				0.18	0.30	0.16
		0.7	5YR 4/6 (yellowish red)	medium heavy clay	35	14	51	0.18	0.28	0.15
	Snake	0.1	grey	sodic cracking clay	38	13	49			0.13
		0.3		similar to mullah but high						0.18
		0.7	5YR 4/4 (reddish brown)	sodium throughout the profile	35	14	51			0.20
Trangie	Wilga	0.1	5YR 3/3 (dark reddish brown)	clay loam	52	29	19	0.07	0.20	0.18
Cowal		0.3	5YR 4/7 (yellowish red)	medium clay				0.09	0.21	0.17
Alluvial Plain		0.7	7.5YR 4/6 (strong brown)	clay loam	50	21	29	0.10	0.21	0.16
	Byron	0.1	7.5YR 3/4 (dark brown)	silty clay	40	35	25	0.09	0.18	0.14
		0.3	5YR 3/3 (dark reddish brown)	medium clay				0.15	0.20	0.08
		0.7	5YR 4/5 (yellowish red)	medium clay	17	42	41	0.15	0.23	0.12
	Buckshot	0.1	similar to wilga and byron	similar to wilga and byron	21	19	25			0.12
		0.3	but with a paler B horizon	but with manganese concretions						0.10
		0.7	7.5YR 5/4 (brown)	and coarse sand at depth	13	11	45			0.08

Table 2 Summary of the additional pedoderms present at the Warren study area (adapted from McKenzie, 1992)

Pedoderm	Soil Class	Depth (m)	Colour	Texture	Particle Size (%)			Moisture (cm^3/cm^3)		
					sand	silt	clay	PWP	FC	AWC
Macquarie	Ellengerah	0.1	10YR 3/2 (very dark greyish brown)	light clay	32	29	39	0.16	0.21	0.08
Alluvium		0.3	10YR 3/2 (very dark greyish brown)	medium clay				0.16	0.24	0.12
Backplain		0.7	7.5YR 4/4 (medium brown)	medium clay	25	33	42	0.17	0.23	0.09
	Mullah	0.1	10YR 4/2 (dark greyish brown)	medium heavy clay	37	13	50	0.19	0.27	0.11
	(black)	0.3	10YR 4/1 (dark grey)	medium heavy clay				0.19	0.25	0.08
		0.7	10YR 4/3 (medium brown)	medium heavy clay	34	15	51	0.21	0.27	0.09
	Buddah	0.1	7.5YR 3/3 (dark brown)	medium clay	38	14	48	0.16	0.26	0.15
		0.3	5YR 3/4 (dark reddish brown)	medium heavy clay				0.18	0.30	0.16
		0.7	5YR 4/6 (yellowish red)	medium heavy clay	35	14	51	0.18	0.28	0.15
	Snake	0.1	grey	sodic cracking clay	38	13	49			0.13
		0.3		similar to mullah but high						0.18
		0.7	5YR 4/4 (reddish brown)	sodium throughout the profile	35	14	51			0.20
Contemporary	Macquarie	0.1	accumulation of organic matter	laminae with contrasting textures	30	40	30			0.09
Macquarie		0.3		often considerable fine sand and silt						0.14
		0.7	7.5YR 4/3 (medium brown)	distinct from other soils in the valley	32	24	38			0.11

Table 3 Summary of the additional pedoderms present at the Trangie study area (adapted from McKenzie, 1992)

Pedoderm	Soil Class	Depth (m)	Colour	Texture	Particle Size (%)			Moisture (cm^3/cm^3)		
					sand	silt	clay	PWP	FC	AWC
Gin Gin	Gin Gin	0.1	2.5YR 3/6 (dark red)	sandy clay	65	10	25	0.07	0.12	0.09
Hills		0.3	2.5YR 5/8 (red)	light medium clay				0.08	0.12	0.09
		0.7	2.5YR 3/6 (dark red)	sandy clay	58	7	35	0.09	0.14	0.05

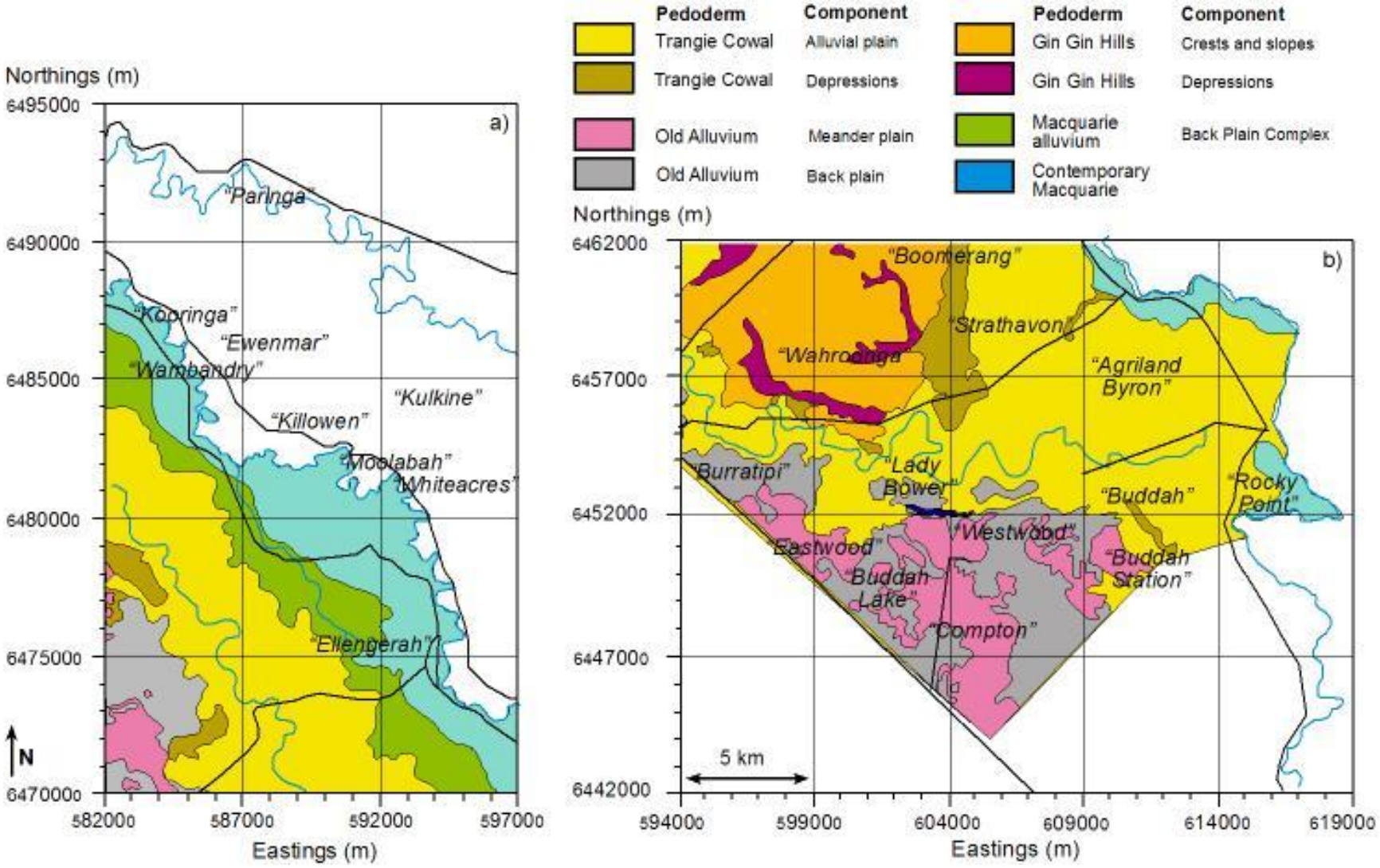

Fig. 2. The spatial distribution of soil pedoderms (after McKenzie, 1992) across a) Warren and b) Trangie study areas

2.1.3. Land Use

Until the completion of the Burrendong Dam in 1967, Trangie and Warren had been extensively developed for dryland cropping and grazing (McKenzie, 1992). As shown in Plate 1, the areas associated with the Macquarie River previously supported *Eucalyptus camaldulensis* (River Red Gum) while only a few stands still exist (Biddiscombe, 1963). The cracking clays supported mostly *Acacia pendula* (Weeping Myall) and *Atriplex nummularia* (Old Man Salt Bush). The remainder of the area was covered by *E. populnea* (Poplar box) (Biddiscombe, 1963). Following completion of the dam and a ready supply of water, irrigated agriculture was introduced with cotton one of the main crops planted in rotation with wheat (see Plate1b) and legumes. As of 1992, 58,000 hectares of the lower Macquarie Valley are licensed for irrigation, with 25,000 hectares of this is cotton (McKenzie, 1992). Shown in Fig. 3 is the extent of irrigated agricultural development in the Warren and Trangie study areas.

Plate. 1. Images showing a) the Macquarie River in Trangie with remnant *E. camaldulensis* and b) furrow irrigated field in Trangie with a rotation crop of wheat planted and emu's running across the field

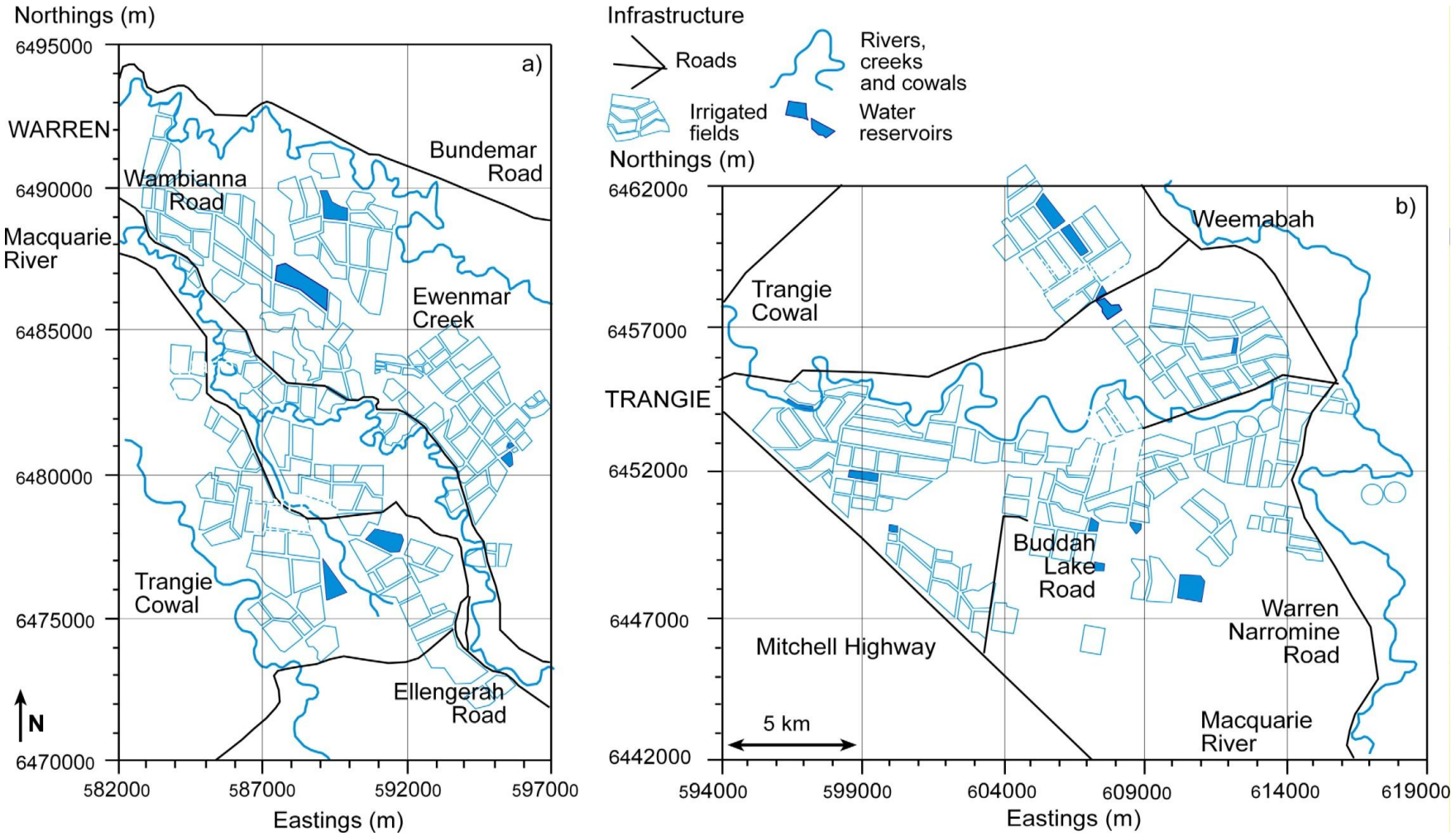

Fig. 3. Location of irrigated agriculture infrastructure across a) Warren and b) Trangie study areas

2.2. Methods

2.2.1. Gamma Spectrometry

Gamma radiation is emitted by the beta and alpha decay of soil constituents in the topsoil, and the decay of minerals in exposed geology. In Australia the majority of the continent (~80%) has been mapped by aerial gamma spectrometry for the purpose of geological exploration. Although gamma spectrometry is primarily used to identify ore, mineral and petroleum deposits (Lesher et al., 2001), other uses of gamma spectrometry data includes geological mapping, geomorphological studies, and soil mapping. The four main spectra which are used in gamma spectrometry are Potassium, Uranium, Thorium, and the total count of radiation (dose rate) (Bierworth, 1996). The theory of the method results from the emission of gamma rays from unstable isotopes which have sufficient strength and energy to be measured by a gamma spectrometer (Minty, 1997). Potassium (K) is measured directly using the decay of ^{40}K, whilst Uranium and Thorium abundances are inferred from the gamma-emitting daughter products of Bismuth (^{214}Bi) and Thallium (^{208}Tl), respectively and are therefore referred to as ‘equivalent’ Uranium (eU) and ‘equivalent’ Thorium (eTh).

Potassium is a major component of the earth’s crust and occurs predominantly in granites. Within granite, the isotope ^{40}K undergoes beta decay, releasing a gamma ray of 1.46 MeV (Grasty, 1997). This gamma ray is measured by a gamma spectrometer, giving an indication to the concentration of silt sized particles (usually micas) in the landscape or K held in secondary clay minerals (e.g. illite).

Uranium and Thorium are rarer elements, and as such are frequent at low concentrations. They are similarly concentrated in felsic rocks high in silica, such as

granite and rhyolite. When they are weathered out, ^{238}U and ^{232}Th tend to concentrate in shales and sandstones as bedrock, and iron oxides and clay minerals as alluvium (Dickson and Scott, 1997). Because ^{238}U and ^{232}Th do not emit gamma rays during their decay, the gamma rays emitted by their most energetic daughter isotope are measured to give eU and eTh. In case of ^{238}U, it has a decay chain where ^{214}Bi emits a gamma ray of 1.76 MeV. The decay series for ^{232}Th sees ^{208}Tl emit a gamma ray of 2.61 MeV (Minty, 1997). As such, gamma radiometric maps are used in soil science to provide information on the spatial distribution of soil forming minerals (Cook et al., 1996), and to delineate between soil classes at a large scale for further analysis (Nelson & Odeh, 2009)

The gamma-spectrometer data was obtained from the New South Wales Department of Mineral Resources. The data was acquired from an aerial geophysical survey undertaken in July 1995 for assistance in geological mapping and mineral exploration. Flight lines were predominantly east-west, with a line spacing of 0.4 km and survey height of 80 m. The spectrometer separated the voltage into a number of classes from windows centered on the K, U, and Th photopeaks. The total count was also measured (dose rate in counts per second-cps). The gamma-ray detection system was calibrated using procedures described in Minty *et al.* (1997). The data recorded was transformed to equivalent concentrations of the radio-elements (K-%, U-ppm and Th-ppm). Prior to numerical analysis, negative values which coincided with mountainous regions or where large bodies of water were present were removed.

2.2.2. Electromagnetic (EM) Induction

Electromagnetic induction operates on the principle of a primary electromagnetic field being able to induce a current in a conductive medium. The induced current, in turn creates its own magnetic field, whereby the strength of this secondary magnetic field is compared to the primary magnetic field. The ratio of the two is termed apparent electrical conductivity (EC_a) and gives an indication to the conductivity of the medium over which the instrument was used (McNeill, 1980a).

The properties of soils which influence conductivity are primarily clay type (Cockx et al., 2009, Friedman, 2005, Triantafilis et al., 2009b), clay content (Cockx et al., 2009, da Silva et al., 2001), and water content (Kachanoski et al., 1988, McCutcheon et al., 2006). EM instruments have been used in soil science for over 30 years as a tool to estimate soil properties, investigate correlations between conductivity and soil properties, and to observe the spatial distribution of soil properties. As such, EM instruments are a valuable tool for soil scientists and are being used ever more frequently to obtain increasing amounts of data at large scales cheaply and quickly.

In order to determine the validity of EM data for use in defining areas of spatially different soil water content at the district scale, an EM34/38 survey was performed across Warren and Trangie. The EM34 instrument is more commonly used to measure the vadose zone of the soil profile because of the depths achieved in its readings (McNeill, 1980b). Whilst the EM38 instrument is more commonly used to measure the root zone and sub-soil because it depth of measurement is shallower (McNeill, 1990). The EM34 was used with 10, 20 and 40 m coil spacing in the horizontal orientation (ie.

EM34-10, EM34-20, and EM34-40), whilst the EM38 was used in the horizontal (EM38-h) and vertical (EM38-v) modes. In these modes of operation the EM34-10 measures to a depth of 7 m; the EM34-20 measures to 15 m; the EM34-40 to 30 m (McNeill, 1980b). The EM38-h measures to 0.75 m whilst the EM38-v measures to 1.5 m (McNeill, 1990). The EM34 readings were taken at the same time as EM38 readings: with a total of 564 measurement locations across the Warren area and 755 southeast Trangie (Figure 4).

2.2.3. Soil Sampling and Preliminary Analysis

Soil samples were taken across the Warren and Trangie districts to gain a representative sample of the various pedoderms and to enable interpolation of laboratory AWC. Sample sites were chosen by sampling within the various soil conductivity zones as identified by the EM survey (Triantafilis et al., 2004). There were 35 sample sites in Warren and 96 in Trangie (Fig. 4). Samples were taken every 30 cm to 1.5 m by hand auger then every meter to 15 m where possible. Samples were initially analysed for effective cation exchange capacity (ECEC-mmol(+)/kg) (Tucker, 1974), pH of 1 part soil to 5 parts water, and electrical conductivity of a soil paste extract (EC_e-dS m^{-1}) and particle-size fraction using the pipette method (Coventry and Fett, 1979).

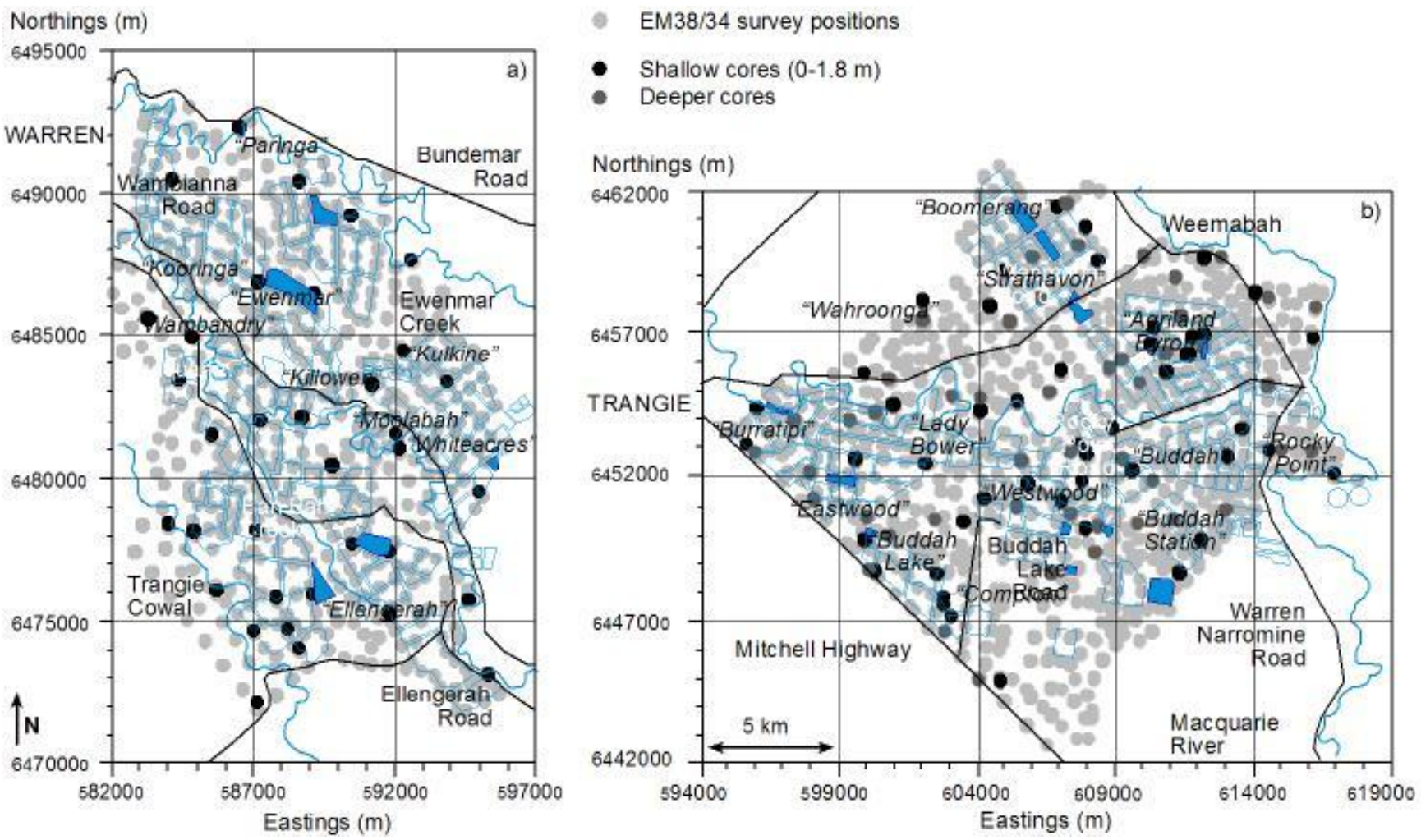

Fig. 4. The spatial distribution of the locations of EM34/38 measurement sites in a) Warren and b) Trangie study areas

2.2.4. Laboratory determination of Available Water Content

The measurement of water in the soil is commonly determined gravimetrically and is defined as soil wetness ($\boldsymbol{w}$). However, and in order to manage soil moisture status, this value needs to be converted into a measurement on a volumetric basis. This is termed volumetric soil moisture (θ) and calculated using the equation:

$$\boldsymbol{\theta = w \times \rho} \quad (1)$$

where ρ is the bulk density of the soil. However, not all the water in soil is available to a plant. This is because water molecules closest to the mineral fraction are held by the soil matrix by a number of forces.

The most dominant of these is the matric forces which are the forces of attraction between the soil particles and individual water molecules. Water is held by matric forces because water is a polar molecule and as such, the slightly positively charged hydrogen atoms are attracted to the predominantly negatively charged clay particles. Water adhering to the soil matrix is known as adhesion water and is held too tightly for a plant to be able to extract the water. This is known as the Permanent Wilting Point (PWP) and is the lower limit of θ. The PWP of a soil corresponds to a θ of -1,500 J/kg matric potential. Conversely, Field Capacity (FC) is the upper limit of θ, and is commonly defined as the amount of water remaining in the soil two days after free drainage from complete saturation. The FC of a soil corresponds to θ between -10 to -33 J/kg matric potential. Of interest here therefore is the Available Water Content (AWC) of a soil, which is the water held between FC and PWP in the soil matrix (Foth, 1990).

The θ of a soil can be determined by either in-field or laboratory methods. The most common field methods are neutron probe (Acworth et al., 2005, Al-Ain et al., 2009), capacitance probe (Chanzy et al., 1998, Paige and Keefer, 2008), or time domain reflectometry (Robinson et al., 2003, Topp and Davis, 1985). Laboratory methods include the filter paper method (Leong et al., 2002), vapour equilibrium (Nam et al., 2010), or pressure plate apparatus (Lu et al., 2008). Field methods are useful for determining θ in situ, however they often need to be calibrated with other equipment or laboratory methods (Stafford, 1988, Wessolek et al., 1994, Wraith and Or, 2001). In addition to this they cannot accurately determine the AWC of a soil because they calculate the variation in θ rather than the discrete FC and PWP. Because laboratory methods can accurately determine the FC and PWP of a soil with a high level of precision, they are used more frequently to determine the AWC (Nam et al., 2010). In this study the pressure plate apparatus was chosen for its ease of use, and ability to determine the precise FC and PWP (Cresswell et al., 2008, Jones and Graham, 1993).

The relationship between FC and soil texture can be described by a convex curve as shown in Figure 5, whereby sand has the lowest ability to hold water and clay the highest. Specifically, as shown in Table 4, sandy soils hold between 0.07-0.17 cm^3/cm^3 water, and clayey soils hold between 0.32-0.40 cm^3/cm^3 water at FC. Conversely, the relationship between PWP and soil texture can be described as a concave curve as shown in Figure 5. At PWP, sandy soils hold 0.02-0.07 cm^3/cm^3, and clayey soils 0.20-0.24 cm^3/cm^3. The result of the convex and concave curves is that silty soil, which occurs in the middle of each curve, has the highest AWC, and is thus considered the best soil for irrigated agriculture.

Table 4 Range of proven experimental values for Available Water Content as it varies across soil texture class (adapted from (Peverill *et al.*, 1999)

soil texture class	Field Capacity (cm^3/cm^3)	Permanent Wilting Point (cm^3/cm^3)	Available Water Content (cm^3/cm^3)
sand	0.07-0.17	0.02-0.07	0.05-0.10
loamy sand	0.11-0.19	0.03-0.10	0.08-0.09
sandy loam	0.18-0.28	0.06-0.16	0.12-0.14
loam	0.20-0.30	0.07-0.17	0.13-0.13
silt loam	0.22-0.36	0.09-0.21	0.11-0.15
silt	0.28-0.36	0.12-0.22	0.14-0.14
silty clay loam	0.30-0.37	0.17-0.24	0.13-0.13
silty clay	0.30-0.42	0.17-0.29	0.13-0.13
clay	0.32-0.40	0.20-0.24	0.12-0.16

The AWC of soil samples was determined by calculating the FC and PWP gravimetrically in the laboratory using the pressure plate apparatus, converting them to θ, and then taking the difference between the two values. A 15 bar pressure plate chamber with two ceramic plates (Fig. 6a) was used to determine PWP at 15 bars of pressure (which corresponds to -1,500 J/kg matric potential). Simultaneously a 5 bar pressure plate chamber with two ceramic plates (Fig. 6b) was used to determine FC at 1 bar of pressure (which corresponds to -10 J/kg matric potential). Each plate held 12 samples in rubber rings. Prior to each analysis the plates were soaked overnight, then the samples were allowed to wet overnight on the soaked plates. Compressed air was used to maintain a positive pressure in the chambers and they were allowed to equilibrate. PWP and FC were determined by the mass of later lost on drying once the samples had equilibrated. These gravimetric water contents were then converted to volumetric water content by using the bulk density for each pedoderm as calculated by McKenzie (1992). And the AWC the difference between FC and PWP. A detailed laboratory procedure is included in Appendix A.

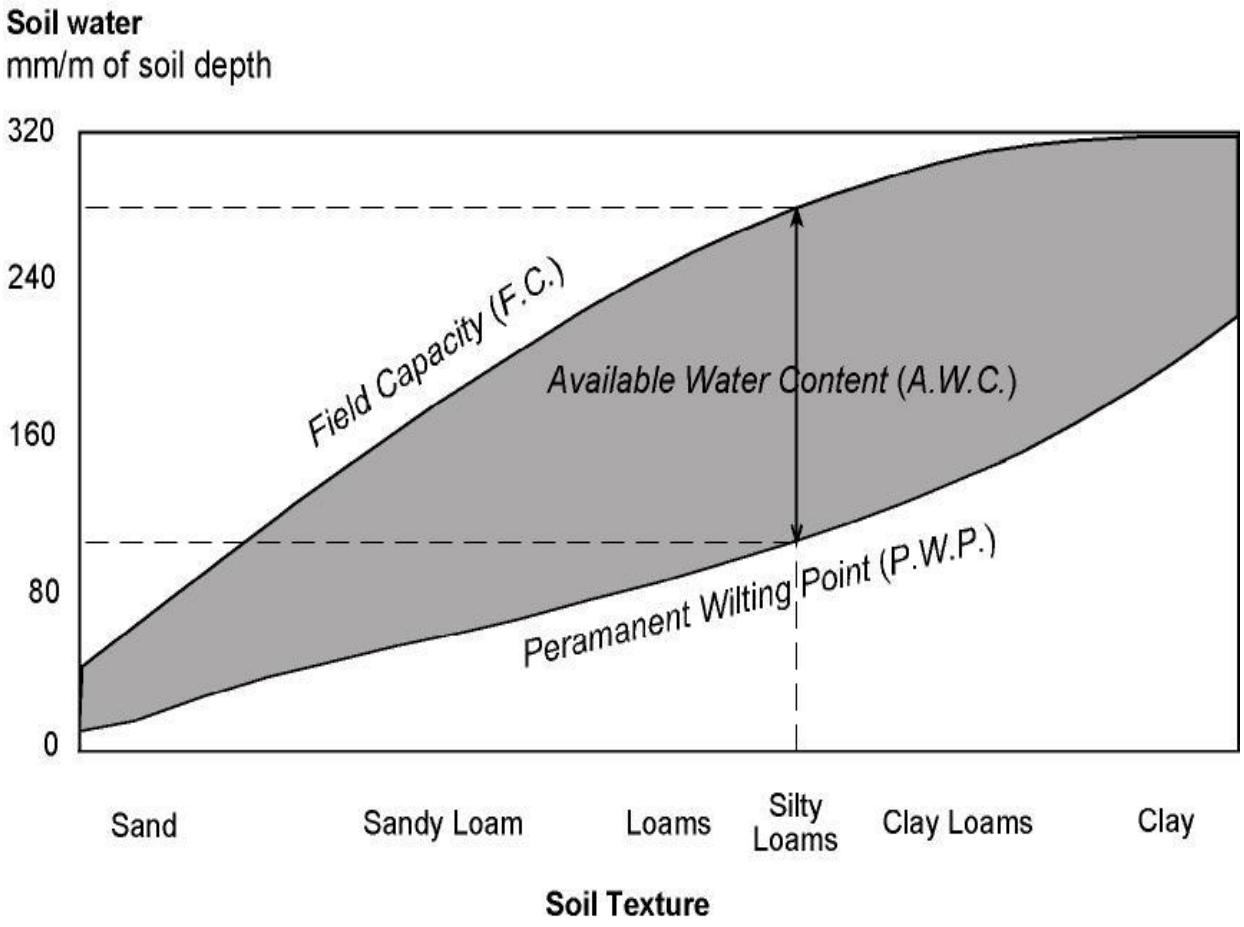

Fig. 5. The relationship of soil texture to Available Water Content (adapted from (Foth, 1990)

2.2.5. Statistical Methods

In order to observe and quantify similarities between various forms of soil data such as sampling, pressure plate and ancillary, statistical analysis is required (Contador et al., 2006, McBratney et al., 2003). Such statistical tools used in soil science are Artificial Neural Networks (ANNs) (Behrens et al., 2005, Chang and Islam, 2000, Jiang and Cotton, 2004, McBratney et al., 2003), Linear Models (Domsch and Giebel, 2004, Kachanoski et al., 1988, Sheets and Hendrickx, 1995), and Multiple Linear Regression (MLR) (Hezarjaribi and Sourell, 2007, Triantafilis et al., 2009b). An ANN is a powerful

statistical tool which aim to establish a relationship between input parameters and the desired output through hidden pathways and weighting (Laffan and Lees, 2004). They are effective at handling complex relationships but the resulting algorithm is rigid and cannot be used by other researchers easily (Gahegan, 2003). LM have been used extensively in soil science, especially to establish relationships between basic soil properties such as clay content or soil texture (Hedley et al., 2004). They operate on the basis of a linear relationship existing between an independent and dependent soil property which can be expressed as:

$$y = \beta x + \varepsilon \quad (2)$$

where y is the dependent variable and x is the independent variable, β represents the empirical regression parameter, and ε is the error term. Once the equation is developed, it can be used to estimate the property y for further sample sites or datasets. MLR is similar to a LR, except that there is more than one dependant variable:

$$y = \beta_0 + \beta_1 x_1 + \ldots + \beta_n x_n + \varepsilon \quad (3)$$

where β_n represents empirical regression parameters which must be estimated, x_n represents the independent variables used in the regression, and ε represents the residual error distribution.

Simple LR have been observed between clay content and θ (Kuhn et al., 2009), bulk density and θ (Kachanoski et al., 1988), and soil conductivity and clay content (Hedley et al., 2004). MLR has also been used to model parameters such as soil class based on terrain attributes and gamma spectrometry (Nelson & Odeh, 2009), and CEC

using EM38, EM31, and spectral brightness (Triantafilis, et al. 2009a). Taking into account that there are relationships between clay content, CEC, gamma spectrometry, soil moisture content, and EC_a (Friedman, 2005, Sudduth et al., 2005, Triantafilis and Lesch, 2005), and that there are multiple soil properties which influence θ (Gebbers et al., 2009, Kuhn et al., 2009), a MLR incorporating the most significant properties in the form of ancillary data is the best method of estimating the two components of AWC (i.e. PWP and FC).

In this thesis four models are developed to determine which is most suited for the purpose of developing DSM of AWC from PWP and FC:

Model 1 - a standard least squares effect model developed for both Warren and Trangie using all ancillary data available (i.e. EM34-10, EM34-20, EM34-40, EM38-v, EM38-h, K, eU, eTh, and dose rate as well as eastings and northings);

Model 2 – a forward sequential stepwise model developed for both Warren and Trangie using only the statistically significant ancillary data (e.g. EM34-10, EM38-v, eU, eTh, and eastings and northings);

Model 3 - a forward sequential stepwise model developed for Warren using only the statistically significant ancillary data (e.g. EM38-h, and dose rate);

Model 4 - a standard least squares effect model developed Trangie using only the statistically significant ancillary data (e.g. EM38-v and eU, as well as eastings and northings).

In addition and in order to interpolate the estimates of PWP and FC to obtain their variation at the district scale, a model which incorporates the spatial nature of the data is required. Geo-statistical modeling techniques such as co-kriging, kriging with external drift, and regression kriging are common techniques for multibavariate spatial data interpolation. However hierarchical spatial regression (HSR) models are used when the ancillary data has its own spatial distribution (i.e. EM and gamma spectrometry) (Royle and Berliner, 1999). The theoretical development of the model is described by Trantafilis and Lesch (2005), but can be explained as such. A HSR first specifies *y* (conditional on observed *z* data) is linearly related to the co-located *z* ancillary data and a linear combination of additional regression variables (such as trend surface vectors). In this case, *z* represents a dense grid of EM and gamma spectrometry data, and *y* represents a subset of FC or PWP data acquired at a co-located set of EM and gamma spectrometer sites. The relationship between *y* and *z* can be specified as:

$$(y \mid z = z_0) = \beta_0 + \beta_1 z_0 + \beta_2 x_1 + \beta_3 x_2 + \eta \qquad (4)$$

where z_0 represents the observed *z* ancillary data readings, x_1 and x_2 represent scaled location coordinates, β_0 through β_3 represent empirical regression parameters that must be estimated, and η represents the residual error distribution, which may exhibit some type of spatial dependence. In practice, this regression component of the HSR model is estimated using the subset of jointly observed (*y*, *z*) data.

The second part of the HSR model specifies that *z* also follows a stationary spatial distribution of some type. This might mean the covariance function for *z* being

specified to follow an isotropic exponential model defined by known parameters such as a nugget, sill, and range. Here, the VESPER software package (Minasny et al., 2005) was used to generate local semi-variograms (i.e. exponential) and enable prediction of $\hat{Z}_{\mathbf{u}}$ at unsampled locations using the 90 nearest neighbors.

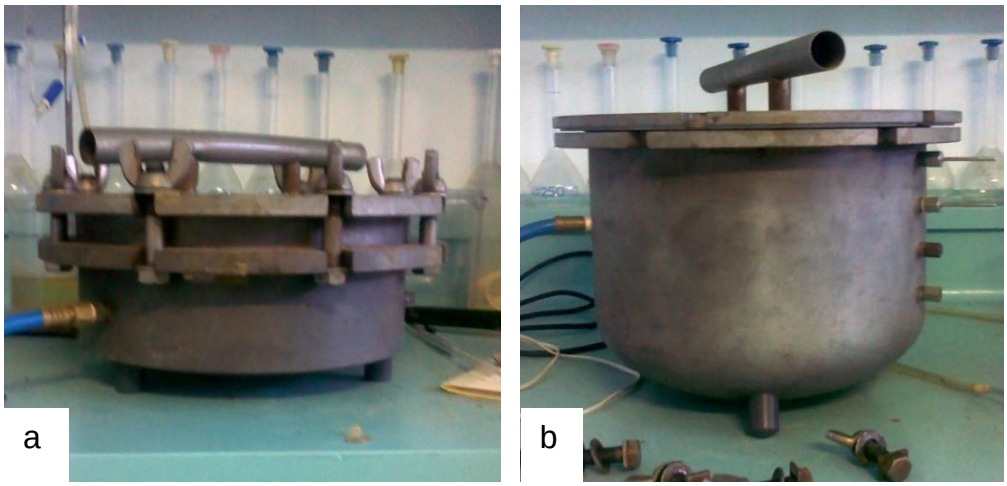

Fig. 6. Images showing the a) 15 bar pressure plate and b) 5 bar pressure plate used in the laboratory

2.2.6 Validation

For the purpose of validating the HSR prediction models, a jackknifing procedure was performed. This consisted of the removal of a random sample of 20% of the calibration data at a time with the remaining 80% used to develop a MLR for either PWP and FC using the ancillary data identified in the initial model (i.e. Models 1-4). The MLR from the jackknifed calibration data was used to predict PWP and FC to the 20% of sites removed previously. This procedure was repeated five times for each MLR that was developed, with two measures of prediction accuracy determined. These were the mean error (ME) as an indication of bias, and the root mean square error (RMSE) as an indication of precision (Voltz and Webster, 1990).

The indices are calculated from the observed values $z(s_j)$ and the predicted values $z^*(s_j)$ where there are *l* sample sites. RMSE and ME are commonly used measurements of prediction performance (Liu et al., 2002, Odeh and McBratney, 2000). RMSE is a measure of prediction accuracy, with the most accurate being close to zero, and is expressed as:

$$RMSE = \left\{\frac{1}{l}\sum_{j=1}^{l}\left[z(\mathrm{s_j}) - z^*(s_j)\right]^2\right\}^{0.5} \quad (5)$$

ME is a measure of bias in the prediction, with unbiased predictions being close to zero, and is expressed as:

$$ME = \frac{1}{l}\sum\left[z(s_j) - z^*(s_j)\right] \quad (6)$$

3. Results

3.1. Gamma Spectrometry

Table 5 shows the basic summary statistics of the gamma spectrometry for the Warren study area. Table 6 shows the equivalent data for Trangie. In general, the gamma spectrometric data is slightly higher in the Warren study area. For example, average K for Warren (1.12 %) is approximately 12.5 % higher than for Trangie (0.98 %). This suggests that the sediments associated with the Warren district are younger and consistent with McKenzie's (1992) pedoderms and Watkins (1996) soil units which describe the area as being characterised by the most recent soil unit (Macquarie Contemporary Alluvium and Marrah Creek formation, respectively). Part B of Tables 5 and 6 show the Pearson Correlation Coefficients for the different gamma spectrometric data. For both study areas, the largest correlations are between the dose rate and K (0.94 and 0.83). This is understandable given K is the largest component of the dose rate (Dickson & Scott, 1997).

Table 5 Gamma spectrometric summary statistics for Warren

Part A. Summary Statistics

	n	average	SD	min	max
K (%)	22504	1.12	0.17	0.01	1.69
U (ppm)	22504	2.05	0.32	0.02	4.74
Th (ppm)	22504	7.09	0.78	0.01	9.82
dose (cps)	22504	1911.84	203.61	253.75	2495.21

Part B. Pearson Correlation Coefficients

K	eU	eTh	dose
1.00	0.44	0.49	0.83
	1.00	0.48	0.75
		1.00	0.67
			1.00

Table 6 Gamma spectrometric summary statistics for Trangie

Part A. Summary Statistics

	n	average	SD	min	max
K (%)	25971	0.98	0.28	0.01	1.59
eU (ppm)	25971	1.86	0.28	0.03	3.58
eTh (ppm)	25971	6.34	0.78	0.02	9.00
dose (cps)	25971	1692.15	273.70	363.90	2367.95

Part B. Pearson Correlation Coefficients

K	eU	eTh	dose
1.00	0.69	0.69	0.94
	1.00	0.68	0.78
		1.00	0.84
			1.00

Fig. 7 shows the spatial distribution of K across both study areas. A prominent feature of the Warren (Fig. 7a) study area is that the Contemporary Macquarie pedoderm is characterised by very high K (>1.25 %) indicating a high silt component. Additionally, the Trangie Cowal pedoderm is evident as being characterised by high-very high K (>1.00 %). In Trangie (Fig. 7b), the Contemporary Macquarie and Trangie Cowal pedoderms are characterised by very high K (>1.25 %) indicating that the youngest soils are identifiable by the higher K. Also, the Old Alluvium and Gin Gin Hills pedoderms can by identified be intermediate-very low K (<1.00 %) indicating weathering and that these soils are higher in clay and sand respectively. Of particular interest is in the Warren study area, where the area to the north of the Macquarie River has not been mapped in Fig. 2a. Here the K signal along the length of Ewenmar Creek is similar to that along the length of the Macquarie River, indicating recent, silty textured sediments. The area between the Creek and the River is more similar to the Macquarie Alluvium indicating that this is perhaps a more weathered form of the Contemporary Macquarie. In addition to this, there is a clear contrast in Trangie with the Trangie Cowal Alluvial Plain with lower counts being found away from the Cowal, but within the same pedoderm. This indicated that the soils closest to the Cowal are more recent than those at a distance from the Cowal in the same pedoderm.

Fig. 8 shows the spatial distribution of eU across both study areas. A prominent feature of the Warren study area (Fig. 8a) is the Contemporary Macquarie pedoderm being characterised by very high eU (> 2.25 ppm). Additionally, the Trangie Cowal pedoderm is evident as being characterised by intermediate-very high eU (>1.75 ppm). This is somewhat similar to the spatial distribution of K in Fig. 7a, and indicates that

these soils are the youngest given that the U has not weathered extensively from the minerals it is bound to. In Trangie (Fig. 8b), the Contemporary Macquarie and Trangie Cowal Alluvial Plain are characterised as being intermediate-very high eU (>1.75 ppm). As well as this, the Old Alluvium and Gin Gin Hills pedoderms can be identified by predominantly low-very low eU (<1.75 ppm), indicating that they are the oldest soils.

Fig. 9 shows the spatial distribution of eTh across both study areas. A prominent feature of Warren (Fig. 9a) is that the majority of the study area is characterised as very high eTh (>7.00 ppm). Of particular interest is that the lowest eTh in the study area (<6.50 ppm) is associated with water features, and that the pedoderms in Fig. 2 are undistinguishable from the spatial distribution of eTh. In the Trangie study area (Fig. 9b), the Contemporary Macquarie and Trangie Cowal pedoderms are largely characterised by high-very high eTh (>6.50 ppm). In addition to this, the Old Alluvium Backplain and Gin Gin Hills are characterised as low-very low eTh (<6.00 ppm) indicating they are older than the Contemporary Macquarie and Trangie Cowal Alluvial Plain. The Old Alluvium Meander Plain is characterised by high eTh (6.50-7.00 ppm). This may be the result of Th weathering from its constituent mineral and being absorbed onto iron oxides which similarly weather from granitic parent material (Dickson and Scott, 1997). The iron oxides persist in the soil and are particularly evident in sandier soil (e.g. Old Alluvium Meander Plain) (Charman and Murphy, 2003). This is evidenced by sand grains which have red (5R), orange (7.5YR) or yellow (10YR) hues. As a result these areas of the landscape have generally elevated eTh signal.

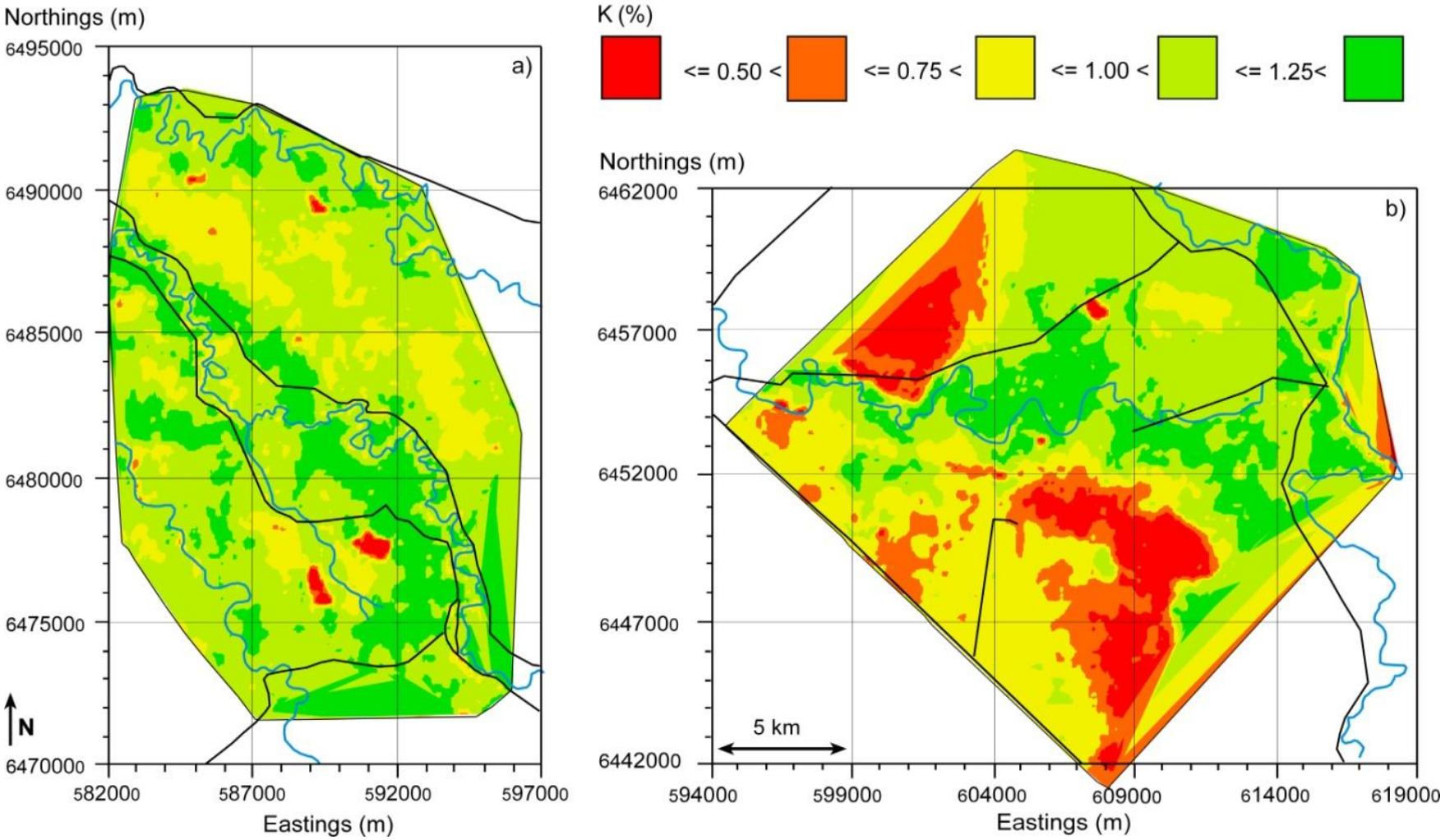

Fig. 7. The spatial distribution of Potassium (K - %) across a) Warren and b) Trangie study areas

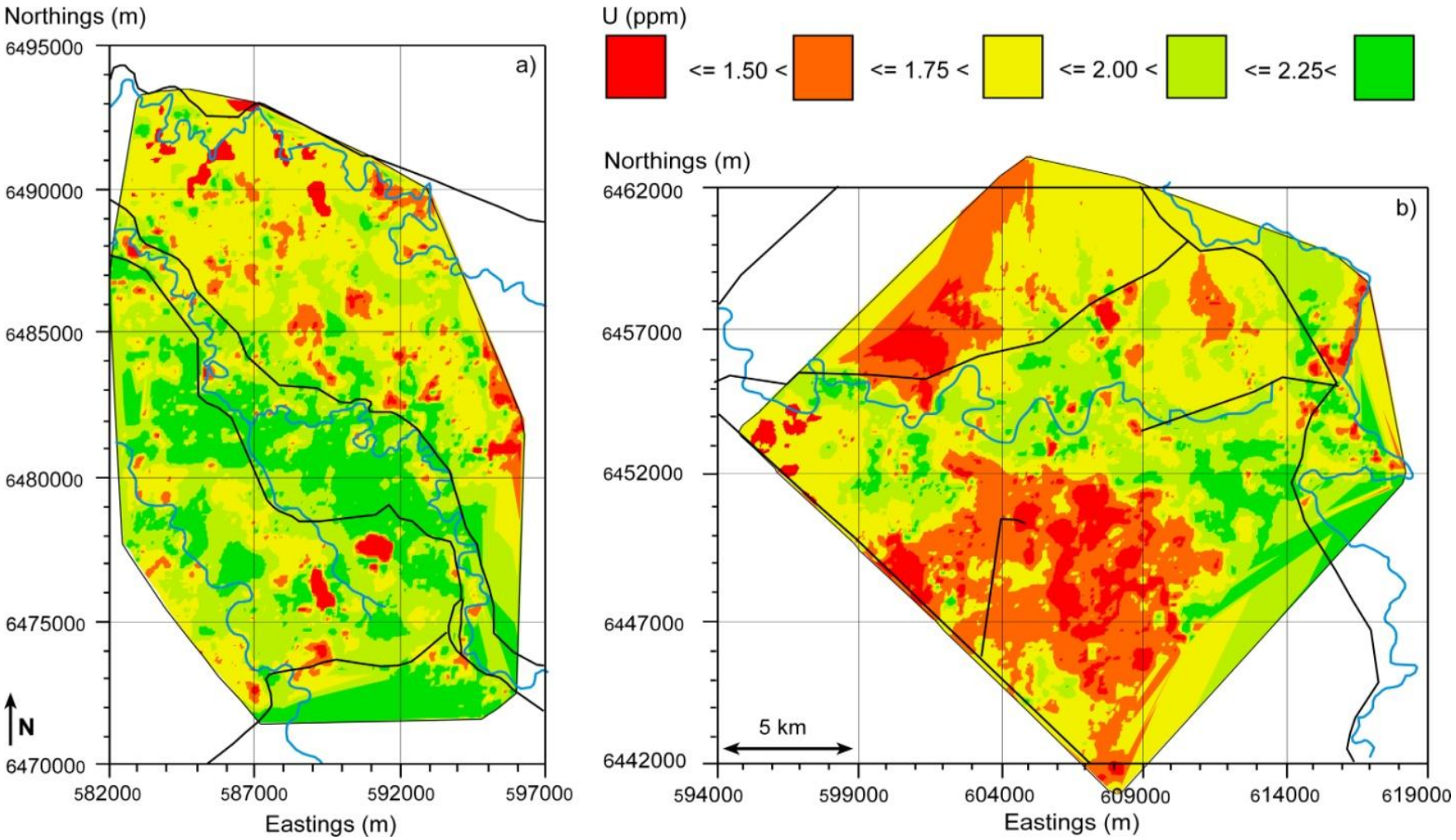

Fig.8. The spatial distrubution of Uranium concentration (eU – ppm) across a) Warren and b) Trangie study areas

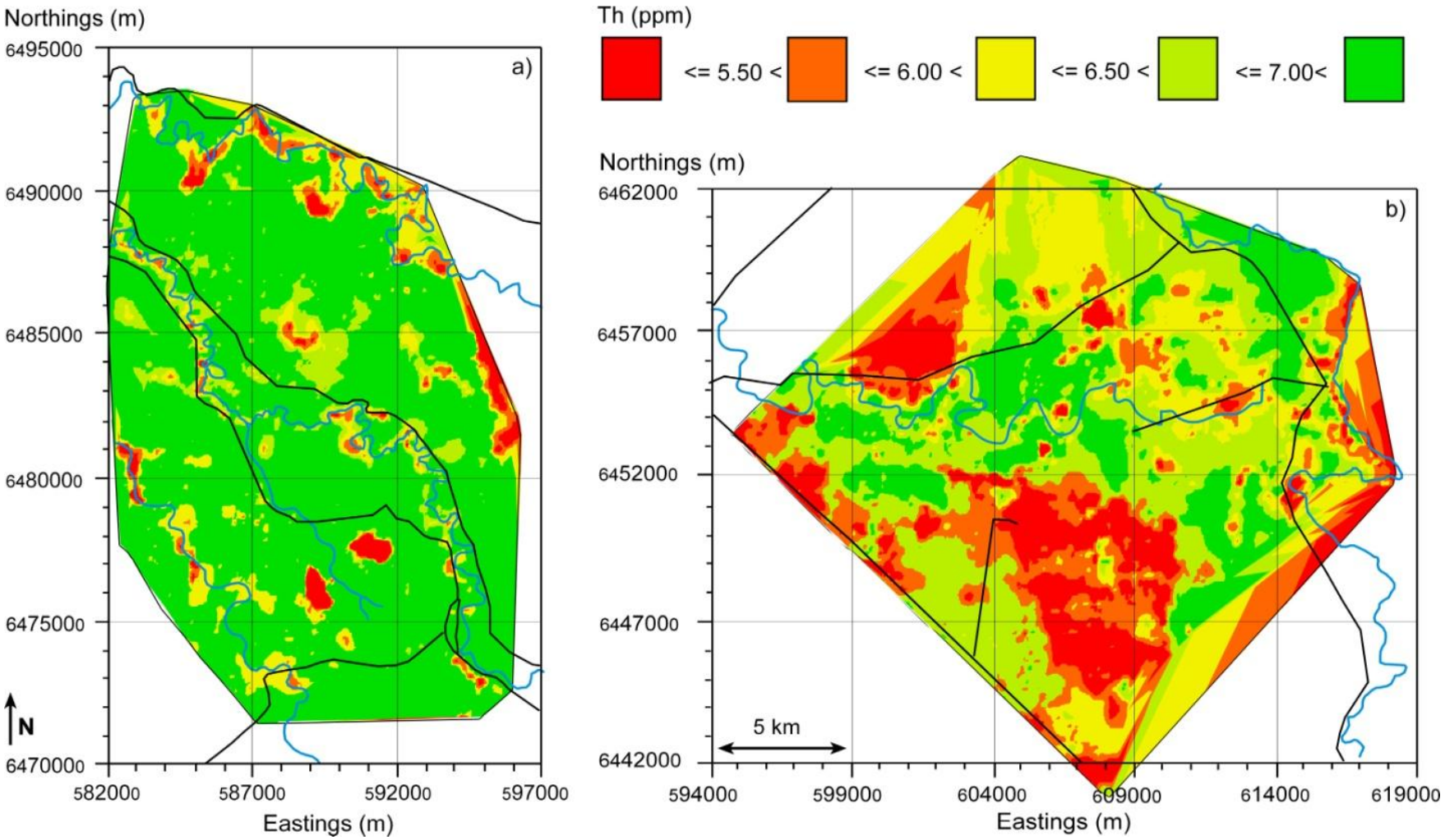

Fig. 9. The spatial distribution of Thorium concentration (eTh – ppm) across a) Warren and b) Trangie study areas

3.2. Electromagnetic

Table 7 shows the basic summary statistics of the EM data for the Warren study area. Table 8 shows the equivalent data for the Trangie study area. In both study areas, the EM34 tended to produce signal readings slightly larger than the EM38. For example in the Warren study area, average EM34-10 (92.67 mS/m) is 1.08% larger than the average EM38-v data (85.25 mS/m). This suggests that there is more conductive material such as clay at depth than in the near surface. As well as this, for both study areas the EM38-v (0-1.5m) is higher than the EM38-h (0-0.75m), further implying a more conductive subsoil than topsoil. This is consistent with McKenzie (1992) who characterises the Mitchell, Wilga, and Byron soils – which are the most commonly occurring – as duplex, that is having a strong texture contrast between horizons with more conductive material at depth.

Part B of Tables 4 and 5 show the Pearson Correlation Coefficients for the various EM data. For both study areas, the largest correlations are between the EM38-h and EM38-v readings (0.94 and 0.95). The across EM class correlation appears to be the lowest, particularly with the EM34-40 in both instances. This is most likely due to the fact that the EM34-40 measures the entire profile to the vadose zone, where-as the EM38-h and –v measures the root zone and are most sensitive to this signal depth.

Table 7 EM34 and EM38 summary statistics for Warren

A. Summary Statistics

	n	average	SD	min	max
EM34-10	564	92.67	33.1	15	171
EM34-20	564	98.64	33.99	22	190
EM34-40	564	110.92	29.48	44	190
EM38-v	564	85.25	38.38	12	252
EM38-h	564	68.24	29.74	12	246

B. Pearson Correlation Coefficients

	EM34-10	EM34-20	EM34-40	EM38-v	EM38-h
EM34-10	1.00	0.94	0.81	0.84	0.78
EM34-20		1.00	0.92	0.73	0.68
EM34-40			1.00	0.57	0.54
EM38-v				1.00	0.95
EM38-h					1.00

Table 8 EM34 and EM38 summary statistics for Trangie

A. Summary Statistics

	n	average	SD	min	max
EM34-10	755	88.44	37.54	17	187
EM34-20	755	92.59	38.13	10	205
EM34-40	755	115.08	40.49	35	223
EM38-v	755	88.26	43.96	7	256
EM38-h	755	74.31	33.13	14	204

B. Pearson Correlation Coefficients

EM34-10	EM34-20	EM34-40	EM38-v	EM38-h
1.00	0.89	0.74	0.76	0.68
	1.00	0.87	0.67	0.58
		1.00	0.55	0.47
			1.00	0.94
				1.00

Fig. 10 shows the spatial distribution of EC_a across both study areas as mapped by an EM38-v. A prominent feature of the Warren study area (Fig. 10a) is that the Contemporary Macquarie and Trangie Cowal pedoderms are characterised by low-very low EC_a (< 100 mS/m), which is consistent with these soils being silty in texture and hence not very conductive. In addition to this the Macquarie Alluvium Backplain is characterised as intermediate to high EC_a (100-200 mS/m), which is a result of more conductive, clayier soils (Table 2). In the Trangie study area (Fig. 10b), the Gin Gin Hills, Old Alluvium Meander Plain, Trangie Cowal Alluvial Plain, and Contemporary Macquarie pedoderms are characterised by low-very low EC_a (< 100 mS/m). In the Old Alluvium Meander Plain this is the result of a sandy textured soil and kaolin clays which are both unconductive. The Old Alluvium Backplain is characterised by intermediate-very high EC_a (> 100 mS/m) which indicates that there are high activity clay minerals such as smectite at depth. Similar to the distribution of K in Fig. 7, there is a difference in conductivity evident in the Trangie Cowal Alluvial Plain indicating two different soil types within the pedoderm.

Fig. 11 shows the spatial distribution of EC_a across both study areas as mapped by an EM38-h. A prominent feature of the Warren study area (Fig. 10a) is that the

Contemporary Macquarie and Trangie Cowal pedoderms are characterised by very low EC_a (<50 mS/m). In addition to this the Macquarie Alluvium Backplain is characterised by intermediate-high EC_a (100-200 mS/m). This indicates a clayier subsoil with high activity smectite, which is consistent with McKenzie's (1992) description. In the Trangie study area (Fig. 11b), the Contemporary Macquarie is characterised by being very low EC_a (< 50 mS/m). This concurs with McKenzie's (1992) description of the pedoderm being silty with a sand component, both soil minerals which are unconductive. Consistent with the EM38-v, the Gin Gin Gills, Old Alluvium Meander Plain and Trangie Cowal Alluvial Plain are characterised by low-very low EC_a (<100 mS/m). The Old Alluvium Backplain is characterised by intermediate-high EC_a (100-200 mS/m).

Fig. 12 shows the spatial distribution of EC_a across both study areas as mapped by an EM34-10. A prominent feature of Warren (Fig. 12a) is that the Contemporary Macquarie and Trangie Cowal Alluvial Plain pedoderms are characterised by predominantly low EC_a (50-100 mS/m). The Macqaurie Alluvium Backplain is characterised by intermediate EC_a (100-150 mS/m). In the Trangie study area (Fig. 12b), the spatial distribution of EC_a is very similar to that of the EM38-v (Fig. 10b) with the Gin Gin Hills, Old Alluvium Meander Plain, Trangie Cowal Alluvial Plain, and Contemporary Macquarie pedoderms being characterised by low-very low EC_a (< 100 mS/m). The Old Alluvium Backplain can be discerned by intermediate-high EC_a (100-200 mS/m).

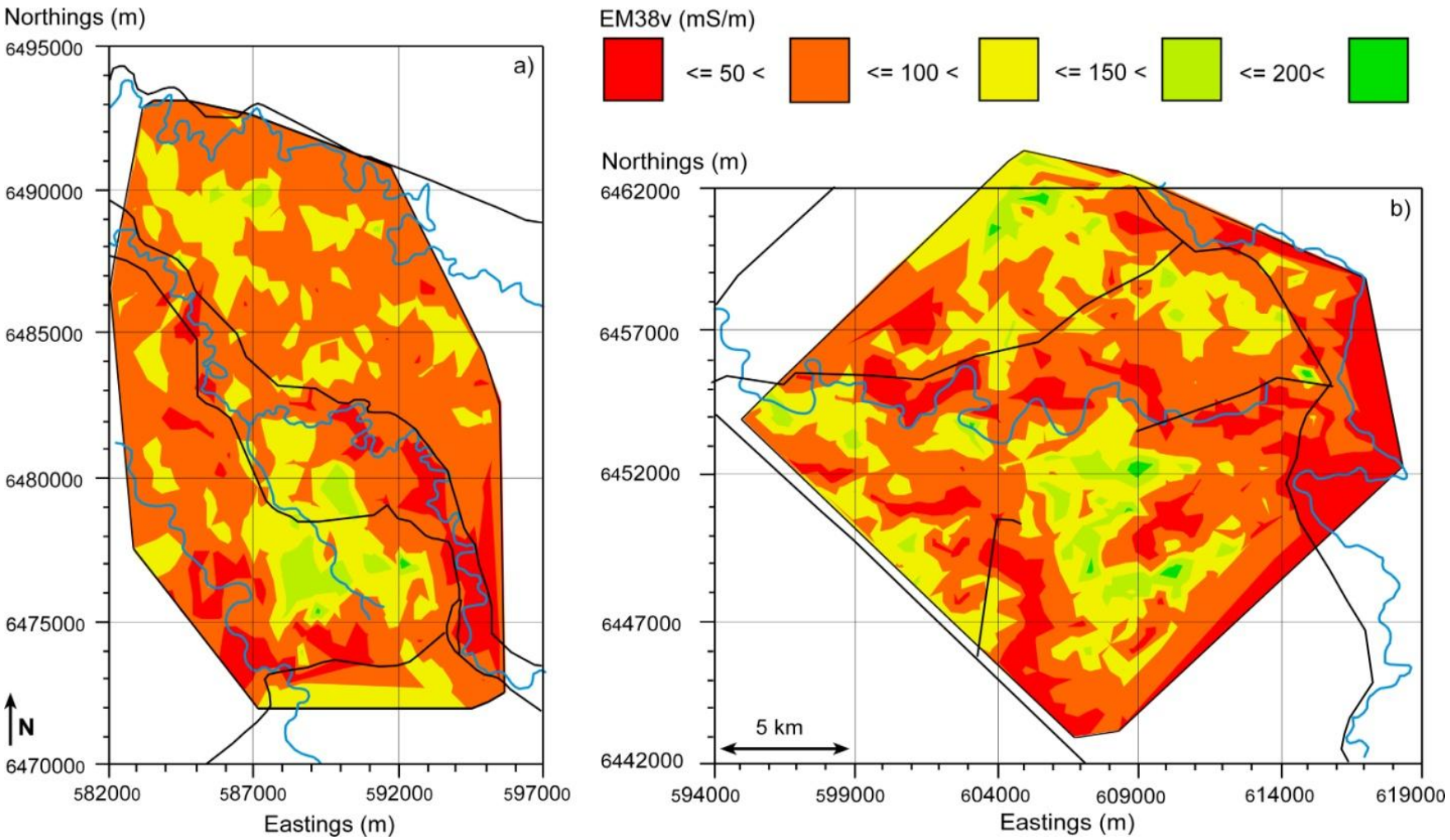

Fig. 10. The spatial distribution of the apparent soil electrical conductivity (ECa – mS/m) measured by an EM38 in the vertical dipole position across a) Warren and b) Trangie study areas

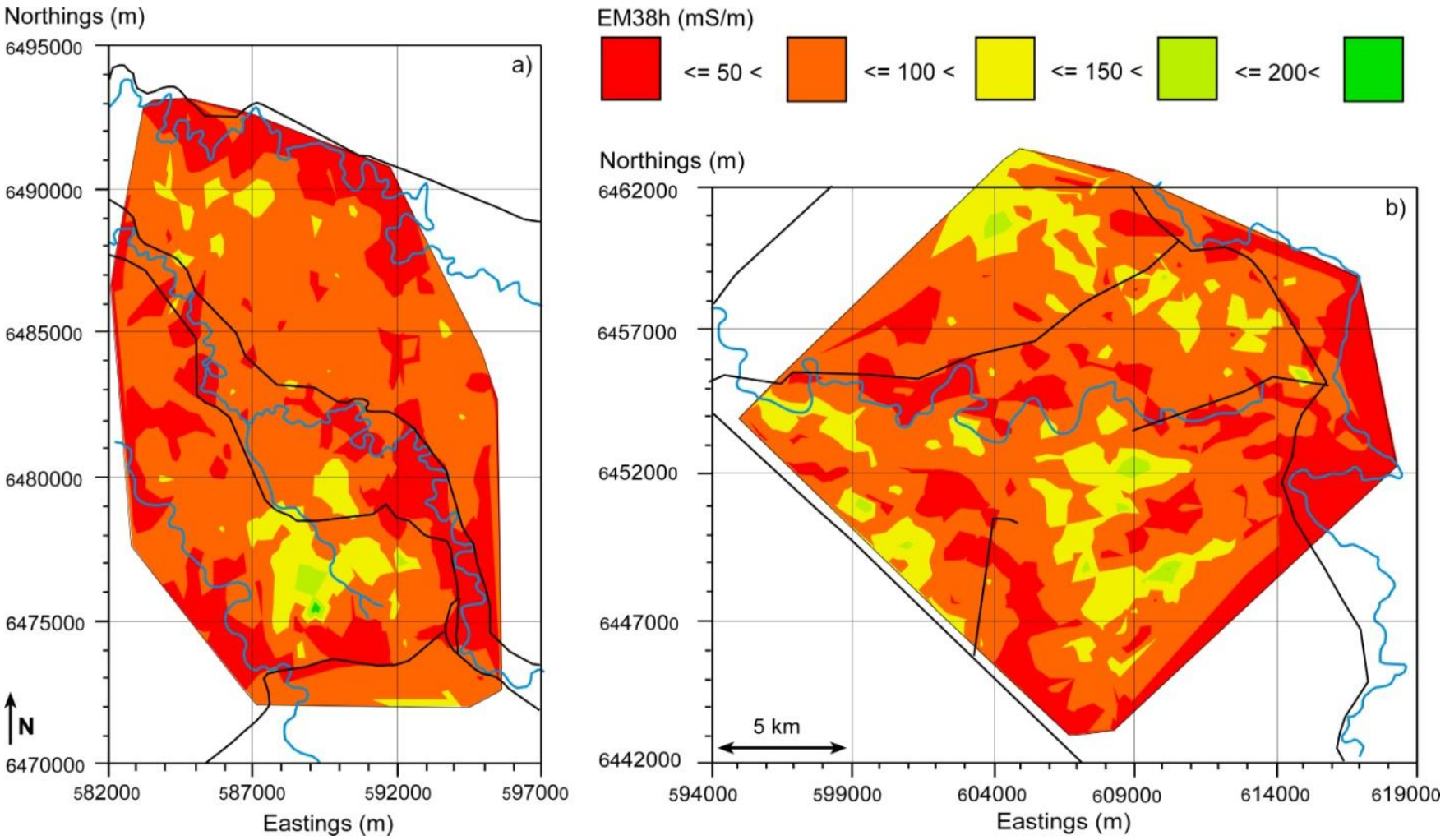

Fig .11. The spatial distribution of the apparent soil electrical conductivity (ECa – mS/m) measured by an EM38 in the horizontal dipole position across a) Warren and b) Trangie study areas

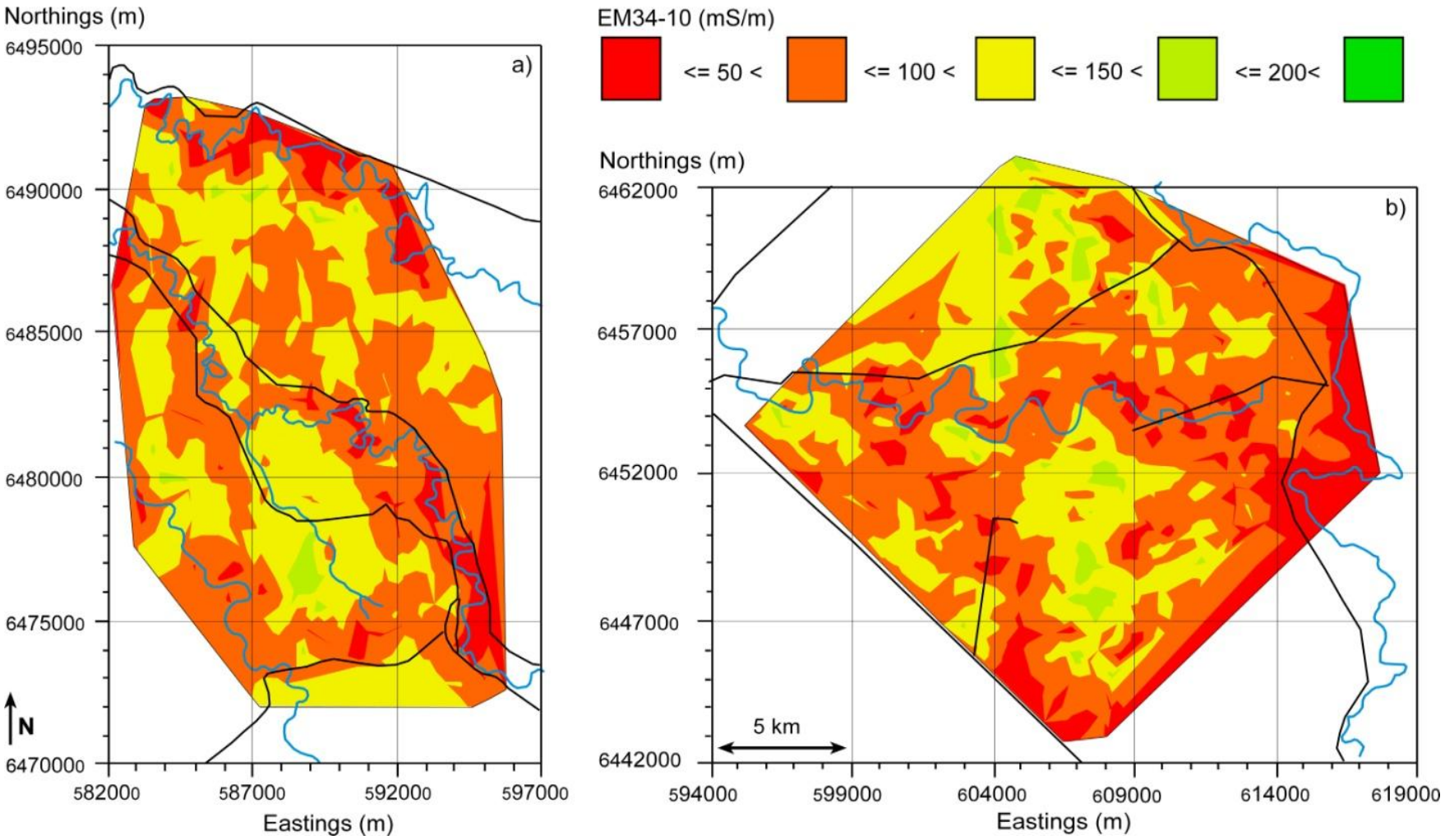

Fig .12. The spatial distribution of the apparent soil electrical conductivity (ECa – mS/m) measured by an EM34 with 10 meter coil spacing across a) Warren and b) Trangie study areas

3.3. Available Water Content (AWC)

In McKenzie's (1992) soil survey of the lower Macquarie Valley, the representative FC and PWP for the identified pedoderms were determined. Of the three pedoderms occurring in the Warren study area, McKenzie calculated the FC and PWP for the Macquarie Alluvium Backplain (0.24 and 0.16 cm^3/cm^3) and the Trangie Cowal Alluvial Plain (0.19 and 0.08 cm^3/cm^3) as shown in Table 9. These values indicate that the Macquarie Alluvium Backplain is a silt loam, and the Trangie Cowal Alluvial Plain is a sandy loam (as per Table 3). Using the samples from this study, as they are located within McKenzie's (1992) pedoderms, the representative FC and PWP for the Macquarie Alluvium Backplain (0.30 and 0.17 cm^3/cm^3) and Trangie Cowal Alluvial Plain (0.19 and 0.08 cm^3/cm^3) are shown in Table 8 alongside McKenzie's (1992) values. The results from this study indicate that the Macquarie Alluvium Backplain is silty, the Trangie Cowal Alluvial Plain is a silt loam, and the Contemporary Macquarie (which McKenzie (1992) did not calculate the FC and PWP for) is a silt loam also (as per Table 3).

Of the seven components that McKenzie (1992) identified in Trangie (Fig. 2b), FC and PWP were calculated for the Gin Gin Crest (0.12 and 0.07 cm^3/cm^3), Gin Gin Depression (0.26 and 0.16 cm^3/cm^3), Old Alluvium Backplain (0.27 and 0.19 cm^3/cm^3), Old Alluvium Meander Plain (0.12 and 0.07 cm^3/cm^3), Trangie Cowal Alluvial Plain (0.19 and 0.08 cm^3/cm^3), and the Trangie Cowal Depression (0.20 and 0.15 cm^3/cm^3) as shown in Table 10. These values indicate that the Gin Gin Hills have a loamy sand to sandy loam texture, the Old Alluvium Backplain has a silt loam texture, the Old Alluvium Meander Plain has a loamy sand texture, and the Trangie Cowal Alluvial Plain has a

sandy loam to loam texture (as per Table 4). Using the samples from this study, as they are located within McKenzie's (1992) pedoderms, the representative FC and PWP values are shown alongside McKenzie's (1992) values in Table 10. The results from this study indicate that the Gin Gin Hills have a sandy loam texture, the Old Alluvium Backplain has a silty loam texture, the Old Alluvium Meander Plain has a sandy loam texture, and the Trangie Cowal Alluvial Plain has a sandy loam to loam texture (as per Table 4).

Table 9 Available Water Content statistics for each pedoderm and component in the Warren study area

	McKenzie (1992)				This Study			
pedoderm	n	FC	PWP	AWC	n	FC	PWP	AWC
Contemporary Macquarie	5			0.09	23	0.24	0.15	0.09
Macquarie Alluvium Backplain	39	0.24	0.16	0.08	1	0.30	0.17	0.13
Trangie Cowal Alluvial Plain	60	0.19	0.08	0.11	9	0.24	0.13	0.11

Table 10 Available Water Content statistics for each pedoderm and component in the Trangie study area

	McKenzie (1992)				This Study			
pedoderm	n	FC	PWP	AWC	n	FC	PWP	AWC
Contemporary Macquarie	5			0.09	3	0.18	0.09	0.09
Gin Gin Crest	11	0.12	0.07	0.05	1	0.25	0.15	0.10
Gin Gin Depression	27	0.26	0.16	0.10	2	0.19	0.13	0.06
Old Alluvium Back Plain	67	0.27	0.19	0.08	12	0.26	0.17	0.09
Old Alluvium Meander Plain	52	0.12	0.07	0.05	11	0.25	0.15	0.10
Trangie Cowal Alluvial Plain	60	0.19	0.08	0.11	30	0.23	0.12	0.11
Trangie Depression	18	0.20	0.15	0.05	3	0.29	0.19	0.10

Table 11 shows a summary of the pressure plate data for the Warren study area. Table 12 shows the equivalent data for Trangie. The high, uniform FC in the Warren study area indicates that this is a more recent soil than the varied FC across the Trangie study area. The higher variation between FC and PWP in the Trangie study area is

indicative of there being more weathered soils here, and varying soils which accounts for the larger range in values than is seen in Warren. The variation between the topsoil (0.0-0.3 m) and subsoil (0.3-0.9 m) in Trangie also indicates that there are duplex soils in the study area, as is described by McKenzie (1992) for the Trangie Cowal Alluvial Plain.

Table 11 Available Water Content summary statistics for Warren

	depth (m)	n	average	SD	min	max
FC	0.0-0.3	33	0.25	0.02	0.20	0.30
(cm^3/cm^3)	0.3-0.6	33	0.25	0.03	0.19	0.31
	0.6-0.9	33	0.25	0.04	0.17	0.31
	0.0-0.9	33	0.25	0.02	0.20	0.30
PWP	0.0-0.3	33	0.16	0.03	0.10	0.20
(cm^3/cm^3)	0.3-0.6	33	0.15	0.03	0.08	0.20
	0.6-0.9	33	0.18	0.04	0.11	0.24
	0.0-0.9	33	0.16	0.03	0.10	0.20
AWC	0.0-0.3	33	0.09	0.02	0.05	0.13
(cm^3/cm^3)	0.3-0.6	33	0.10	0.02	0.06	0.16
	0.6-0.9	33	0.07	0.01	0.04	0.10
	0.0-0.9	33	0.09	0.02	0.05	0.13

Table 12 Available Water Content summary statistics for Trangie

	depth (m)	n	average	SD	min	max
FC	0.0-0.3	63	0.24	0.05	0.13	0.34
(cm^3/cm^3)	0.3-0.6	66	0.27	0.06	0.11	0.40
	0.6-0.9	66	0.27	0.06	0.09	0.41
	0.0-0.9	50	0.26	0.05	0.13	0.36
PWP	0.0-0.3	63	0.14	0.04	0.07	0.24
(cm^3/cm^3)	0.3-0.6	66	0.18	0.05	0.06	0.29
	0.6-0.9	66	0.19	0.05	0.05	0.31
	0.0-0.9	50	0.17	0.04	0.06	0.26
AWC	0.0-0.3	63	0.09	0.03	0.05	0.19
(cm^3/cm^3)	0.3-0.6	66	0.08	0.02	0.04	0.11
	0.6-0.9	66	0.08	0.02	0.02	0.16
	0.0-0.9	50	0.09	0.02	0.05	0.12

3.4. Multiple Linear Regression

In order to determine the FC and PWP at the district level, the use of MLRs using ancillary soil data and laboratory FC and PWP data were assessed. Four training MLR models were developed: Models 1a and 1b the first using FC and PWP data in the 0.0-0.9m depth range from the Warren and Trangie study areas with all ancillary data, shown as equation 7. The second using FC and PWP data in the 0.0-0.9m depth range from the Warren and Trangie study areas, with significant ancillary data, shown as equation 6. The third using FC and PWP data from the Warren study area in the 0.0-0.9m range, with significant ancillary data, shown as equation 9. The fourth using FC and PWP data from the Trangie study area in the 0.0-0.9m range, with significant ancillary data identified, shown as equation 10.

Model 1 was a standard least squares effect screening model developed in JMP 5 using the FC and then PWP data for both Warren and Trangie as the dependant variables. All ancillary data, in the form of EM34-10, EM34-20, EM34-40, EM38-v, EM38-h, K, eU, eTh, and dose rate were used as independent variables, as well as normalised eastings and northings. The equation for Model 1 is:

$$\text{AWC component} = \beta_0 + \beta_1(X_s) + \beta_2(Y_s) + \beta_3(\text{EM34-10}) + \beta_4(\text{EM34-20}) + \beta_5(\text{EM34-40}) \beta_6(\text{EM38-v}) + \beta_7(\text{EM38-h}) + \beta_8(\text{K}) + \beta_9(\text{eU}) + \beta_{10}(\text{eTh}) + \beta_{11}(\text{dose}) + \varepsilon \quad (7)$$

where X_s = (Easting – 600,000)/10,000, Y_s = (Northing – 6,440,000)/10,000, β_0 to β_{10} represent empirical regression parameters, and ε represents the error term. The regression model summary statistics and parameter estimates for this model are shown as Table 13 for FC and Table 14 for PWP.

As shown in Table 13a, Model 1 explains 49% of the FC data; this is lower than the 57% for PWP as shown in Table 14a. The RMSE of 0.026 for PWP indicates a higher precision than FC (0.032). In addition to this, there are a number of parameters in Model 1 which are not significant as indicated by the *p* values greater than 0.05 in Tables 13b and 14b. Despite this, Model 1 shows that it is possible to use ancillary data in the form of EM generated EC_a and aerial gamma spectrometric data, with laboratory AWC data, to predict the FC and PWP at the district scale with a degree of certainty.

Table 13 Regression Model 1 summary statistics for Eq. (7) performed for Field Capacity

a) Model summary statistics	
r^2	0.49
RMSE	0.032

b) Parameter estimates

Coefficient	Parameter Estimate	Standard Error	*t*-test	*p*>|*t*|
β_0	0.2493	0.0340	7.33	<0.0001
β_1	-0.0141	0.0067	-2.12	0.0375
β_2	-0.0117	0.0044	-2.64	0.0102
β_3	-0.0001	0.0003	-0.28	0.7804
β_4	-0.0001	0.0004	-0.29	0.7749
β_5	-0.0002	0.0002	-0.13	0.8972
β_6	0.0006	0.0002	2.39	0.0197
β_7	0.0001	0.0003	0.38	0.7066
β_8	0.0001	0.0001	0.91	0.3666
β_9	-0.0325	0.0489	-0.66	0.5091
β_{10}	0.0062	0.0083	0.74	0.4627
β_{11}	-0.0519	0.0225	-2.30	0.0243

Table 14 Regression Model 1 summary statistics for Eq. (7) performed for Permanent Wilting Point

a) Model summary statistics	
r^2	0.57
RMSE	0.026

b)Parameter estimates

Coefficient	Parameter Estimate	Standard Error	*t*-test	*p*>|*t*|
β_0	0.1671	0.0278	6.02	<0.0001
β_1	-0.0149	0.0054	-2.74	0.0078
β_2	-0.0141	0.0036	-3.90	0.0002
β_3	0.0001	0.0002	0.34	0.7384
β_4	-0.0002	0.0003	-0.64	0.5214
β_5	-0.0001	0.0001	-0.07	0.9473
β_6	0.0004	0.0002	2.24	0.0285
β_7	0.0001	0.0003	0.53	0.5948
β_8	0.0001	0.0001	0.83	0.4116
β_9	-0.0306	0.0399	-0.77	0.4460
β_{10}	0.0046	0.0068	0.68	0.4994
β_{11}	-0.0343	0.0184	-1.86	0.0664

Model 2 was a standard least squares effect screening model developed in JMP 5 using the depth averaged FC, then PWP data for both Warren and Trangie as the dependant variables. The ancillary data for this model was selected from all variables using a forward modeling stepwise function in JMP 5 which selected the variables which were most significant. The equation for model 2 is:

$$\text{AWC component} = \beta_0 + \beta_1(X_s) + \beta_2(Y_s) + \beta_3(\text{EM34-10}) + \beta_4(\text{EM38-v}) + \beta_5(\text{eTh}) + \beta_6(\text{eU}) + \varepsilon \quad (8)$$

The regression model summary statistics and parameter estimates for this model are shown as Table 15 for FC and Table 16 for PWP.

As shown in Table 15a, Model 2 explains 47% of the FC variation across both study areas with a RMSE of 0.032. This is a reduction of 2% from Model 1, however the RMSE remains the same. Table 16a shows that Model 2 explains 55% of the PWP variation across both study areas, with an RMSE of 0.025. Like FC, this is a reduction of 2% accuracy from Model 1, but the RMSE improves by 0.01, indicating this model is more precise. Model 2 also has an improved validation for FC and PWP from the validation for Model 1, further indicating that it is more applicable to both study areas rather than Model 1. Using a forward modeling stepwise function identified which ancillary data is statistically significant. This is shown in Table 15b and 16b. Although the EM34-10 and eTh parameters resulted in a $p>0.05$, removing them from the model results in an $r^2 = 0.42$ and RMSE = 0.033 for FC, and $r^2 = 0.52$ and 0.026 for PWP. Model 2 thus shows the optimum ancillary variables for predicting the AWC at the district scale in this study area.

Table 15 Regression Model 2 summary statistics for Eq. (8) performed for Field Capacity

a) Model summary statistics

r^2	0.47
RMSE	0.032

b)Parameter estimates

Coefficient	Parameter Estimate	Standard Error	*t*-test	*p*>|*t*|
β_0	0.2647	0.0310	8.54	<0.0001
β_1	-0.0157	0.0063	-2.49	0.0150
β_2	-0.0121	0.0043	-2.84	0.0058
β_3	-0.0002	0.0001	-1.66	0.1019
β_4	0.0007	0.0001	5.59	<0.0001
β_5	0.0102	0.0059	1.73	0.0876
β_6	-0.0445	0.0185	-2.41	0.0185

Table 16 Regression Model 2 summary statistics for Eq. (8) performed for Permanent Wilting Point

a) Model summary statistics

r^2	0.55
RMSE	0.025

b)Parameter estimates

Coefficient	Parameter Estimate	Standard Error	*t*-test	*p*>|*t*|
β_0	0.1762	0.0243	7.26	<0.0001
β_1	-0.0139	0.0050	-2.78	0.0069
β_2	-0.0137	0.0034	-4.07	0.0001
β_3	-0.0001	0.0001	-1.01	0.3138
β_4	0.0006	0.0001	5.84	<0.0001
β_5	0.0072	0.0046	1.57	0.1211
β_6	-0.031	0.0144	-2.15	0.0347

Model 3 was a standard least squares effect screening model developed in JMP 5 using the depth averaged FC, then PWP data for Warren as the dependant variable. The ancillary data for this model was selected from all ancillary data using a forward modeling stepwise function in JMP 5 which selected the variables which were most significant. The equation for model 3 is:

$$\text{AWC component} = \beta_0 + \beta_1(\text{EM38-h}) + \beta_2(\text{dose}) + \varepsilon \quad (9)$$

The regression model summary statistics and parameter estimates for this model are shown in Table 17 for FC and Table 18 for PWP.

As shown in Tables 17a and 18a, Model 3 only describes 22% of FC variation and 45% of PWP variation. The very low r^2 indicates that this model is not effective at predicting the FC and PWP across the Warren study area. The exclusion of eastings and northings by the forward modeling stepwise function indicates that using Warren data alone, the datapoints are too closely spaced and violate the assumption of independence. By removing the eastings and northings from the regression the spatial independence issue is solved but it does not give the model a spatial representation of the datapoints, as evidenced by the very low validation. Although in Table 17b, $p>0.5$ for dose rate, it is significant in Table 18b and is hence included in the model.

Table 17 Regression Model 3 summary statistics for Eq. (9) performed for Field Capacity

a) Model summary statistics	
r^2	0.22
RMSE	0.022

b) Parameter estimates

Coefficient	Parameter Estimate	Standard Error	*t*-test	*p*>|*t*|
β_0	0.2048	0.0331	6.19	<0.0001
β_1	0.0003	0.0001	2.91	0.0067
β_2	0.0001	0.0001	0.57	0.5699

Table 18 Regression Model 3 summary statistics for Eq. (9) performed for Permanent Wilting Point

a) Model summary statistics	
r^2	0.45
RMSE	0.020

b)Parameter estimates

Coefficient	Parameter Estimate	Standard Error	*t*-test	*p*>|*t*|
β_0	0.0634	0.0299	2.12	0.0422
β_1	0.0004	0.0001	4.77	<0.0001
β_2	0.0001	0.0001	2.05	0.0494

Model 4 was a standard least squares effect screening model developed in JMP 5 using the depth averaged FC, then PWP data for Trangie as the dependant variable. The ancillary data as the independent variable for this model was selected from all ancillary data using a forward modeling stepwise function in JMP 5 which selected the variables which were most significant. The equation for model 4 is:

$$\text{AWC component} = \beta_0 + \beta_1(X_s) + \beta_2(Y_s) + \beta_3(\text{EM38-v}) + \beta_4(\text{eU}) + \varepsilon \quad (10)$$

The regression model summary statistics and parameter estimates for this model are shown in Table 19 for FC and Table 20 for PWP.

Table 19a shows that Model 4 explains 53% of the FC data across the Trangie study area with a RMSE of 0.035. This is 6% more than is explained using Model 2, but the RMSE is higher by 0.003. Applying Model 4 to the Warren data set results in r^2 = 0.24 and RMSE = 0.022. This indicates that Model 4 is only applicable to the Trangie study area. Table 20a shows that Model 4 explains 60% of the PWP data across the Trangie study site with a RMSE of 0.028. This is 5% more than Model 2, but the RMSE is higher by 0.003. The validation of Model 4 shows that it can explain more variation than Model 2, but with lower precision.

Table 19 Regression Model 4 summary statistics for Eq. (10) performed for Field Capacity

a) Model summary statistics

r^2	0.53
RMSE	0.035

b)Parameter estimates

Coefficient	Parameter Estimate	Standard Error	*t*-test	*p*>|*t*|
β_0	0.3129	0.0427	7.32	<0.0001
β_1	-0.0079	0.0100	-0.79	0.4325
β_2	-0.0191	0.0145	-1.31	0.1953
β_3	0.0007	0.0001	5.29	<0.0001
β_4	-0.0434	0.0211	-2.06	0.0452

Table 20 Regression Model 4 summary statistics for Eq. (10) performed for Permanent Wilting Point

a) Model summary statistics

r^2	0.60
RMSE	0.028

b)Parameter estimates

Coefficient	Parameter Estimate	Standard Error	*t*-test	*p*>|*t*|
β_0	0.2279	0.0345	6.61	<0.0001
β_1	-0.0094	0.0081	-1.16	0.2527
β_2	-0.0202	0.0117	-1.72	0.0920
β_3	0.0006	0.0001	5.83	<0.0001
β_4	-0.0393	0.0170	-2.31	0.0257

3.5. Validation

Using the method described in section 2.2.6, validation was performed for each MLR model using a jackknife procedure. As shown in Table 21, PWP was measured more accurately in all models except Model 4. Model 3 was the most accurate at predicting FC and PWP, with Model 4 the worst. Despite PWP being more accurate in general across the models, FC had a lower bias in all models, with the lowest bias occurring in Model 2. The very low bias, and very good prediction accuracy of Model 2 indicates that it is the best model for predicting FC and PWP. As such Model 2 is selected for further detailed investigation and interpretation in developing DSM of FC and PWP.

Table 21 root mean square error and mean error validation for each of the Multiple Linear Regression models developed

Model		RMSE	ME
1	FC	0.040	0.0026
	PWP	0.032	0.0035
2	FC	0.037	0.0000
	PWP	0.031	0.0004
3	FC	0.029	0.0027
	PWP	0.024	0.0028
4	FC	0.035	0.0030
	PWP	0.045	0.0031

3.6. Spatial Distribution of Available Water Content

Digital Soil Maps were produced for FC, PWP, and AWC across the Warren and Trangie study areas. Each image was produced by applying Model 2 to a grid of interpolated 100m spaced values of predicted EM and gamma spectrometry data. Fig. 13 shows the spatial variation of FC across (a) Warren and (b) Trangie. Although only 47% of the variation is explained, there are readily identifiable soil types and pedoderms apparent across each study area. In Warren (Fig. 13a), the Contemporary Macquarie and Trangie Cowal pedoderms are characterised by low-very low FC (0.200-0.250 cm^3/cm^3), whilst the Macquarie Alluvium is characterised by intermediate-very high FC (> 0.250 cm^3/cm^3). In the Trangie study area: the Gin Gin Hills are defined by intermediate low- intermediate-high FC (0.225-0.300 cm^3/cm^3); the Old Alluvium Backplain is characterised by high-very high FC (>0.275 cm^3/cm^3); the Old Alluvium Meander Plain by low-intermediate (0.225-0.275 cm^3/cm^3); and the Contemporary Macquarie and Trangie Cowal by low-very low FC (< 0.250 cm^3/cm^3).

Fig. 14 shows the spatial distribution of PWP across Warren (Fig. 14a) and Trangie (Fig. 14b). Although only 55% of the variation is explained, there various soil types and pedoderms are visible. In Warren, the Contemporary Macquarie and Trangie Cowal are characterised by low-intermediate PWP (0.125-0.175 cm^3/cm^3), and the Macquarie Alluvium by intermediate-high PWP (0.150-0.200 cm^3/cm^3). In Trangie, the Gin Gin Hills are characterised by intermediate-high PWP (0.150-0.200 cm^3/cm^3), Old Alluvium Backplain is characterised by high-very high PWP (> 0.175 cm^3/cm^3), the Old Alluvium Meander Plain is characterised by intermediate PWP (0.150-0.175 cm^3/cm^3),

and the Contemporary Macquarie and Trangie Cowal by low-intermediate PWP (0.125-0.175 cm^3/cm^3).

Fig. 15 shows the spatial distribution of the AWC across Warren (Fig. 15a) and Trangie (Fig. 15b). The AWC was calculated using the difference between FC and PWP given by Model 2. The small range in values of AWC means it is harder to observe patterns, however there are some relationships with McKenzie's spatial distribution of pedoderms in Fig. 2. In Warren, the Contemporary Macquarie and Trangie Cowal are characterised as intermediate-low AWC (0.080-0.090 cm^3/cm^3), whilst the Macquarie Alluvium is characterised by high-very high AWC (>0.090 cm^3/cm^3). In Trangie, the Gin Gin Hills are characterised by low-high AWC (0.080-0.095 cm^3/cm^3), the Old Alluvium Backplain is characterised by intermediate-high AWC (0.085-0.095 cm^3/cm^3). The Old Alluvium Meander Plain, Trangie Cowal Alluvial Plain, and Contemporary Macquarie are characterised by intermediate-very low AWC (<0.090 cm^3/cm^3).

The Old Alluvium Meander Plain is described as being one of the oldest soils occurring across the study area (McKenzie 1992). In association with this is a sandy soil with some clay at depth (Table 1), in particular kaolin dominant with illite sub-dominant. The intermediate K (<1.00 %) and low eU (<1.75 ppm) in Figs. 7 and 8 respectively give an indication of the age of the soil through extensive weathering and lack of silt sized particles, and an indication of the kaolin clay mineral which has low K. The high eTh (6.50-7.00 ppm) in Fig. 9 is indicative of a sandy soil through Th associating with iron oxides which adhere to sand particles. The low EC_a (< 100 mS/m) in Figs 10-12 also indicates a sandy soil which has little active clay. The FC (0.225-0.275 cm^3/cm^3) and PWP (0.150-0.175 cm^3/cm^3) estimated by Model 2 are consistent with the values for this

study in Table 10 for FC (0.25 cm^3/cm^3) and PWP (0.15 cm^3/cm^3). However the values for FC (0.12 cm^3/cm^3) and PWP (0.17 cm^3/cm^3) calculated by McKenzie are lower than those indicated in the model. Despite this, the values indicate that this soil is loamy sand to sandy loam in texture which is consistent with McKenzie's (1992) initial particle analysis in Table 1.

The Old Alluvium Backplain is described as being a similarly old soil like the Meander Plain, but characterised as being a clayey soil with a sand component, and low silt (Table 1). The clay mineralogy with this soil is smectite dominant with kaolin and illite a minor component. The low gamma spectrometry values across all three spectra in Figs. 7-9 indicate a high degree of weathering through lack of silt sized particles. The intermediate-high EC_a (> 100 mS/m) in Figs 10-12 is indicative of the high activity smectite clay at depth. The FC (>0.275 cm^3/cm^3) and PWP (> 0.175 cm^3/cm^3) estimated by Model 2 is consistent with the values from this study, and McKenzie's (1992) survey Table 10, indicating a silty loam textured soil (Table 4).

The Gin Gin Hills is described as being an old, sandy soil, with a low silt component, and low activity kaolin clay at depth (Table 3). The low gamma spectrometer values in Figs. 8 and 9 indicate a large degree of weathering, and lack of K in Fig. 7 is consistent with the low silt component. Low EC_a (< 100 mS/m) is consistent with kaolin being a relatively unconductive clay mineral. The FC (0.225-0.300 cm^3/cm^3) and PWP (0.150-0.200 cm^3/cm^3) estimated by Model 2 are not very consistent with the values in Table 10, this is most likely the result of only 3 soil samples being collected in this study from the pedoderm.

The Macquarie Alluvium is a fairly recent soil unit, characterised by being a clayey soil with a large silt component (Table 2). It is a similar soil to the Old Alluvium Backplain, however the clays present here are a more active smectite. The intermediate-high K (> 0.75 %), eU (> 1.75 ppm), and eTh (> 7.00 ppm) is consistent with the high silt component and lack of weathering. The intermediate-high EC_a (100-200 mS/m) in Figs. 10-12 is characteristic of a silty clay to clay soil with smectite clay at depth. The high FC (> 0.250 cm^3/cm^3) and PWP (0.150-0.200 cm^3/cm^3) indicated by Model 2 is consistent with the values in Table 9 from both studies, indicating it is a silt-silt loam texture and good for irrigated agriculture, as shown in Fig. 3a.

The Trangie Cowal Alluvial Plain is a recent soil unit characterised by a silt loam texture. It has a high silt component and low hue which indicates a young age (Table 1) as identified earlier, there are two components of the Alluvial Plain identifiable, one occurring along the length of the Cowal, the other to the north of the Cowal in the Trangie study area. The unit occurring along the Cowal is characterised by high K (>1.25 %), eU (>2.00 ppm), and eTh (>7.00 ppm), and low EC_a (<100 mS/m) indicating the high silt component and young age. The low FC (<0.250 cm^3/cm^3) and PWP (<0.150 cm^3/cm^3) indicated by Model 2 is consistent with the values in Tables 9 and 10 and indicate a silt loam texture (Table 4). The area to the north of this first unit is characterised by intermediate K (0.75-1.25 %), eU (1.50-2.00 ppm), eTh (6.00-7.00 ppm), and intermediate EC_a (100-200 mS/m). Model 2 characterises this unit as high FC (> 0.250 cm^3/cm^3) and PWP (0.150-0.200 cm^3/cm^3) which are higher than the values in Tables 9 and 10, but are still characteristic of a silt loam texture.

The Contemporary Macquarie pedoderm as defined in Fig. 2a extends to the Macquarie River, which is the extent of McKenzie's characterisation of the pedoderms. The study area as shown in Fig. 4a extends past the Macquarie River and to Ewenmar Creek along the northern border, with the EM and gamma spectrometer data indicating the Contemporary Macquarie occurs on both sides of the River, and extending to Ewenmar Creek. The known extent of Contemporary Macquarie is characterised by very high K (>1.25 %), eU (> 2.25 ppm) and low EC_a (< 100 mS/m). The very high K and eU are consistent with McKenzie's (1992) description of the Contemporary Macquarie being young with a silty texture (Table 2). Given the very high K counts it is likely the silt sized soil fraction is dominated by K rich secondary minerals such as micas. Model 2 characterises this unit as low FC (0.225-0.250 cm^3/cm^3) and low PWP (1.125-1.150 cm^3/cm^3) which is consistent with Table 9. The unclassified soil to the north of the River is characterised by very high K (>1.25 %) and low EC_a (< 100 mS/m) along Ewenmar Creek, and intermediate K (0.75-1.25 %) with intermediate EC_a (100-200 mS/m) between Ewenmar Creek and the Macquarie River. The soil along Ewenmar Creek is characterised by low FC (0.225-0.250 cm^3/cm^3) and low PWP (1.125-1.150 cm^3/cm^3) which is consistent with the known Contemporary Macquarie. The soil between the two water courses is characterised by high FC (0.250-0.275 cm^3/cm^3) and high PWP (0.150-0.175 cm^3/cm^3) which is similar to the Macquarie Alluvium Backplain.

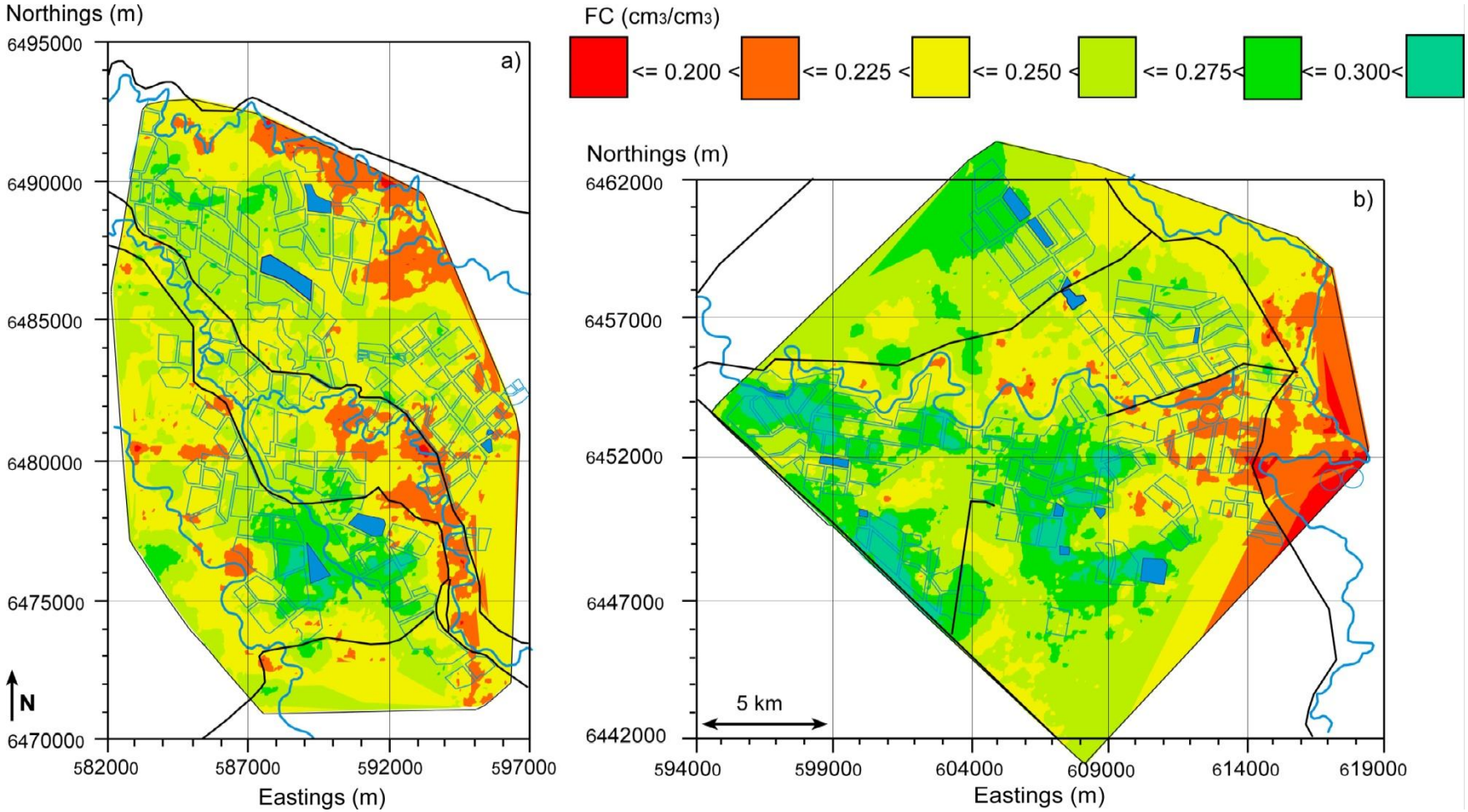

Fig. 13. The spatial variation of Field Capacity (cm^3/cm^3) across a) Warren and b) Trangie study areas as modelled by Model 2, based on average Field Capacity from 0-0.9m

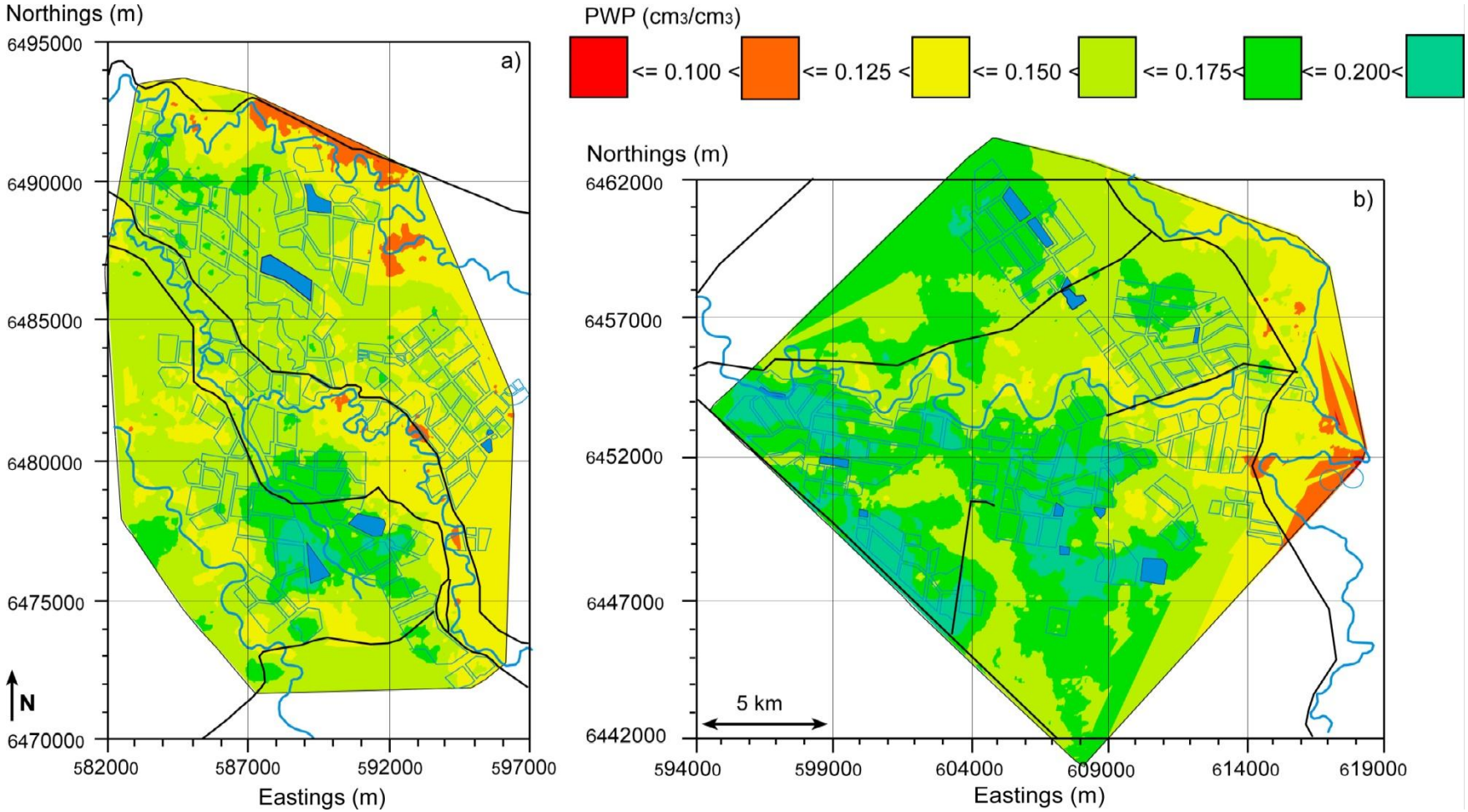

Fig. 14. The spatial variation of Permanent Wilting Point (cm^3/cm^3) across a) Warren and b) Trangie study areas as modelled by Model 2, based on average Permanent Wilting Point from 0-0.9m

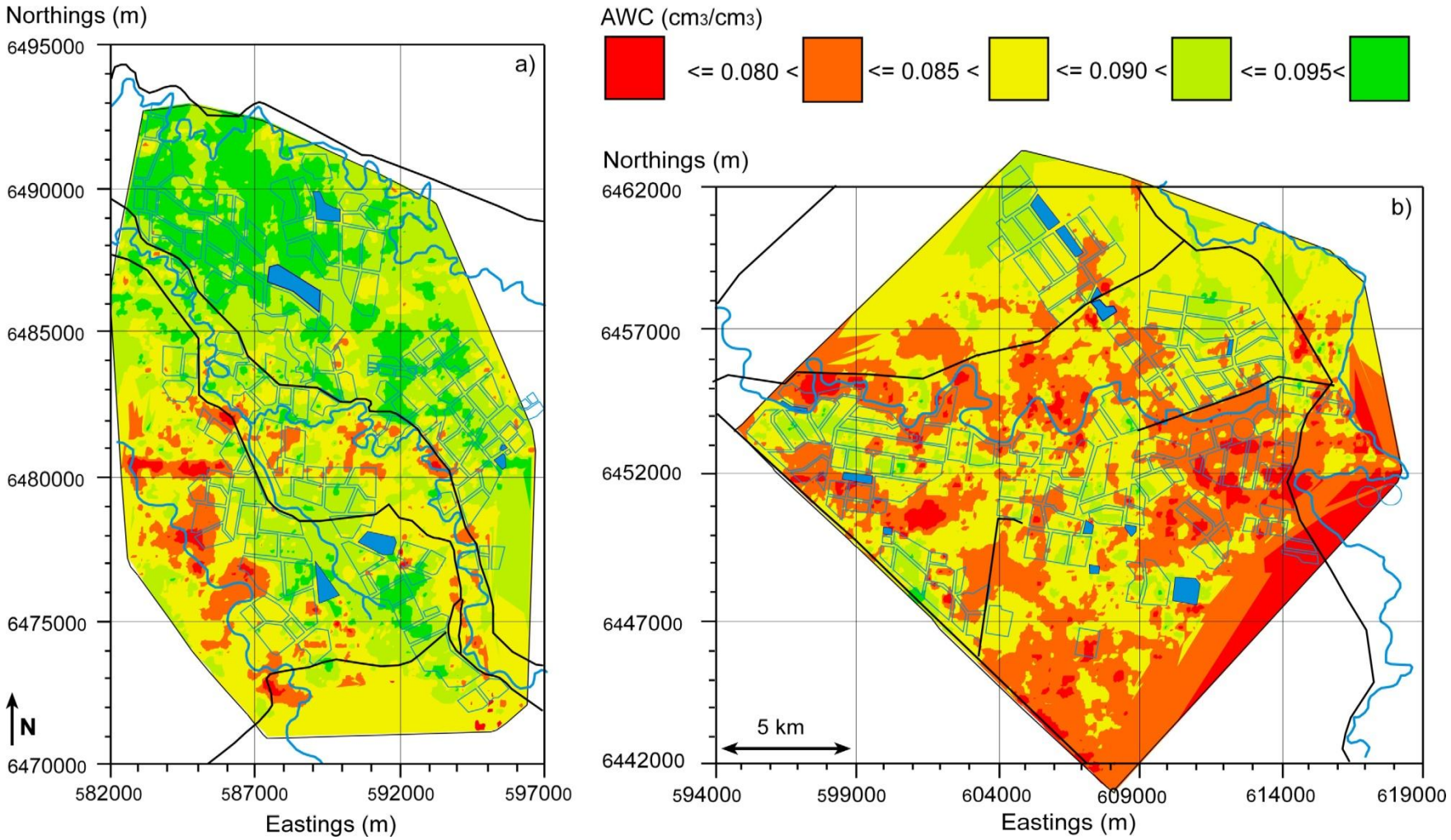

Fig. 15. The spatial variation of Available Water Content (cm^3/cm^3) across a) Warren and b) Trangie study areas as calculated from the difference between the Field Capacity and Permanent Wilting Point as modelled by Model 2.

4. Discussion

In comparison with Fig. 2, Figs. 13 and 14 can be seen to complement the existing soil map of the area. This is the result of being able to distinguish the soil morphological properties of clay content, and soil mineralogy from EC_a and gamma spectrometry data as they relate to FC and PWP. In addition to this the age and degree of weathering of each pedoderm can be distinguished from the ancillary data. Taking into account the survey methods used in the existing soil map, ancillary data can improve the definition of soil boundaries based on a texture definition of the soil unit. The maps produced by Model 2 add further value to the existing soil map by distinguishing between two components of the Trangie Cowal Alluvial Plain not determined using conventional soil mapping methods, and by extending the soil map in the Warren study area.

Previous studies have distinguished the relationships between soil properties, ancillary data and θ (Allred et al., 2006, Robinson et al., 2009), or mapped the variation in θ across seasons (Besson et al., 2010, Reedy and Scanlon, 2003). DSM of the AWC has been minimal within the literature (Curtis and Claassen, 2008, McBratney et al., 2003, Thompson et al., 2007), and non-existent at the district scale. By showing that a MLR model of FC and PWP complements the existing soil map of the district, further EM data needs to be collected to link the two study areas. By creating a MLR using representative, laboratory determined FC and PWP of the soils present, all that is required to extend the maps to a larger district scale is additional EM survey data. In addition, and where appropriate, more detailed EM and gamma radiometric data can be collected at the field level to further improve water use efficiency.

The implications of this work are already evident in observing the distribution of irrigated fields in relation to AWC (Fig. 15). In the areas of low AWC along the Trangie Cowal, the fields are small and predominantly developed for pivot irrigation. This is in contrast to the irrigated fields occurring on the northern parts of the Trangie Cowal Alluvial Plain and Old Alluvium Backplain in Trangie, and on the Macquarie Alluvium in Warren In the locations, the irrigated fields are much larger as they can sustain furrow irrigation. By identifying the areas which have the highest AWC, it allows irrigators to irrigate more efficiently. This can be achieved through choosing the right irrigation nfrastructure, as well as knowing the exact amount of water to apply through irrigation to minimise loss to deep drainage and runoff.

The spatial variation of FC and PWP explained by Model 2 (47% and 55% respectively) indicates that there are some improvements that can be made to the model. One aspect of the methods which is thought to have an impact on the FC and PWP θ values used in the regression is the value of ρ used to create θ from w**.** The value used in this study was derived from McKenzie's calculated average per pedoderm. As it has been established that the boundaries of the pedoderms in Fig. 2 are not definitive, further models would benefit from using individually calculated ρ for each soil sample rather than an average. Other forms of ancillary data which may enhance the predictions in the future could include spectral brightness and/or spectral reflectance. Spectral brightness has been shown to relate to soil texture and organic matter, which both influence the water holding capacity of the topsoil (Triantafilis et al., 2009b, Wuthrich, 1996). Spectral reflectance has been shown to be applicable to measuring surface θ and soil mineralogy (Haubrock et al., 2008, Rossel et al., 2006).

5. Conclusions

The aims of this study were to develop a digital soil map (DSM) of the available soil water content (AWC) across the two predominantly irrigated cotton growing areas of Trangie and Warren in the lower Macquarie valley. To achieve this EC_a data collected with an EM38-v and EM34-10 instruments, gamma spectrometry data of eTh and eU and two trend surface vectors were most suitable to predict FC and PWP. The ECa data appeared to relate FC and PWP to clay content and soil texture, whilst the gamma spectrometry data related to soil mineralogy. The trend surface parameters added information relevant to the distance from the Macquarie River and related somewhat to the age (i.e. degree of weathering) of the sediments.

The resultant DSM showed that the spatial distribution of AWC was consistent with the spatial distribution of soil texture. In particular, that the Old Alluvium Meander Plain which is a sandy soil holds the least water (0.085 cm^3/cm^3). The Old Alluvium Backplain which is a clayier soil holds a large amount of water (0.090 cm^3/cm^3), but it is the silty textured soil which characterizes the Trangie Cowal Alluvial Plain and Macquarie Alluvium which holds the most water (0.095 cm^3/cm^3). The DSM also showed it was possible to improve the existing soil boundaries identified using traditional mapping methods, as well as extend them to unmapped soils.

In terms of the MLR models developed, and despite the intermediate strength of the relationships, the DSM produced using a Hierarchical Spatial Regression (HSR) models is consistent with the irrigation infrastructure. This is most clearly discerned in the area adjacent to the Trangie Cowal and associated with the Trangie Cowal Pedoderm in both study areas. For the most, the Trangie Cowal in the Warren area has

not been overly developed owing to the low water holding capacity of the silty loam textured soil. In the Trangie area, irrigation development has been restricted to pivot irrigation systems (south of the Cowal) and irrigation fields of shorter length north of the Cowal). Interestingly, it is apparent from the DSM that the northern part of the area identified by McKenzie (1992) as being part of the Trangie Cowal pedoderm is perhaps incorrect. This is because of the significantly larger water holding capacity of the soil (). This is consistent with the larger fields which have been developed in this area and which have longer irrigation runs. It would appear that the soil here, on either side of the Weemabah Rd, is more consistent with the AWC of the Old Alluvium Back Plain where the water holding capacity is large. However, the area with the highest water holding capacity occurs in the area southeast of Warren.

The approach developed herein could be applied to other irrigated areas where competition for water is growing. This includes the Hunter valley where irrigation for grape and wine production is competing with coal mining and environmental flow issues. This is similarly the case in other cotton growing areas such as the lower Namoi valley, particularly in the Breeze Plains.

6. References

ABS (Australian Bureau of Statistics). 2008. *Water and the Murray-Darling Basin: A Statistical Profile 2000-01 to 2005-06*, cat. no. 4610.0.55.070, ABS, Canberra.

ACWORTH, R. I., YOUNG, R. R. & BERNADI, A. L. 2005. Monitoring soil moisture status in a Black Vertosol on the Liverpool Plains, NSW, using a combination of neutron scattering and electrical image methods. *Australian Journal of Soil Research,* 43**,** 105-117.

AL-AIN, F., ATTAR, J., HUSSEIN, F. & HENG, L. K. 2009. Comparison of nuclear and capacitance-based soil water measuring techniques in salt-affected soils. *Soil Use and Management,* 25**,** 362-367.

ALLRED, B. J., EHSANI, M. R. & SARASWAT, D. 2006. Comparison of electromagnetic induction, capacitively-coupled resistivity, and galvanic contact resistivity methods for soil electrical conductivity measurement. *Applied Engineering in Agriculture,* 22**,** 215-230.

BEHRENS, T., FORSTER, H., SCHOLTEN, T., STEINRUCKEN, U., SPIES, E. D. & GOLDSCHMITT, M. 2005. Digital soil mapping using artificial neural networks. *Journal of Plant Nutrition and Soil Science-Zeitschrift Fur Pflanzenernahrung Und Bodenkunde,* 168**,** 21-33.

BESSON, A., COUSIN, I., BOURENNANE, H., NICOULLAUD, B., PASQUIER, C., RICHARD, G., DORIGNY, A. & KING, D. 2010. The spatial and temporal organization of soil water at the field scale as described by electrical resistivity measurements. *European Journal of Soil Science,* 61**,** 120-132.

BETHUNE, M. 2004. Towards effective control of deep drainage under border-check irrigated pasture in the Murray-Darling Basin: a review. *Australian Journal of Agricultural Research,* 55**,** 485-494.

BIDDISCOMBE, E. F. 1963. A Vegetation Survey in the Macquarie Region, New South Wales.: CSIRO Division of Plantt Industry Tech. Paper No. 18.

BIERWORTH, P. 1996. Investigation of Airborne Gamma-Ray Images as a Rapid Mapping Tool for Soil and Water Degradation. Australian Geological Survey Organisation.

BREWER, R., CROOK, K. A. W. & SPEIGHT, J. G. 1970. Proposal for Soil-Stratigraphic units in the Australian Stratigraphic code. *Australian Journal of Earth Sciences,* 17**,** 103-111.

CHANG, D. H. & ISLAM, S. 2000. Estimation of soil physical properties using remote sensing and artificial neural network. *Remote Sensing of Environment,* 74**,** 534-544.

CHANZY, A., CHADOEUF, J., GAUDU, J. C., MOHRATH, D., RICHARD, G. & BRUCKLER, L. 1998. Soil moisture monitoring at the field scale using automatic capacitance probes. *European Journal of Soil Science,* 49**,** 637-648.

CHARMAN, P. E. V. & MURPHY, B. W. (eds.) 2003. *Soils: Their Properties and Management*: Oxford University Press.

COCKX, L., VAN MEIRVENNE, M., VITHARANA, U. W. A., VERBEKE, L. P. C., SIMPSON, D., SAEY, T. & VAN COILLIE, F. M. B. 2009. Extracting Topsoil Information from EM38DD Sensor Data using a Neural Network Approach. *Soil Sci Soc Am J,* 73**,** 2051-2058.

CONTADOR, J. F. L., MANETA, M. & SCHNABEL, S. 2006. Prediction of near-surface soil moisture at large scale by digital terrain modeling and neural networks. *Environmental Monitoring and Assessment,* 121**,** 213-232.

COOK, S. E., CORNER, R. J., GROVES, P. R. & GREALISH, G. J. 1996. Use of airborne gamma radiometric data for soil mapping. *Australian Journal of Soil Research,* 34**,** 183-194.

COVENTRY, R. J. & FETT, D. E. R. 1979. *A pipette and sieve method of particle size analysis and some observations on its efficacy*, CSIRO Australia Division of Soils, Divisional Report, No. 38. CSIRO, Australia.

CRESSWELL, H. P., GREEN, T. & MCKENZIE, N. J. 2008. The adequacy of pressure plate apparatus for determining soil water retention. *Soil Science Society of America Journal,* 72**,** 41-49.

CURTIS, M. J. & CLAASSEN, V. P. 2008. An Alternative Method for Measuring Plant Available Water in Inorganic Amendments. *Crop Science,* 48**,** 2447-2452.

DA SILVA, A. P., NADLER, A. & KAY, B. D. 2001. Factors contributing to temporal stability in spatial patterns of water content in the tillage zone. *Soil and Tillage Research,* 58**,** 207-218.

DICKSON, B. L. & SCOTT, K. M. 1997. Interpretation of aerial gamma-ray surveys - adding the geochemical factors. *AGSO Journal of Australian Geology & Geophysics,* 17**,** 187-200.

DOMSCH, H. & GIEBEL, A. 2004. Estimation of Soil Textural Features from Soil Electrical Conductivity Recorded Using the EM38. *Precision Agriculture,* 5**,** 389-409.

FOTH, H. D. 1990. *Fundamentals of Soil Science. 8E*, John Wiley & Sons.

FRIEDMAN, S. P. 2005. Soil properties influencing apparent electrical conductivity: a review. *Computers and Electronics in Agriculture,* 46**,** 45-70.

GAHEGAN, M. 2003. Is inductive machine learning just another wild goose (or might it lay the golden egg)? *International Journal of Geographical Information Science,* 17**,** 69 - 92.

GAWNE, B., CRASE, L. & WATSON, A. S. 2010. Can a collaborative focus on solutions improve our capacity to achieve sustainable water management? *Marine and Freshwater Research,* 61**,** 814-820.

GEBBERS, R., LUCK, E., DABAS, M. & DOMSCH, H. 2009. Comparison of instruments for geoelectrical soil mapping at the field scale. *Near Surface Geophysics,* 7**,** 179-190.

GRASTY, R. L. 1997. Radon emanation and soil moisture effects on airborne gamma-ray measurements. *Geophysics,* 62**,** 1379-1385.

GREEN, S. R., KIRKHAM, M. B. & CLOTHIER, B. E. 2006. Root uptake and transpiration: From measurements and models to sustainable irrigation. *Agricultural Water Management,* 86**,** 165-176.

HAUBROCK, S. N., CHABRILLAT, S., KUHNERT, M., HOSTERT, P. & KAUFMANN, H. 2008. Surface soil moisture quantification and validation based on hyperspectral data and field measurements. *Journal of Applied Remote Sensing,* 2.

HEDLEY, C. B. & YULE, I. J. 2009. A method for spatial prediction of daily soil water status for precise irrigation scheduling. *Agricultural Water Management,* 96**,** 1737-1745.

HEDLEY, C. B., YULE, I. Y., EASTWOOD, C. R., SHEPHERD, T. G. & ARNOLD, G. 2004. Rapid identification of soil textural and management zones using electromagnetic induction sensing of soils. *Australian Journal of Soil Research,* 42**,** 389-400.

HEZARJARIBI, A. & SOURELL, H. 2007. Feasibility study of monitoring the total available water content using non-invasive electromagnetic induction-based and electrode-based soil electrical conductivity measurements. *Irrigation and Drainage,* 56**,** 53-65.

HULUGALLE, N. R., WEAVER, T. B. & FINLAY, L. A. 2010. Soil water storage and drainage under cotton-based cropping systems in a furrow-irrigated Vertisol. *Agricultural Water Management,* 97**,** 1703-U3.

JIANG, H. L. & COTTON, W. R. 2004. Soil moisture estimation using an artificial neural network: a feasibility study. *Canadian Journal of Remote Sensing,* 30**,** 827-839.

JONES, D. P. & GRAHAM, R. C. 1993. WATER-HOLDING CHARACTERISTICS OF WEATHERED GRANITIC ROCK IN CHAPARRAL AND FOREST ECOSYSTEMS. *Soil Science Society of America Journal,* 57**,** 256-261.

KACHANOSKI, R. G., GREGORICH, E. G. & VANWESENBEECK, I. J. 1988. ESTIMATING SPATIAL VARIATIONS OF SOIL-WATER CONTENT USING NONCONTACTING ELECTROMAGNETIC INDUCTIVE METHODS. *Canadian Journal of Soil Science,* 68**,** 715-722.

KIM, Y., EVANS, R. G. & IVERSEN, W. M. 2008. Remote sensing and control of an irrigation system using a distributed wireless sensor network. *Ieee Transactions on Instrumentation and Measurement,* 57**,** 1379-1387.

KOTHAVALA, Z. 1999. The duration and severity of drought over eastern Australia simulated by a coupled ocean-atmosphere GCM with a transient increase in CO2. *Environmental Modelling & Software,* 14**,** 243-252.

KUHN, J., BRENNING, A., WEHRHAN, M., KOSZINSKI, S. & SOMMER, M. 2009. Interpretation of electrical conductivity patterns by soil properties and geological maps for precision agriculture. *Precision Agriculture,* 10**,** 490-507.

LAFFAN, S. W. & LEES, B. G. 2004. Predicting regolith properties using environmental correlation: a comparison of spatially global and spatially local approaches. *Geoderma,* 120**,** 241-258.

LEONG, E. C., HE, L. & RAHARDJO, H. 2002. Factors affecting the filter paper method for total and matric suction measurements. *Geotechnical Testing Journal,* 25**,** 322-333.

LESHER, C. M., BURNHAM, O. M., KEAYS, R. R., BARNES, S. J. & HULBERT, L. 2001. Trace-element geochemistry and petrogenesis of barren and ore-associated komatiites. *Canadian Mineralogist,* 39**,** 673-696.

LIU, W. D., BARET, F., GU, X. F., TONG, Q. X., ZHENG, L. F. & ZHANG, B. 2002. Relating soil surface moisture to reflectance. *Remote Sensing of Environment,* 81**,** 238-246.

LU, S., REN, T., GONG, Y. & HORTON, R. 2008. Evaluation of Three Models that Describe Soil Water Retention Curves from Saturation to Oven Dryness. *Soil Science Society of America Journal,* 72**,** 1542-1546.

MCBRATNEY, A. B., SANTOS, M. L. M. & MINASNY, B. 2003. On digital soil mapping. *Geoderma,* 117**,** 3-52.

MCCUTCHEON, M. C., FARAHANI, H. J., STEDNICK, J. D., BUCHLEITER, G. W. & GREEN, T. R. 2006. Effect of soil water on apparent soil electrical conductivity and texture relationships in a dryland field. *Biosystems Engineering,* 94**,** 19-32.

MCKENZIE, N. J. 1992. *Soils of the Lower Macquarie Valley, New South Wales*, CSIRO Division of Soils, Divisional Report No 117, Canberra, Australia.

MCNEILL, J. D. 1980a. Electrical Conductivity of Soils and Rocks. *Technical Note TN-5.* Geonics Ltd: Mississauga, ON, Canada.

MCNEILL, J. D. 1980b. Electromagnetic terrain conductivity measurement at low induction numbers. *Technical Note TN-6.* Geonics Ltd, Mississauga ON, Canada.

MCNEILL, J. D. 1990. Geonics EM38 Ground Conductivity Meter: EM38 Operating Manual. Geonics Ltd: Mississuaga, ON, Canada.

MERTENS, F. M., PAETZOLD, S. & WELP, G. 2008. Spatial heterogeneity of soil properties and its mapping with apparent electrical conductivity. *Journal of Plant Nutrition and Soil Science-Zeitschrift Fur Pflanzenernahrung Und Bodenkunde,* 171**,** 146-154.

MINASNY, B., MCBRATNEY, A. B. & WHELAN, B. M. 2005. VESPER version 1.62. *Australian Centre for Precision Agriculture, The University of Sydney*.

MINTY, B. R. S. 1997. Fundamentals of airborne gamma-ray spectrometry. *AGSO Journal of Australian Geology & Geophysics,* 17**,** 39-50.

NAM, S., GUTIERREZ, M., DIPLAS, P., PETRIE, J., WAYLLACE, A., LU, N. & MUNOZ, J. J. 2010. Comparison of testing techniques and models for establishing the SWCC of riverbank soils. *Engineering Geology,* 110**,** 1-10.

NELSON, M. A. & ODEH, I. O. A. 2009. Digital soil class mapping using legacy soil pro. le data: a comparison of a genetic algorithm and classification tree approach. *Australian Journal of Soil Research,* 47**,** 632-649.

NSW Government. 2010. $2 billion expansion of the Cadia Valley gold and copper mining complex. <http://www.nsw.gov.au/projects/2-billion-expansion-cadia-valley-gold-and-copper-mining-complex>

NSW Department of Primary Industries. (2005) New Mines and Projects in NSW – Coal. <http://www.dpi.nsw.gov.au/minerals/resources/coal/new-mines-and-projects>

ODEH, I. O. A. & MCBRATNEY, A. B. 2000. Using AVHRR images for spatial prediction of clay content in the lower Namoi Valley of eastern Australia. *Geoderma,* 97**,** 237-254.

PAIGE, G. B. & KEEFER, T. O. 2008. Comparison of field performance of multiple soil moisture sensors in a semi-arid rangeland. *Journal of the American Water Resources Association,* 44**,** 121-135.

PEVERILL, K. I., SPARROW, L. A. & REUTER, D. J. (eds.) 1999. *Soil Analysis: an interpretation manual*: CSIRO publishing.

REEDY, R. C. & SCANLON, B. R. 2003. Soil water content monitoring using electromagnetic induction. *Journal of Geotechnical and Geoenvironmental Engineering,* 129**,** 1028-1039.

ROBINSON, D. A., JONES, S. B., WRAITH, J. M., OR, D. & FRIEDMAN, S. P. 2003. A Review of Advances in Dielectric and Electrical Conductivity Measurement in Soils Using Time Domain Reflectometry. *Vadose Zone Journal,* 2**,** 444-475.

ROBINSON, N. J., RAMPANT, P. C., CALLINAN, A. P. L., RAB, M. A. & FISHER, P. D. 2009. Advances in precision agriculture in south-eastern Australia. II. Spatio-

temporal prediction of crop yield using terrain derivatives and proximally sensed data. *Crop & Pasture Science,* 60**,** 859-869.

ROSSEL, R. A. V., WALVOORT, D. J. J., MCBRATNEY, A. B., JANIK, L. J. & SKJEMSTAD, J. O. 2006. Visible, near infrared, mid infrared or combined diffuse reflectance spectroscopy for simultaneous assessment of various soil properties. *Geoderma,* 131**,** 59-75.

ROYLE, J. A. & BERLINER, L. M. 1999. A hierarchical approach to multivariate spatial modeling and prediction. *Journal of Agricultural Biological and Environmental Statistics,* 4**,** 29-56.

SANKARANARAYANAN, K., PRAHARAJ, C. S., NALAYINI, P., BANDYOPADHYAY, K. K. & GOPALAKRISHNAN, N. 2010. Climate change and its impact on cotton (Gossypium sp.). *Indian Journal of Agricultural Sciences,* 80**,** 561-575.

SCHMUGGE, T. J., JACKSON, T. J. & MCKIM, H. L. 1980. SURVEY OF METHODS FOR SOIL-MOISTURE DETERMINATION. *Water Resources Research,* 16**,** 961-979.

SHEETS, K. R. & HENDRICKX, J. M. H. 1995. NONINVASIVE SOIL-WATER CONTENT MEASUREMENT USING ELECTROMAGNETIC INDUCTION. *Water Resources Research,* 31**,** 2401-2409.

SHERWIN, L. 1996. *Narromine 1:250 000 Geological Sheet*. Geological Survey of New South Wales; Department of Mineral Resources.

STAFFORD, J. V. 1988. REMOTE, NON-CONTACT AND INSITU MEASUREMENT OF SOIL-MOISTURE CONTENT - A REVIEW. *Journal of Agricultural Engineering Research,* 41**,** 151-172.

SUDDUTH, K. A., KITCHEN, N. R., WIEBOLD, W. J., BATCHELOR, W. D., BOLLERO, G. A., BULLOCK, D. G., CLAY, D. E., PALM, H. L., PIERCE, F. J., SCHULER, R. T. & THELEN, K. D. 2005. Relating apparent electrical conductivity to soil properties across the north-central USA. *Computers and Electronics in Agriculture,* 46**,** 263-283.

THOMPSON, R. B., GALLARDO, M., VALDEZ, L. C. & FERNÁNDEZ, M. D. 2007. Determination of lower limits for irrigation management using in situ assessments of apparent crop water uptake made with volumetric soil water content sensors. *Agricultural Water Management,* 92**,** 13-28.

TOPP, G. C. & DAVIS, J. L. 1985. MEASUREMENT OF SOIL-WATER CONTENT USING TIME-DOMAIN REFLECTROMETRY (TDR) - A FIELD-EVALUATION. *Soil Science Society of America Journal,* 49**,** 19-24.

TRIANTAFILIS, J. & LESCH, S. M. 2005. Mapping clay content variation using electromagnetic induction techniques. *Computers and Electronics in Agriculture,* 46**,** 203-237.

TRIANTAFILIS, J., LESCH, S. M., LA LAU, K. & BUCHANAN, S. M. 2009. Field level digital soil mapping of cation exchange capacity using electromagnetic induction and a hierarchical spatial regression model. *Australian Journal of Soil Research,* 47**,** 651-663.

TRIANTAFILIS, J., ODEH, I. O. A., JARMAN, A. L., SHORT, M. G. & KOKKORIS, E. 2004. Estimating and mapping deep drainage risk at the district level in the lower Gwydir and Macquarie valleys, Australia. *Australian Journal of Experimental Agriculture,* 44**,** 893-912.

TUCKER, B. M. 1974. *Laboratory procedure for cation exchange measurements in soils*, CSIRO Division of Soils, Technical Paper No. 23, CSIRO, Australia.
VOLTZ, M. & WEBSTER, R. 1990. A COMPARISON OF KRIGING, CUBIC-SPLINES AND CLASSIFICATION FOR PREDICTING SOIL PROPERTIES FROM SAMPLE INFORMATION. *Journal of Soil Science,* 41**,** 473-490.
WATKINS, J. J. & MEAKIN, N. S. 1996. *Nyngan 1:250 000 Geological Sheet*. Geological Survey of New South Wales; Department of Mineral Resources.
WESSOLEK, G., PLAGGE, R., LEIJ, F. J. & VAN GENUCHTEN, M. T. 1994. Analysing problems in describing field and laboratory measured soil hydraulic properties. *Geoderma,* 64**,** 93-110.
WIATRAK, P., KHALILIAN, A., MUELLER, J. & HENDERSON, W. 2009. Applications of Soil Electrical Conductivity in Production Agriculture. *Better Crops,* 93**,** 16-17.
WRAITH, J. M. & OR, D. 2001. Soil water characteristic determination from concurrent water content measurements in reference porous media. *Soil Science Society of America Journal,* 65**,** 1659-1666.
WUTHRICH, M. 1996. Thermal infra-red underflights compared to ERS-1 C-band synthetic aperture radar focusing soil moisture distribution. *Theoretical and Applied Climatology,* 53**,** 69-78.

APPENDIX A – Detailed Laboratory Method

Samples were analysed by depth layer for each study area using a pressure plate apparatus. A 15 bar pressure chamber with two 15 bar ceramic plates were used to determine the PWP in conjunction with a 5 bar pressure chamber and 5 bar pressure plates to determine the FC. A compressed air system manifold was used to regulate air flow to each chamber. A positive air pressure of 15 bars was applied to the 15 bar pressure chamber to simulate the soil matric suction of -1500 J/kg at PWP, and 1 bar of pressure was applied to the 5 bar pressure chamber to simulate the soil matric suction of -100 J/kg at FC.

Each ceramic plate was allowed to soak overnight it regular tap water to ensure all the pores were filled. Soil samples were then placed onto each plate within the 5cm rubber rings so that 12 samples were on one plate. Identical samples were placed in each chamber to ensure ease of later calculating the AWC. The samples on the plates were then indirectly wet by pouring ~200 mL of regular tap water onto each plate. The samples were then left to soak overnight to ensure complete wetting and good contact with the plate.

Excess water was removed from the surface of each plate by a Millipore pump and the lids of the pressure chambers secured. Compressed air was gradually introduced into the manifold system and then into the 15 bar pressure chamber until 15 bars of pressure was reached, upon completion of this, the pressure was gradually increased in the 5 bar pressure chamber until 1 bar of pressure was achieved. The output of water was measured by a burette connected to each pressure chamber. Once

the equilibrium was reached for each chamber, the burettes were disconnected and the pressurized air gradually released from the chambers. Equilibrium was judged to be no noticeable output of water for a period of three or more hours.

Samples were removed individually from the plates and placed into a weighed aluminium soil tin. The samples were then weighed again so the wet mass could be established and placed into a drying oven overnight to dry. Once the samples were dry, they were weighed again to determine the dry mass of the soil. The water lost from each sample was then calculated as the difference between the wet sample and the oven dry sample. The gravimetric soil moisture content was then calculated as:

$$\text{gravimetric moisture } (\text{g/g}) = \frac{\text{water lost (g)}}{\text{wet sample (g)}}$$

To convert gravimetric moisture into volumetric moisture, the following equation was used:

$$\text{volumetric moisture } (\text{cm}^3/\text{cm}^3) = \text{gravimetric moisture } (\text{g/g}) \times \frac{\text{bulk density } (\text{g/cm}^3)}{\text{density of water } (\text{g/cm}^3)}$$

where the bulk density was derived from McKenzie (1992) for each soil sample as they were located across his pedoderms. And the density of water was assumed to be 1 g/cm^3. It is important that the volumetric moisture content is used because it takes into account the volume of the soil through incorporating the bulk density. Without this, the moisture content is dimensionless.

APPENDIX B – Literature Review

Digital Soil Mapping
Available Water Content
using ancillary data
across the Warren and Trangie districts
of the Lower Macquarie Valley, NSW.

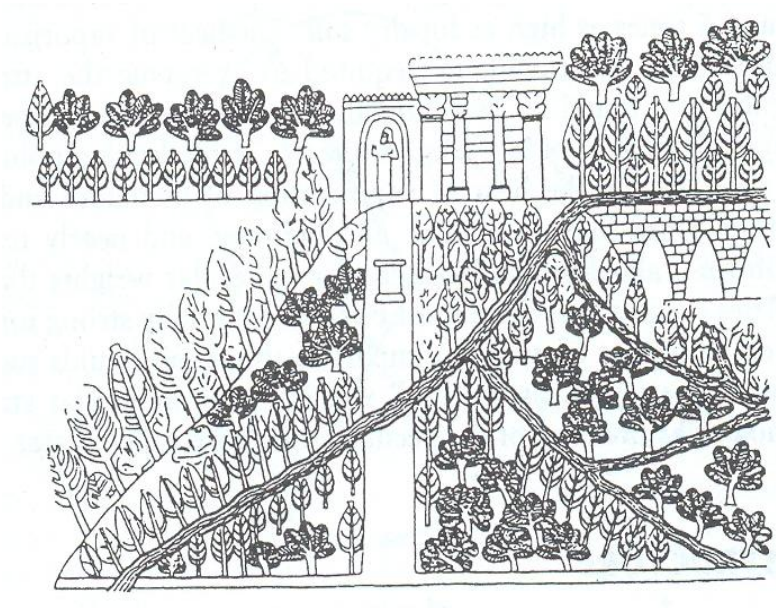

The Hanging Gardens of Babylon - Assyrian interpretation

Liam Gooley
z3216661

School of Biological, Earth and Environmental Sciences
The University of New South Wales
Australia

Digital Soil Mapping
Available Water Content
using ancillary data
across the Warren and Trangie districts
of the Lower Macquarie Valley, NSW.

A Review of the Literature

Contents

Abstract

Three quarters of all irrigated agriculture in Australia is undertaken within the Murray Darling Basin (MDB). Unfortunately, given the geographic location and the change in climate predicted, water use efficiency in irrigated areas will need to be improved. In order to understand where improvements need to be made irrigators need to be aware of the spatial distribution of soil texture and available moisture content of their soil. Owing to the expense of collecting this information, digital soil mapping techniques are increasingly being employed. This is the coupling of soil laboratory measurements and ancillary data sets which are collected much more readily. In this literature review the various laboratory methods (e.g. filter paper and pressure plate apparatus) and field methods (e.g. neutron probes) available to measure available soil moisture are introduced. In addition, various ancillary data sets (e.g. electromagnetic induction and infra-red spectra) capable of being coupled to these measurements are described. In order to calibrate the ancillary data to laboratory measurements of available moisture, various statistical tools (e.g. linear regression and artificial neural networks) are outlined. It is concluded that of the laboratory methods, the pressure plate apparatus seems most appropriate given its speed and ability to measure both the available water content with high precision. Of the ancillary data, the electromagnetic induction and gamma radiometrics appear suitable owing to their speed of data collection and their relationship with soil properties which influence soil mositure (i.e. electromagnetic induction) and increasing ubiquity (i.e. radiometrics). In terms of an optimal method of statistical analysis, artificial neural networks appear to be the most robust, however linear regression has proved useful and will be compared.

1. Introduction

The Murray Darling Basin (MDB) is one of the largest agricultural regions in Australia accounting for 40% of all Australian farms and producing one third of all of Australia's food. Within the MDB there is a high degree of irrigated agriculture which accounts for three quarters of all irrigated agriculture in Australia. Irrigated agriculture is one of the largest users of water in Australia, but it also gives a greater return in profit than conventional farming. Increasing water scarcity due to climate change (Kothavala, 1999) and demand for food in the MDB is leading to the massive buyback of water licenses and increasing need for water use efficiency. In order to increase water use efficiency we need to understand the sources of water in the environment and where that water goes to once it is in the environment. To do this, we look at the water balance equation: Precipitation + Irrigation = Evapotranspiration + Runoff + Deep Drainage + the change in soil moisture. There has been much research focusing on deep drainage and evapotranspiration, but little work done on understanding the ability of soils to store specific amounts of moisture. Soil moisture storage is significant because different soil types store different amounts of water. Because soil varies at the field and district level, it is important to understand this spatial variation and map it in order to irrigate more efficiently.

The change in soil moisture is also known as the available water content (AWC) and is given by the difference between the field capacity (FC) and permanent wilting point (PWP) of the soil. FC is defined as the amount of water adhering to soil particles after two days of drainage from irrigation or heavy precipitation, and PWP is the amount of water left in the soil after plants have drawn it all out. The AWC of soils can be determined in the field or by laboratory methods, with the field methods often being approximations based on calibrated laboratory methods. Common field

methods include Neutron Probes, Capacitance Probes and Time Domain Reflectometry. Laboratory methods such as the filter paper method, vapour equilibration, and pressure plate apparatus are used to equilibrate the field methods. The greatest issue with these lab methods is that they are time consuming, and combined with field methods only provide point based information about the soils in a field. Because soil type can vary across the field and district, it is important to gain an understanding of the spatial variation of soils and their AWC across an area.

In order to gain a more complete picture of the spatial variation of soils across a district or field, proximal and remote methods are used. The most common proximal methods are direct current resistivity, and electromagnetic induction, whilst common remote methods are infra-red imagery and gamma radiation. The proximal methods mentioned provide information regarding the conductivity of the soil, most commonly the bulk soil conductivity which is then extrapolated to cover the entire area. Whilst infra-red imagery provides information as a whole image on the crops in an area and gamma radiation the soil type.

Because there is no single instrument that can accurately measure soil moisture content at the field or district scale, this literature review will be looking at three key aspects aiming to solve this problem. These are: the various methods for measuring soil moisture content in the field and the lab, the various remote and proximal methods available which give us information on soil properties, and the variety of statistical models used in soil science. In doing this, I am aiming to elicit a method using a statistical model to link lab measured soil moisture content at point based locations with proximal soil data at the district scale in order to create a high resolution digital soil map (DSM) at the field scale of field capacity, permanent wilting point, and the available water content.

2. Materials and Methods

2.1. Biophysical Background

2.1.1. Study Area

The study area is located in the lower Macquarie valley in the central west of New South Wales. Specifically, two predominantly irrigated areas will be studied: Trangie and Warren (Figure 1), NSW. The lower Macquarie Valley is part of the Murray-Darling Basin (Figure 1) and the field sites lie on the floodplain of the Darling river. The soils associated with the district have been deposited over the last 40,000 years with a variety of sedimentary environments. The controlling geomorphology of the district is a basement of metamorphic and granitic rocks under the Macquarie floodplain with the alluvial plains being underlaid by sandstones and shales (McKenzie, 1992). Following extensive deposition since the late Pleistocene has seen 20-60m of recent alluvium from an extensive river network. The climate has been relatively stable for the development of soils with alternating dry cold periods and moist wet periods, the recent climate has been relatively stable with low rainfall and being relatively warm. Land uses have change extensively over the last 100 years going from native vegetation to dryland agriculture to the present irrigated agriculture.

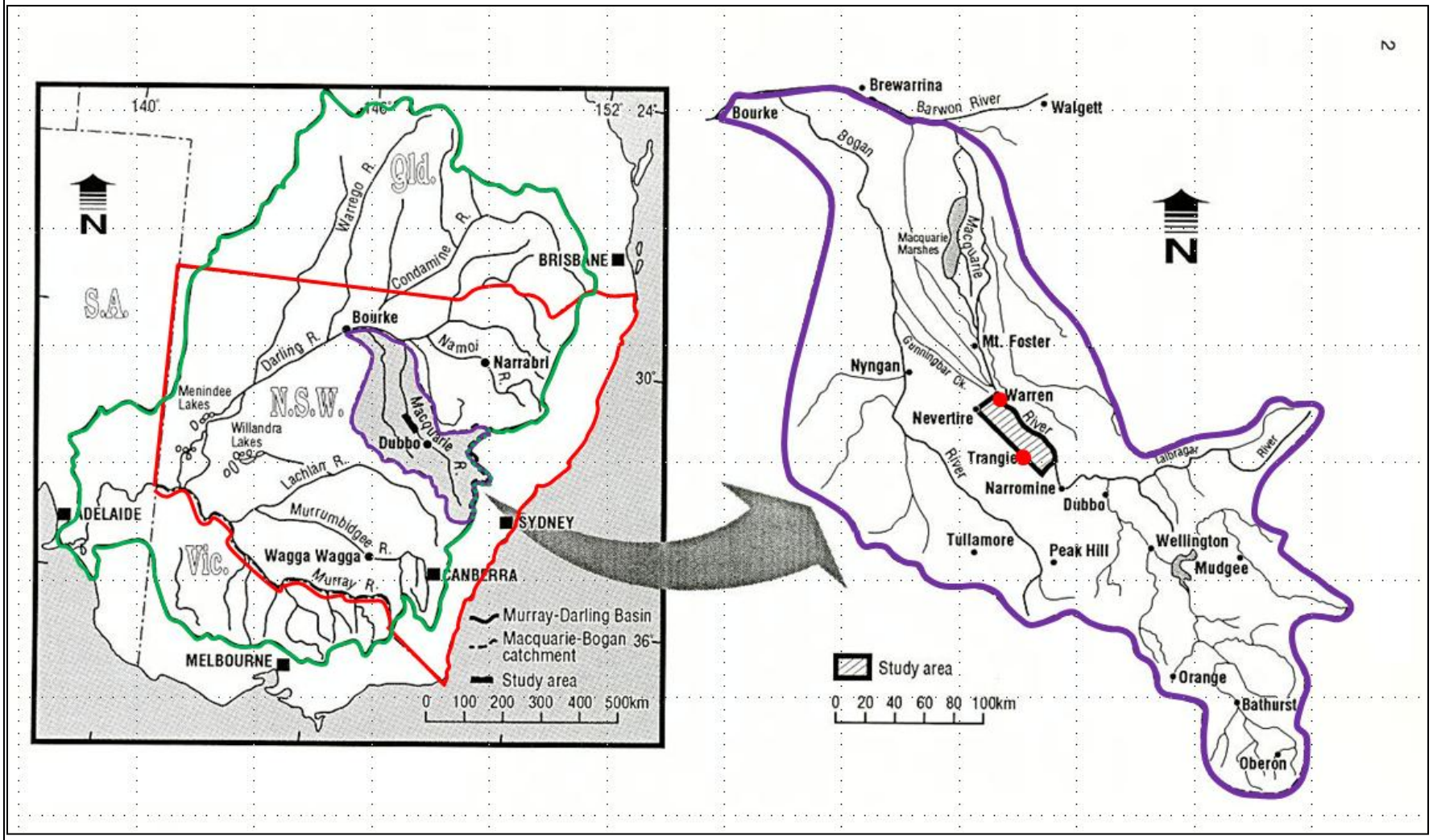

Figure 1: Location of Trangie and Warren in respect to NSW (red), the lower Macquarie Valley (purple), and the Murray Darling Basin (green). Adapted from (McKenzie, 1992).

2.1.2. Soils

An extensive soil survey of the study area was carried out by McKenzie (1992) where ten main pedoderms were classified and mapped (Figure 2). McKenzie (1992) identified three main pedoderms occurring in Trangie and five across Warren. The three common pedoderms are old alluvium meander plain, old alluvium back plain, and trangie cowal alluvial plain. Two additional Pedoderms were identified in Warren. These are the Macquarie alluvium backplain complex and comtemporary Macquarie alluvium. From this variety of pedoderms it is possible to see that soil increases with age away from the Macquarie river in the North East to the South West. The soils along the Trangie Cowal and Macquarie River alluvial plains are the youngest and contain high fertility silty loams. The next soil unit of the backplain contains high levels of clay due to the distance from the river. The oldest soil unit is also the most unfertile as is largely a sandier soil than the others due to its location on the meander plain. Overall, the majority of soils in the area vertosols or dermasols with interspersed kurasols and kandosols.

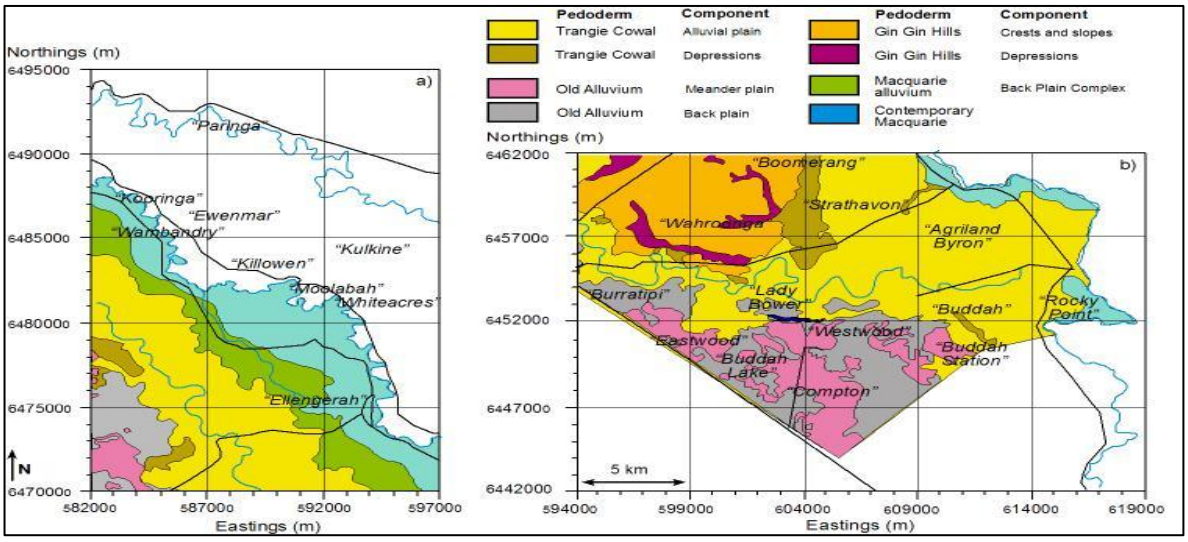

Figure 2: pedoderms as identified by McKenzie (1992) in Warren (left) and Trangie (right)

2.1.3. Geomorphology

Prior to the development of the current soils from heavy bedload stream systems and distributary networks from the Quaternary, this area of NSW was controlled by extensive deposition and sedimentation. The oldest formations are Paleozoic and Mesozoic sedimentary, metamorphic and granitic sequences. The extended periods of depostition and sedimentation were controlled by a fluctuating climate of cold and dry (deposition) to warm and moist (erosional). Towards the end of the tertiary was an extended erosional period where extensive weathering occurred across NSW and saw the alluvium deposited as the current contemporary Riverine plains.

2.1.4. Climate

The climate of this region is typical of inland NSW, it is a semi-arid region with annual precipitation of 493mm. Rainfall is slightly summer dominant but highly variable, temperatures are also highest across the summer period as is mean evaporation. The climatic averages are summarised below in Table 1. Although the current climate is drought prone and has low rainfall, climate change predictions indicate that prolonged periods of more intense drought will increase over the next 20 years (Kothavala, 1999).

Table 1: climatic averages at the Trangie Agricultural Research Centre (BOM)(Dickson et al., 1996)(Dickson et al., 1996)

	Jan	Feb	Mar	Apr	May	Jun	Jul	Aug	Sep	Oct	Nov	Dec	**Annual**
air temperature (°C)													
mean max	33.2	32.1	29.3	24.4	19.8	16.0	15.3	17.3	20.9	25.2	28.8	31.9	24.5
mean min	18.4	18.4	15.6	11.2	7.2	4.4	3.2	4.0	6.4	10.2	13.6	16.6	10.8
mean soil Temp °C at 9am													
	16.3	16.1	12.7	8.2	4.8	1.6	0.0	0.5	3.1	6.9	10.6	13.2	7.8
rainfall													
mean (mm)	53.5	52.1	46.4	40.1	37.3	35.7	34.5	32.2	31.2	45.4	44.4	40.3	492.8
rain days	5.8	5.4	5.4	4.9	6.0	6.9	7.7	6.6	6.3	7.0	6.0	5.7	73.7
mean daily evaporation (mm)													
	9.8	8.8	6.9	4.6	2.6	1.8	1.8	2.7	4.0	6.0	8.1	9.7	5.6

2.1.5. Land Uses

Until the completion of the Burrendong Dam in 1967, Trangie and Warren had been extensively redeveloped for dryland cropping and grazing (McKenzie, 1992). Prior to this, the region supported *Eucalyptus camldulensis* (River Red Gum) along the Macquarie River, where a few strands still exist (Biddiscombe, 1963). The cracking clays of the region supported mainly *Acacia pendula* (Myall) and *Atriplex nummularia* (Old Man Salt Bush). The rest of the region was covered by *E. populnea* (poplar)(Biddiscombe, 1963). Following completion of the dam and a ready supply of water, irrigated agriculture was introduced to the region with cotton being one of the main crops. As of 1992, 58,000 hectares are licensed for irrigation and 25,000 hectares of this is cotton (McKenzie, 1992).

2.2. Laboratory Methods

Water occurs within soil in three different forms; adhesively to individual soil particles, cohesively to other water particles, and within soil pores. Adhesive water occurs as a thin layer about 10 molecules thick around soil particles because of the asymmetrical charge on water molecules and positive or negative charge of soil particles. Adhesion water is bonded so tight to the soil particles it cannot be removed by plants. Cohesion water is that which bonds to the adhesion water by hydrogen bonding. This bond between the water molecules is not as strong as an adhesive bond, allowing cohesion water to move more freely and be available to plants via respiration. Soil which exists in the pores of soil is known as gravitational water because it drains out of the profile within two days of irrigation or rainfall. Overall, all water occurring in the soil is known as the volumetric water content (θ) (Foth, 1990).

Water moves through the soil profile as a function of its total potential. Total potential is the work which must be done to move the water to a zero energy state. Total potential is compromised of three main mechanisms of potential energy; gravitational, osmotic, and matric. The gravitational potential in soil means water flows downward, for example from the surface to depth. Osmotic potential is when it is difficult for plants to remove water from the soil because of high solute concentration in the soil (ie. saline soil). Matric potential is the adhesion of water to the soil matrix, and differs across soil types. For example, clay particles hold onto water more tightly than sand particles, so a clayey soil will retain more water than a sandy soil. Total potential primarily depends on matric potential because osmotic potential is minimal as is gravitation when there is water in the soil. Matric potential is important because each soil type (i.e. textures) has a different matric potential, this affects θ (figure 3). The relationship between matric potential and θ is known as the

soil moisture characteristic (figure 4). From the soil moisture characteristic, it is possible to distinguish the upper and lower limits of water that is available to plants. The upper limit is known as the Field Capacity (FC) and is the most water that can be stored in the soil by cohesion without draining by gravitational forces. The matric potential of soil at FC has been experimentally determined to be -33 J/kg (figure 3). As water is used by plants, θ is reduced until there is only adhesion water left occurring in the soil. At this point, θ is said to be at its permanent wilting point (PWP) because plants will remain wilted. The matric potential of soils at PWP has been experimentally determined to be -1500 J/kg. The difference between PWP and FC is then the amount of water freely available to plants to use, otherwise known at the available water content (AWC). As shown by Figure 4, FC, PWP and the AWC for a specific soil type can be determined by its soil moisture characteristic because the theoretical values of matric potential are known. In order to determine the soil moisture characteristic of a soil, specific laboratory methods are needed. The three most commonly used laboratory methods for determining the soil moisture characteristic are the filter paper method, vapour equilibrium, and pressure plate. In the following section each of these methods is introduced and described.

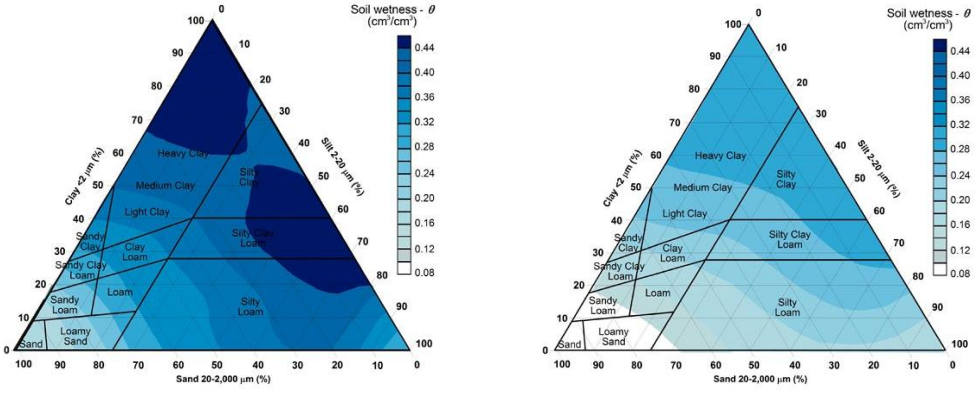

Figure 3: Volumetric water content (*θ-cm3/cm3)* at FC (left) and PWP (right) relative to soil texture. Source (http://www.terragis.bees.unsw.edu)

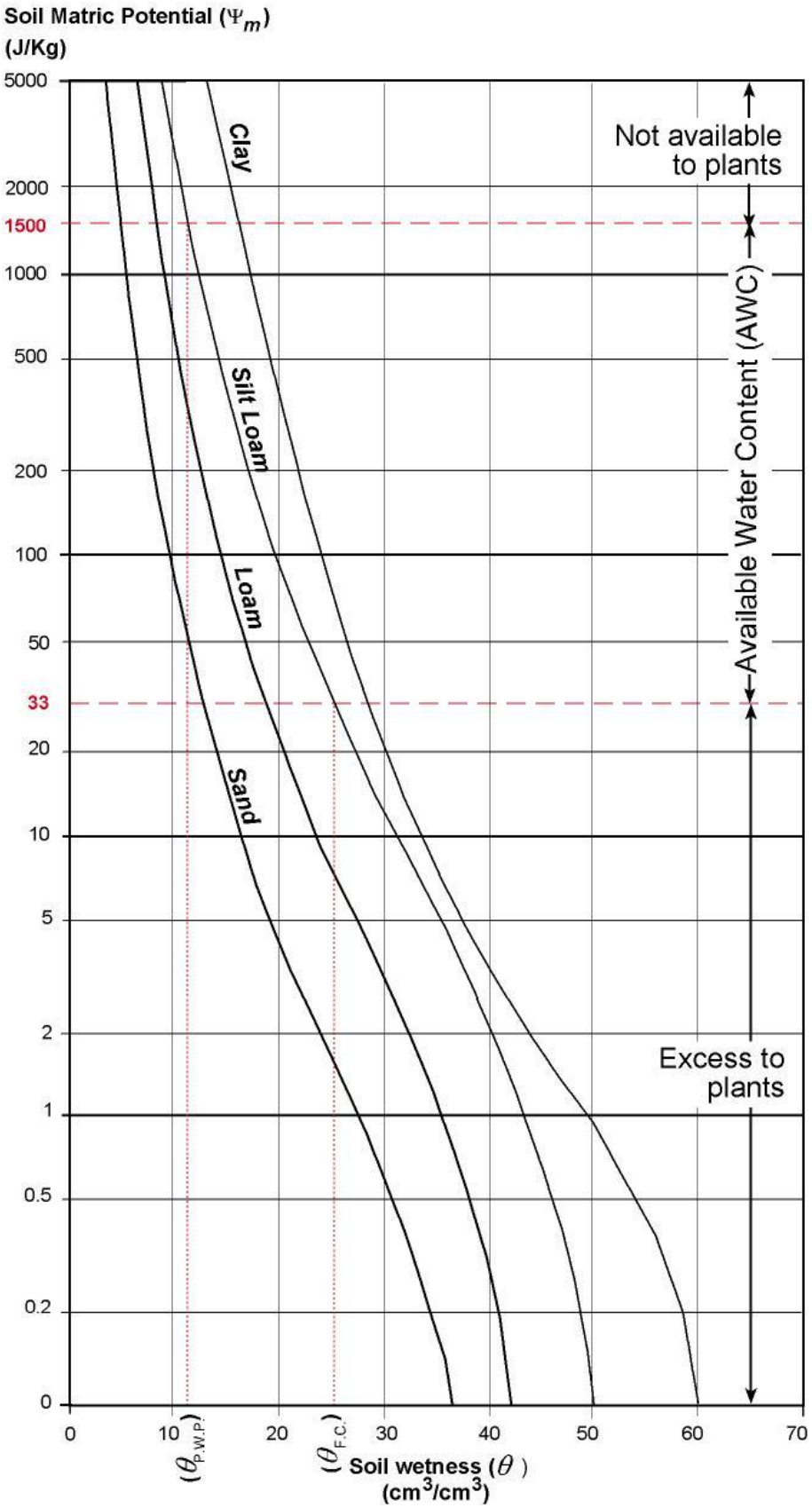

Figure 4: soil moisture characteristic curve. (Triantafilis, 2009c)

2.2.1. Vapour Equilibrium

Vapour equilibrium is a method which provides information above PWP on the soil moisture characteristic curve (Figure 4). The vapour equilibrium technique uses chemical solutions in an enclosed desiccator with the soil samples placed above the solution (Figure 5). The solution creates constant suction conditions which force the soil samples to reach equilibrium with the enclosed space (Nam et al., 2010). Adaptations to this technique include using an unsaturated acid solution which draws the water out of the soil samples and into the solution, thus achieving a specific matric potential (Nam et al., 2010). Alternatively it is possible connect the desiccator to a fixed source of air pressure to speed up the equilibrium time. This is done because it can take up to 15 days for the samples to reach equilibrium with the chemical solutions. Once it has been determined that the samples have equilibrated, θ is calculated by the mass lost on drying of the samples. This technique is seldom used on its own for the determination of the soil moisture characteristic because it only provides matric potentials above -1500J/kg due to the variety of solutions used. Although it is possible to apply models to predict the soil moisture characteristic based on limited data, the data range required to work from is 0 to -1500J/kg (Lu et al., 2008), and these models are often not entirely accurate. However, vapour equilibrium is a useful method if the upper part of the soil moisture characteristic is required with a high degree of accuracy.

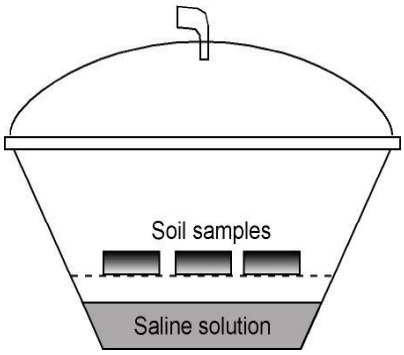

Figure 5: Schematic showing the components of the vapour equilibrium method (Triantafilis, 2009c)

Figure 6: Students filling aluminium tins with moist soil and Whatman No. 42 paper in the middle. (Triantafilis, 2009c)

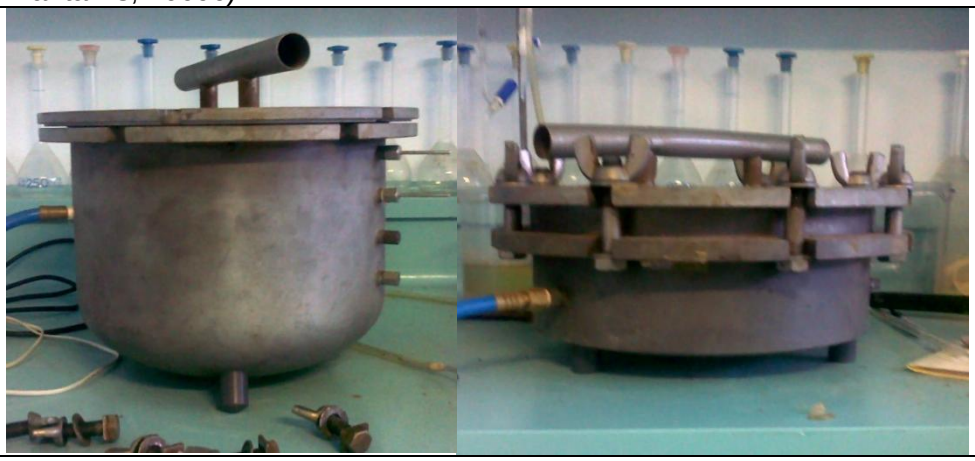

Figure 7: 1 bar pressure plate apparatus (left) and 15 bar pressure plate apparatus (right). (Photo taken by author)

2.2.2. Filter Paper

The filter paper method is more used to determine the soil moisture characteristic curve (Figure 4) of a soil because it gives matric potential values in the range of -10 to -2000J/kg. There is a standard test method (ASTM Standard, 1997) which involves placing a Whatman No.42 filter paper in an aluminium tin in contact with the soil sample (Figure 6). In order to achieve a full range of matric potentials, at least eight different samples should be prepared of increasing wetness. After seven days the filter paper is removed, weighed, oven dried, and weighed again. Then using the moisture calibration curve of Whatman No.42 filter paper the soil matric potential can be determined and plotted into a soil moisture characteristic curve. Whatman No.42 filter paper is used because it is porous and has a specific water release characteristic. That is, that when in contact with soils at a specific wetness, it exerts a matric potential on the soil and then equilibrates to the specific soil wetness. Following this, Whatman No.42 filter paper's water release characteristic has been calibrated and plotted so it is possible to determine the soil matric potential at a specific wetness. Schleicher and Schuell No. 589 filter paper is also commonly used as it has similar water release characteristic and a calibration curve exists for it as well, although it has been experimentally determined that Whatman No.42 filter paper is more consistent (Leong et al., 2002). The filter paper method is effective at determining the soil moisture characteristic of soils, however the relatively long equilibrium period, number of experiments required for a single sample, and use of materials is intensive. The result of this is that the filter paper method is primarily used in comparative studies with other methods to determine their effectiveness at determining the soil moisture characteristic.

2.2.3. Pressure Plate

Pressure Plates (Figure 7) are used to determine the soil moisture characteristic (Figure 4) of soils between the range of 0 to -1500 J/kg (Lu et al., 2008, Jones and Graham, 1993). Pressure Plate Apparatus operate on the principle of using suction gained by positive atmospheric pressure to mimic the negative pressure observed in the field and attain the corresponding soil matric potentials. For example we know that PWP occurs at -1500 J/kg, this is a negative force exerted by the soil particles to hold onto the water. To replicate this with pressure plates a positive force of 15 bars is used in the laboratory.

To do this a sample is placed on a porous ceramic plate with a rubber diaphragm which has been soaked overnight in water (12 samples fit on a plate), the sample is then wetted by pouring excess water onto the plate and left for a second night. The wet soil samples on the wet ceramic plate are then placed inside the pressure chamber where compressed air is let into the chamber using a pressure manifold system, up to the desired atmospheric pressure. By having a pressure difference between the liquid phase water in the soil (1500 kPa) and the water in the diaphragm of the pressure plate (100 kPa), this maintains suction. The result of this maintained suction is that water flows from the soil matrix onto the other side of the pressure plate and out of the extractor. When the flow of water from the extractor has ceased (no noticeable output for three hours) the samples are said to be at equilibrium and are removed from the chamber to be weighed, oven dried then weighed again to determine the moisture content.

Using this method it is possible to create the soil moisture characteristic using a variety of pressures and fit a water retention function to this data (Bittelli and Flury,

2009). However it is also possible to determine the FC and PWP of soils using this method by using a 15 bar apparatus at 1500 kPa to determine PWP, and a 5 bar apparatus at 100 kPa to determine FC. Pressure plates have been used since the 1940's in determining the soil moisture characteristic (Richards, 1948) and have been used extensively in this field as well being the subject to comparisons with other instruments (Nam et al., 2010, Waters, 1980, Wessolek et al., 1994, Cancela et al., 2006). In addition this the apparatus has been used to determine the AWC of soils (Jones and Graham, 1993, Duniway et al., 2007, Curtis and Claassen, 2005) , has had adjustments made to the standard operating procedure relevant to particular soil types (Curtis and Claassen, 2008, Montagne et al., 1992, Cresswell et al., 2008), and had its adequacy investigated with positive results (Bittelli and Flury, 2009, Cresswell et al., 2008).

2.3. Field Methods

With the increasing need for site specific irrigation regimes due to the spatial variability of soils, there has been the development of infield systems that monitor θ. These systems operate primarily by calculating θ from various soil properties such as the dielectric constant of soil and system uses different theories of operation. The dielectric constant of soil varies across soil types and is the ability of soil to transmit an electric current, this property varies across soil textures and it directly related to θ. As it is, there have been three main instruments used in the soil science literature and in practice. These are neutron probes, capacitance probes and time domain reflectometry, which will be introduced and explained in the following sections.

2.3.1. Neutron Probe

Neutron Probes are an instrument that gives point readings of θ across a field. This is because it requires a pre-installed access tube into which the probe it lowered. The probe consists of a radiation source – usually americium-241 and beryllium – and a detector (Figure 8), it is connected to the control unit which houses the probe when not in use and gives the soil moisture reading (Figure 8). It operates by measuring the ratio of fast neutrons from alpha decay exiting the probe to the returning slow neutrons from collision with soil water hydrogen molecules. From this an estimate of θ is obtained. However there are significant limitations with this device in that it requires calibration in the field for soil type and access tube material, required an access tube, is unreliable for the top 10cm of soil – due to the escape of fast neutrons – and is a health risk due to radioactivity. The main benefits in using this device are its high degree of accuracy (from directly measuring the amount of water molecules in the soil) and the ability to have precise measurements at a known location at various times during the drying and wetting cycle.

Neutron Probes have been in use since the late 1940's in soil science but were used extensively from the 1950's through to the 1970's due to their high accuracy of θ compared to the previously used resistance blocks. The use of neutron probes during this period was extensive and much of the progress with their development was during this period. Use of neutron probes diminished with the advent of Time Domain Reflectometry and Capacitance Probes, but they are still used to assess the accuracy of new techniques and equipment (Acworth et al., 2005, Al-Ain et al., 2009). Neutron probes are still common place today in farms across Australia and used particularly by irrigation consultants (DPI, 2004) because of their relatively low cost and where there are pre-existing access bores.

2.3.2. Time Domain Reflectometry

Time Domain Reflectometry (TDR) has been available since the late 1970's and consists of a microprocessor and a series of waveguides along a transmission line (Figure 9) (Topp and Davis, 1985). It directly measures θ content by converting the time travel of a high frequency electromagnetic pulse reflected between the open ends of the waveguides to the dielectric constant of the soil (Topp and Davis, 1985). The waveguides (probes) are placed around the field and linked to the central processor unit allowing the electromagnetic pulse to travel back along the original path. The central processor then displays the waveform, actual time delay and correlated θ. TDR has significant benefits over Neutron Probes in that it does not require radioactive material or highly trained personnel (Schmugge et al., 1980, Stafford, 1988), can auto log soil moisture over time to see the effect of irrigation in a field (Hedley and Yule, 2009), is portable across districts, does not require pre-installation of any components or calibration (Wessolek et al., 1994), and it can be left unattended to record measurements(Green et al., 2006). In addition to these points, TDR is also used in the calibration and testing of new equipment where neutron probes are not practical (Kelleners et al., 2009, McCutcheon et al., 2006). Although there are many benefits, TDR does have some downfalls. Chiefly, it can only measure to the depth of the relatively short probe (Topp and Davis, 1985), requires very good soil contact for accurate measurements (Robinson et al., 2003, Ghezzehei, 2008), and there is a relatively high level of technical expertise required to install the TDR and analyse the results (Topp and Davis, 1985). Despite all these factors, it is a relatively easy to use, cheap, readily available piece of technology for use in the field to determine θ.

2.3.3. Capacitance Probes

The last piece of equipment is the capacitance probe (Figure 10). Capacitance Probes operate on the same principle of TDR – calculating the dielectric constant of the soil (Paltineanu and Starr, 1997). However as you can see in Figure 10, it is a singular probe with multiple sensors located along its length. These multiple sensors measure the dielectric constant at different depths in the soil profile and convert it to θ. Each sensor consists of an oscillator to induce an electromagnetic field, and two electrodes (Figure 10) which function as the capacitor. As the current oscillated between the electrodes, the dielectric constant of the surrounding soil is measured. Ancillary to this, the probe is installed in a water-tight access tube in the field and requires full soil contact to ensure the most accurate results (Mohamed et al., 1997). The issue of full soil contact can become problematic with incorrect installation, or a shrink-swelling clay where air gaps form around the probe and affects the dielectric loop (Al-Ain et al., 2009, Paltineanu and Starr, 1997). Like the neutron probe, capacitance probes only offer soil moisture data at fixed points and several probes are needed across a field to get a representative view of the spatial variability of soils in the field (Chanzy et al., 1998). There is also soil specific calibration required and it is also sensitive to other soil conductive properties such as bulk density, clay content and temperature (Vera et al., 2009). Despite these shortcomings, capacitance probes offer accurate site-specific measurements (Tromp-van Meerveld and McDonnell, 2009), can operate in highly saline conditions (Al-Ain et al., 2009), can be attached to a conventional data logger for ease of use, and produce a better resolution of data than TDR . As such, capacitance probes are more robust than TDR and provide data that can be analysed more easily than TDR data and at a greater depth (Paige and Keefer, 2008).

Source: ICT International

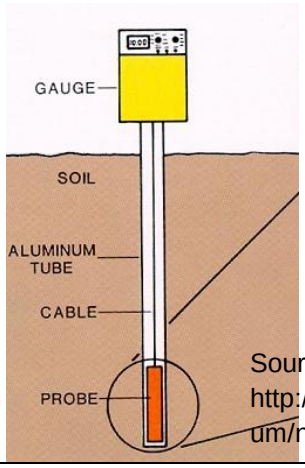

Source: http://safiles.tamu.edu/agronomy/sorghum/neutron.htm

Figure 8: neuron probe with schematic of use

Source: soilmoisture equipement corp.

Figure 9: time domain reflectometry equipment

Figure 10: capacitance probe

2.4. Ancillary Data

Ancillary data is secondary information which can be directly related to a soil property being investigated. Ancillary data is used in soil science literature for determining θ in the field because field methods offer only point based information, as do laboratory methods. θ is a function of clay content, soil mineralogy, and bulk soil density. Hence in order to determine θ, it is necessary to measure a parameter such as clay content or soil mineralogy, or alternatively another soil attribute which directly relates to any of these. Apparent soil electrical conductivity (EC_a) is the conductivity of the soil as measured by an ancillary instrument using either passive or active techniques. EC_a is has been linked to all the soil properties that influence θ through a variety of studies. Ancillary data can be collected by a number of instruments, active sensing instruments such as Direct Current Resistivity and Electromagnetic Induction which pass a signal into the soil in order to measure the resulting signal, and passive sensing instruments which measure radiation given off by the soil such as gamma radiation or spectral radiation.

2.4.1. Contact Methods

Contact methods of gaining ancillary data in soil science literature and involves having an instrument in direct contact with the soil. The most commonly used method is direct current resistivity (DCR). DCR is the measurement of the potential generated by two electrodes in the ground when a direct current (DC) is passed through them. Measuring potential gives a reading of resistivity; because resistivity is the inverse of conductivity it is possible to measure EC_a using DCR methods.

Using different spacings and configurations of current and potential electrodes, the potential of the earth can be measured from the topsoil to the depth of entire aquifers. DCR is commonly used in geophysics and hydrogeology because of the depth of investigation achieved is useful for studying aquifers and contamination plumes (Sailhac et al., 2009). In soil science literature, because it is only the very near subsurface being investigated, there are two instruments used to measure soil resistivity by DCR instead of traditional electrode arrays. These are the the Veris Technologies, Veris 3100 (Figure 12) and a MultiContinuous Electrical Profiling (MuCEP) device (ARP patented, Geocarta society, Paris, France) (Figure 13).

The Veris 3100 consists of six coulter electrodes (circular discs) (Figure 12), two act as current electrodes (2 and 5) whilst the other four act as potential electrodes. Because of the configuration of electrodes, the Veris 3100 measures resistivity at two different depths, 0-0.3m and 0-0.9m. The shallow readings are taken by electrodes 3 and 4, whilst the deeper readings are taken by the outer electrodes, 1 and 6. The MuCEP device consists of three arrays, each composed of

four wheels which act as electrodes (Figure 13). Because of the spacings involved between the current (A and B) electrodes and the potential (M and N) electrodes, it is only smallest array (A-B – M_1-N_1) which measures the near subsurface resistivity.

The Veris 3100 has been primarily used as a data source for generating high resolution maps of EC_a at the field scale (Johnson et al., 2001). Johnson et al. (2001) used a Veris 3100 device on a 250ha farm in the United States of America with the aim of mapping EC_a across the field site to identify soil management zones (Figure 11). Once these zones of EC_a had been determined the authors sampled within the zones with the aim of identifying physical parameters which correlated to the EC_a zones. It was established from this study that bulk density and percentage clay were positively correlated with EC_a enabling specific farm management strategies to be implemented based on a Veris 3100 EC_a survey.

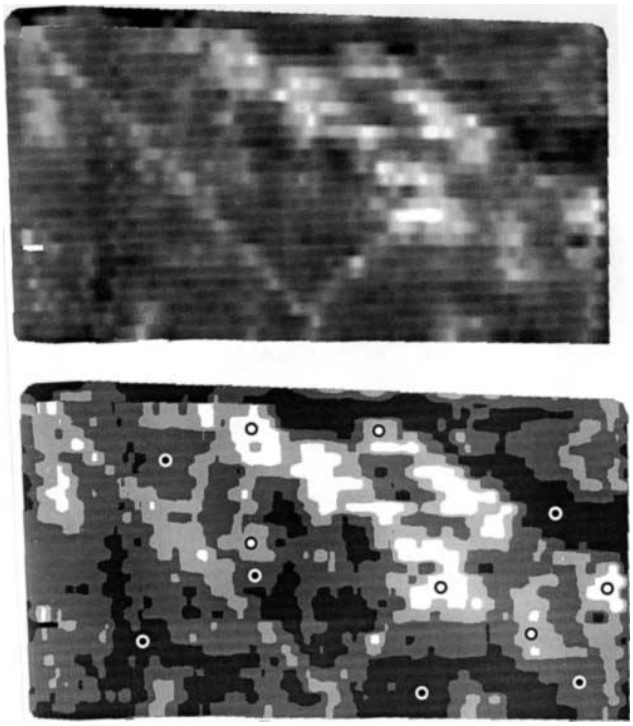

Figure 11: a greyscale electrical conductivity map for the field site (top) and the same map following recoding into four electrical conductivity classes (bottom). Variations in coulour, from light to dark, correspond to increasing conductivity, and “O” symbols represent selected soil sampling sites. From (Johnson et al., 2001)

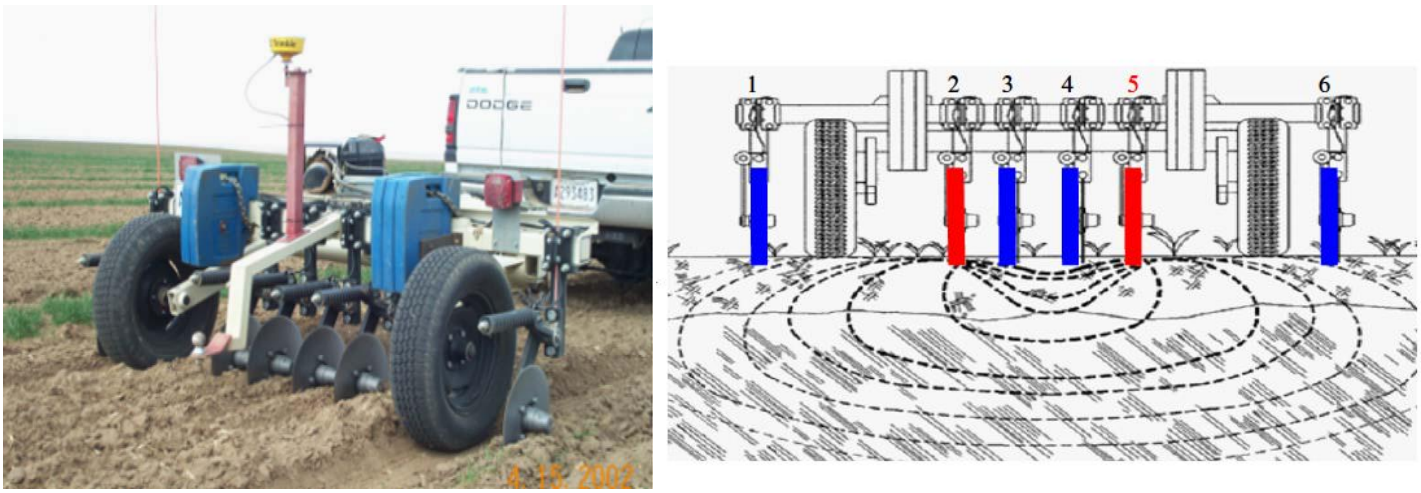

Figure 12: Veris 3100 device (left) with schematic of operation (right) (McCutcheon et al., 2006)

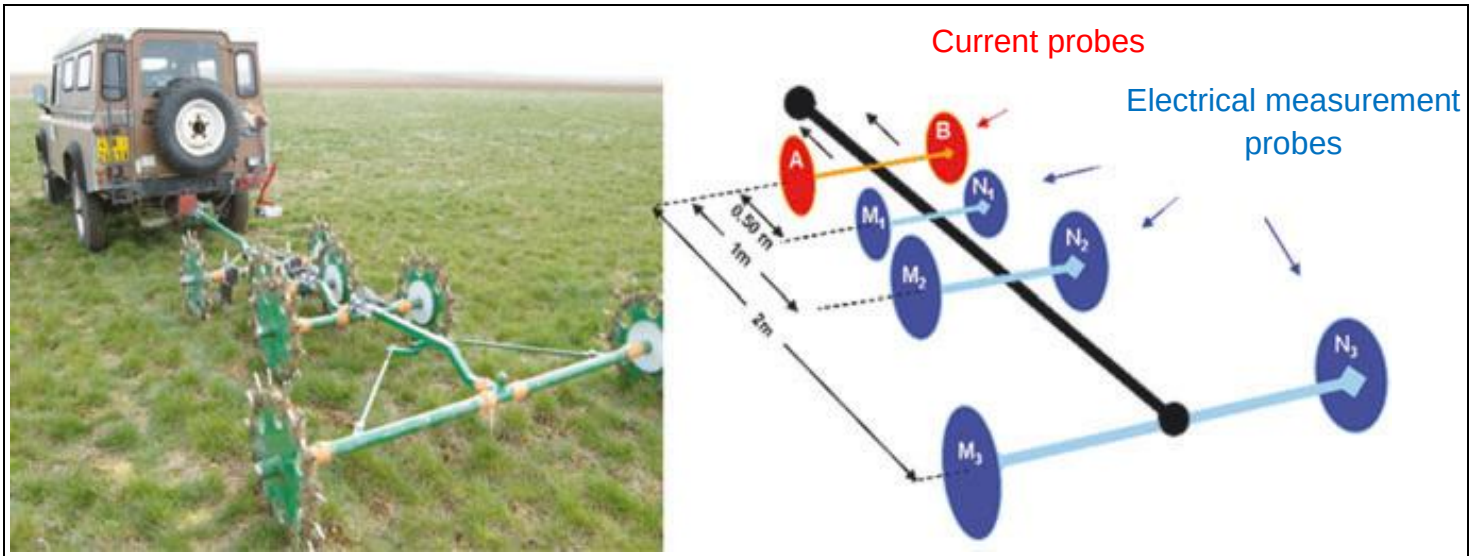

Figure 13: MuCEP device (left) with schematic of operation (right) (Besson et al., 2010)

Similarly, McCutcheon et al. (2006) used a Veris 3100 to map soil EC_a at the field scale (Figure 14) with the aim of identifying management zones through inferring soil texture as soil moisture changed across sampling dates. To do this they mapped soil EC_a on four different dates as well as taking 198 soil samples which were analaysed in a laboratory for θ and texture. Subsequent mapping events saw the authors use TDR to determine θ at various sampling sites. It was found that no single soil parameter could explain the variations in EC_a with confidence, but that θ and elevation could predict EC_a through spatial regression ($R^2 = 0.87$). They concluded that soil texture and EC_a have a temporally spatial relationship, with θ being the soil property that influences EC_a the most.

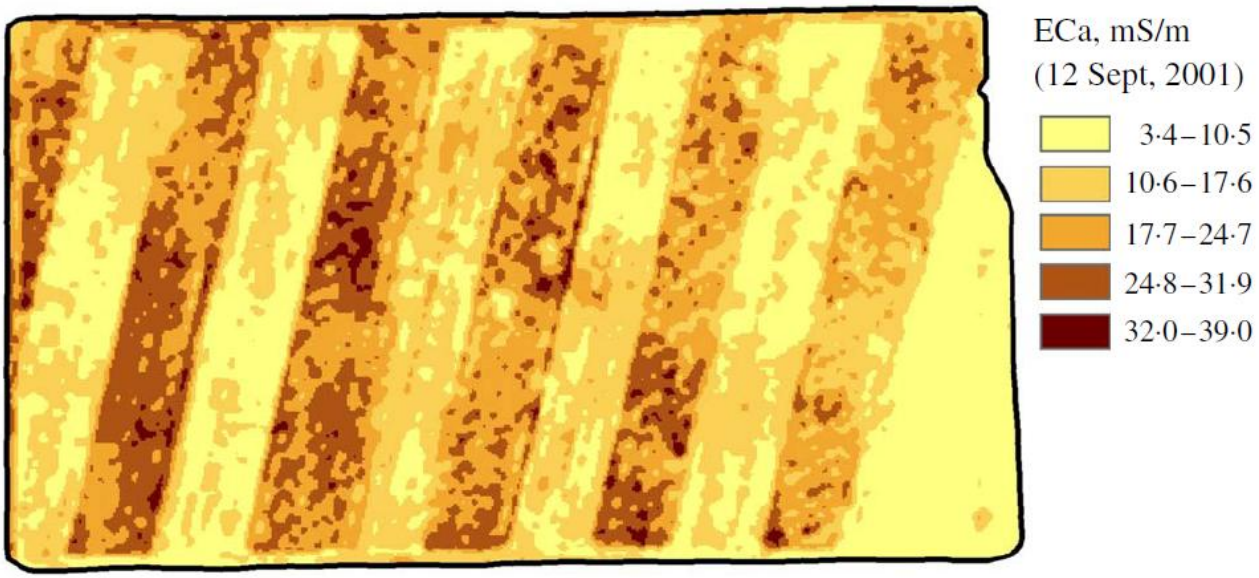

Figure 14: map of continuous shallow EC_a using measurements taken on 12 September 2001 across fallow and cropping strips. From (McCutcheon et al., 2006)

Hezarjaribi and Sourell (2007) outline a method by which they attempted to map the AWC at the field scale using a Veris 3100. To do this they mapped EC_a across their study area and used EC_a to identify different zones. They then sampled within these zones and used the pressure plate apparatus to determine FC and PWP. Using their laboratory determined AWC values they applied a linear calibration to determine the AWC as a function of EC_a which was highly correlated ($R^2 = 0.77$). From this, they were able to produce a map of the spatial variation in AWC as a function of EC_a across their study area (Figure 15). The shallow Veris 3100 readings have been shown to be correlated to lab determined AWC values which relates to the spatial variation in soil texture across the field. However, the model applied in this study did not take into consideration other soil factors which have been shown to affect the variation in AWC such as clay content or bulk density (Friedman, 2005).

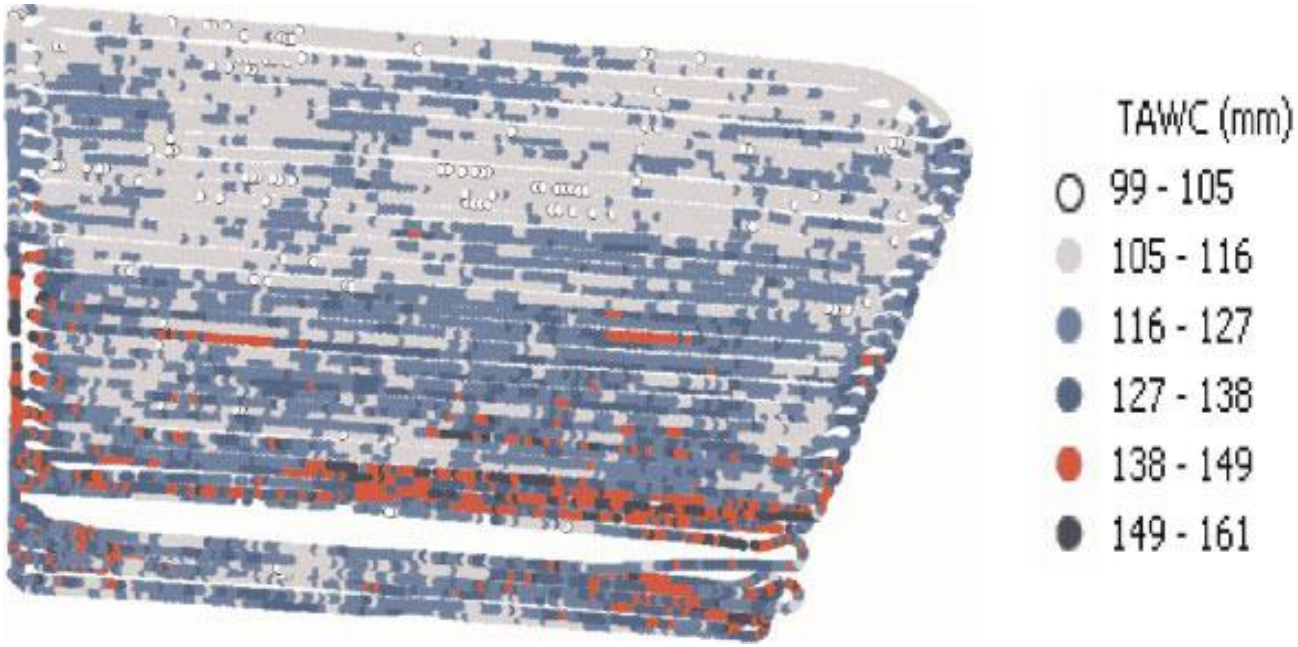

Figure 15: Interpolated EC_a and AWC map standardised to 25°C obtained with Veris 3100 shallow. From (Hezarjaribi and Sourell, 2007)

The MuCEP is a relatively new device and little work has been done using it. It is similar to the Veris 3100 in that it uses DCR to determine EC_a whilst being towed across a field. It has recently been shown that the MuCEP can be used to map the spatial variation in EC_a at the field scale in high resolution (Besson et al., 2010). In their study, Besson et al. (2010) took EC_a reading across a 2ha field site in France on four different dates throughout a single year (Figure 16). With this multiple survey of EC_a they took soil samples at each date to determine θ (Figure 17). From this it was seen that EC_a follows soil texture patterns (Figure 18), but also that a spatial analysis of EC_a is inadequate in describing the variation θ. The authors concluded from this study that in order to gain a reliable estimation of the spatial variability of θ across a field, the two main controlling factors are EC_a and soil texture.

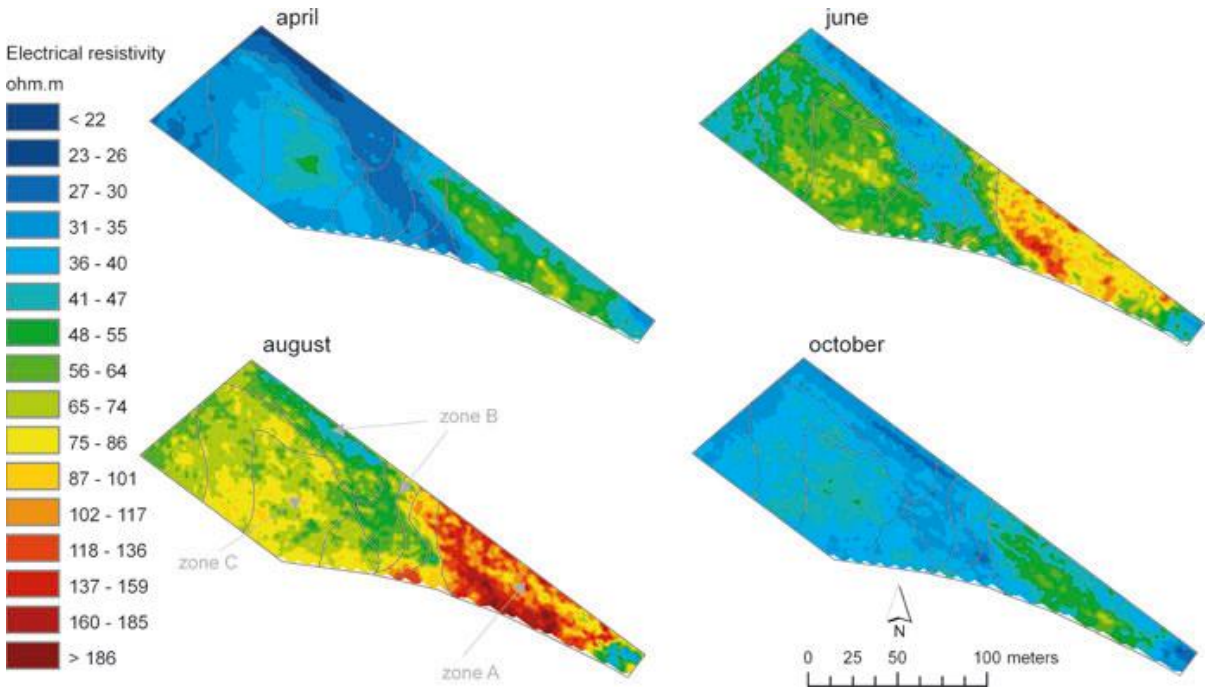

Figure 16: Maps of EC_a measured by the V1 array interpolated by normal kriging. From (Besson et al., 2010)

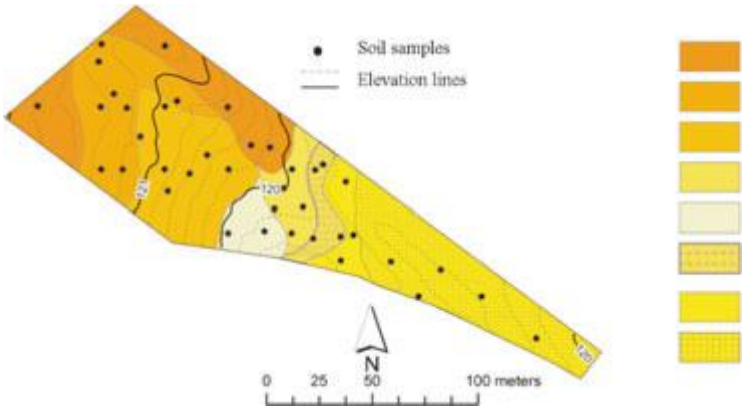

Figure 17: Field map of the area studied, black dots represent sampling sites. From (Besson et al., 2010)

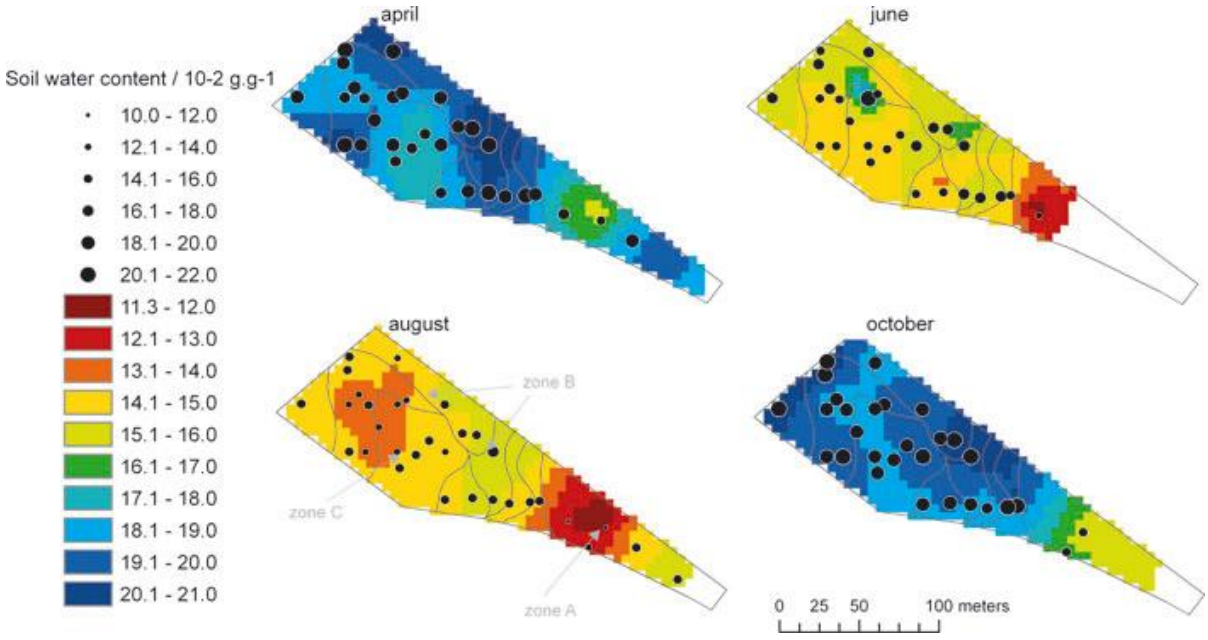

Figure 18: Maps of θ of the 0 to -0.7m layer interpolated using normal kriging. From (Besson et al., 2010)

2.4.2 Non-Contact Methods

Non-Contact methods involve the use of an instrument that does not touch the soil surface, or is not inserted into the soil profile. They are useful pieces of equipment because they do no disturb the soil profile. Electromagnetic (EM) induction (EMI) of soils using EM instruments such as Geonics EM31 and EM38 (Table 2) is one such non-contact method and is an increasingly popular method of proximal data acquisition. This is because EM instruments are relatively lightweight and mobile compared to DCR instruments.

EM instruments contain two coils of wire a fixed distance from each other, one coil is the transmitter, the other the receiver (Hezarjaribi and Sourell, 2007). An alternating current is passed through the transmitter coil, inducing an EM field which passes into the soil. This primary magnetic field then induces eddy currents in any conductive medium within the soil profile, which in turn induce their own magnetic field (Figure 19). This secondary magnetic field then passes out of the soil and is measured by the receiver coil.

The properties of soils which influence conductivity are primarily clay type (Cockx et al., 2009, Friedman, 2005, Triantafilis et al., 2009b), clay content (Cockx et al., 2009, da Silva et al., 2001), and water content (Kachanoski et al., 1988, McCutcheon et al., 2006). Other factors which have an influence on conductivity are temperature, bulk density and salinity (da Silva et al., 2001, Hedley et al., 2004, Sheets and Hendrickx, 1995, Tromp-van Meerveld and McDonnell, 2009). By measuring the ratio of the primary magnetic field to the secondary, it is possible to determine the conductivity of the soil and hence EC_a. Because the strength of the secondary field is a function of the various conductors, then a higher EC_a reading

indicates the presence of a certain clay type, higher clay content, or soil water. The depth of investigation of EMI instruments is a function of the spacing between the coils, the orientation of the coils – vertical or horizontal to the ground, and the frequency of the AC.

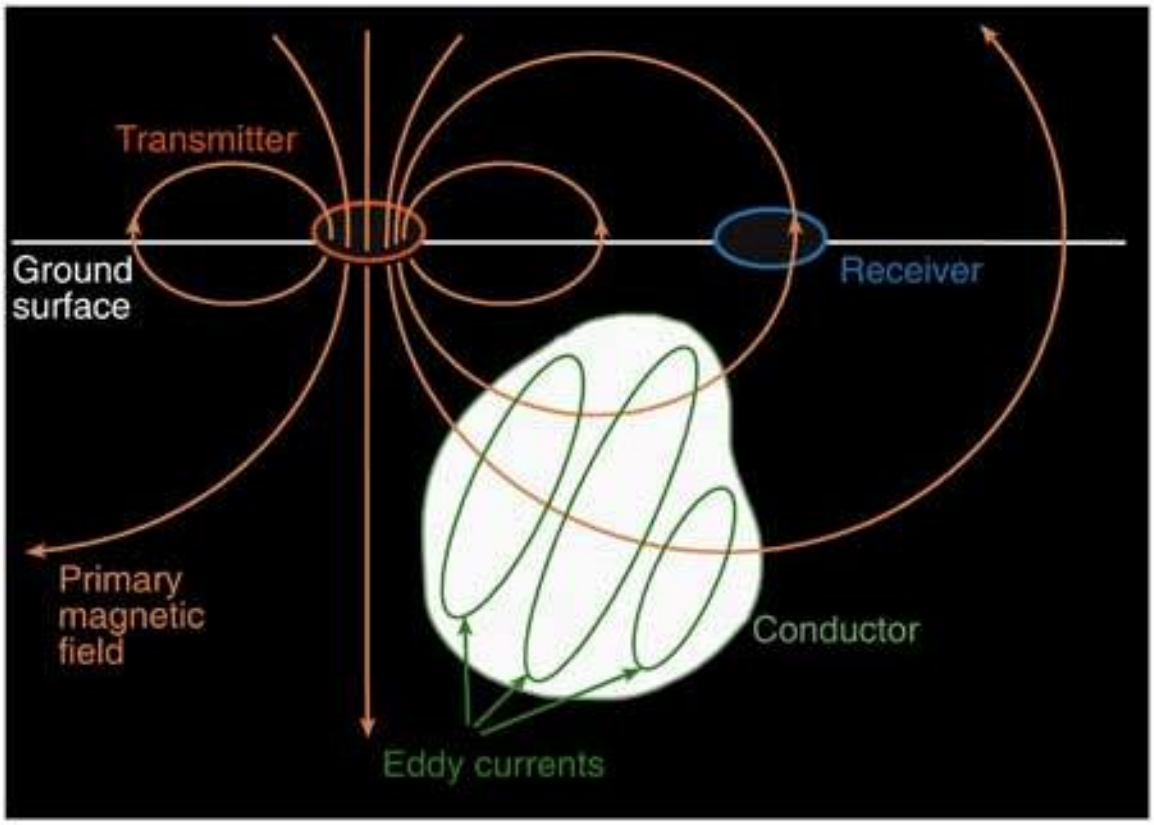

Figure 19: Schematic showing the primary magnetic field inducing eddy currents in a conductive medium within the soil profile. Source (http://www.terragis.bees.unsw.edu.au)

There is a wide range of commercially available EM instruments that are used in scientific investigations. Listed below in Table 2 is a sample of these that relate to investigations into soil moisture and other soil properties.

Table 2: variety of commercially available EM instruments

Instrument	Image	Depth of investigation V=vertical H=horizontal	References
Geonics **EM38**		**V = 1.5m** **H = 0.75m**	**(Hedley et al., 2004, Triantafilis et al., 2009b)**
Geonics EM38DD		**1.5m and 0.75m**	**(Cockx et al., 2009)**
Geonics EM34		**10m spacing** **V =3.8m** **H = 8.7m** **20m spacing** **V = 7.6m** **H = 17.4** **40m spacing** **V = 15.2m** **H = 34.8m**	**(Triantafilis and Buchanan, 2010)**

Geonics EM31		**5-6m**	**(Triantafilis et al., 2009b, Kachanoski et al., 1988, Sheets and Hendrickx, 1995)**
DualEM 421		**Multiple depths due to dual-geometry sensors:** **0.5m** **1m** **1.5m** **2m** **3m** **6m**	**(Santos et al., 2010)**
GEM-300		**Varies due to its range of operating frequencies**	**(Tromp-van Meerveld and McDonnell, 2009)**

Kachanoski, et al. (1988) investigated the relationship between EMI EC_a values, and TDR θ with soil texture (particle sizes). They did this by taking 52 point measurements in a grid system across a study area with a Geonics EM38 and Geonics EM31 for EC_a, a TDR hand probe for θ, and three soil cores which were analysed for percent sand, silt, and clay using the pipette method. Using simple linear regression, the authors found significant relationships (R^2 above 0.88 in all cases) with the EM31 and EM38 EC_a values and θ. In each case it was found to be a linear relationship and was postulated that EC_a could be mapped across a site in order to optimise experimental designs into soil water content. This study highlighted the potential to relate EC_a values gathered by EM techniques to be interpreted with the aim of investigating the spatial variations in soil moisture at the field scale.

With the recent stresses of water and agriculture in the last decade, EM techniques for predicting soil moisture have gathered large interest. They have proved particularly useful in precision irrigated agriculture (Hedley and Yule, 2009). In this case, a Geonics EM38 was used to map EC_a and define soil textural boundaries and hence soil texture zones (Figure 20). Samples were taken within these zones and analysed in the laboratory for FC and PWP, these values were then fitted to a linear regression with EC_a (R^2 = 0.76 for AWC). The authors then used daily TDR measurements to monitor the water status of the field in reference to their AWC map derived from the relationship to EC_a. This experiment shows that it is possible to create a map of EC_a defined zones using EMI to which sample within to determine the AWC of that texture class.

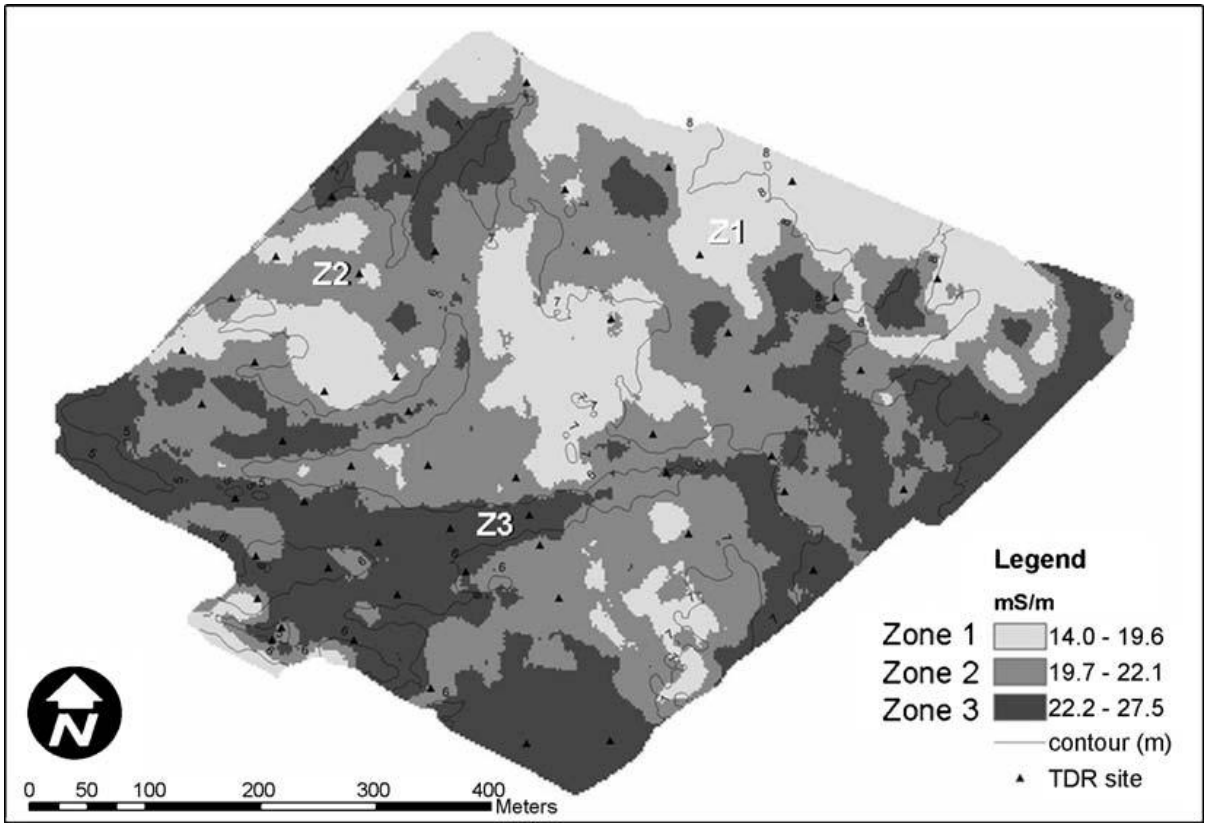

Figure 20: Soil EC_a map of the study area. From (Hedley and Yule, 2009)

Similar studies have been undertaken with the aim of using EM EC_a values to categorise soil units based on the correlation between EC_a and soil texture (Hedley et al., 2004, Triantafilis et al., 2009a). Hedley et al. (2004) found that EC_a values taken at different times of the year all correlated well with the clay percentage across a field (Figure 21). The correlation was not very high (R^2 = 0.72) which indicates that there are indeed other factors which influence EC_a. Triantafilis et al. (2009a) showed this again, that EC_a values from an EMI relate to soil texture but other values are needed to further discriminate texture based on other soil properties. The correlation between EC_a and soil texture has now been shown conclusively through many other studies (Hezarjaribi and Sourell, 2007, Mertens et al., 2008).

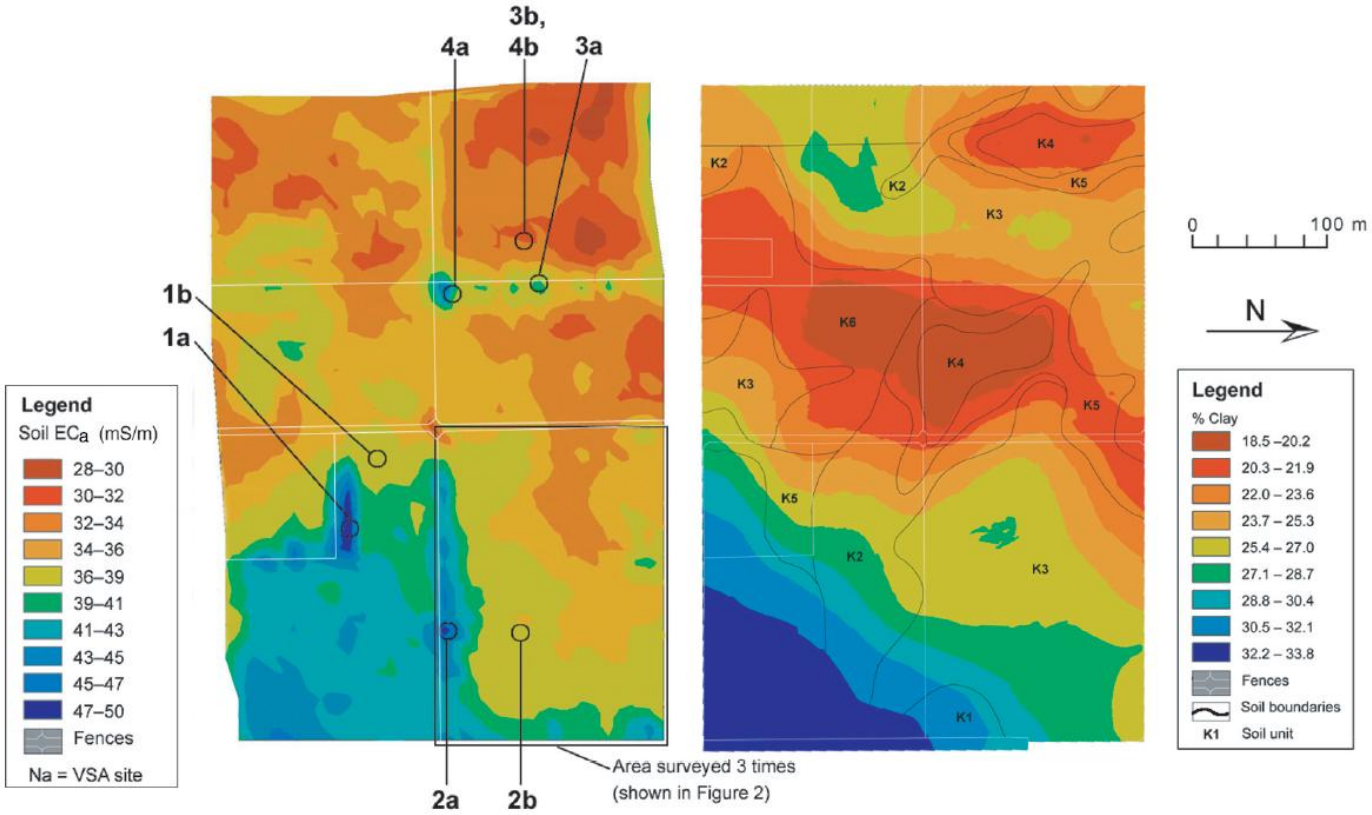

Figure 21: Average EC_a (left) and clay map (right) of the study area. (Hedley et al., 2004)

Although AWC, FC or PWP has been mapped solely using EM methods to date, it has been established that EM EC_a values can be correlated to θ (Jiang et al., 2007, Reedy and Scanlon, 2003, Sheets and Hendrickx, 1995, Tromp-van Meerveld and McDonnell, 2009). Jiang et al. (2007) used lab determined FC and PWP values and found a linear relationship with EC_a and PWP by means of a simple regression model. Reedy and Scanlon (2003) used spatially averaged neutron probe θ measurements across a field site and were able to predict these using a simple linear regression from EC_a after three years of calibration. This relationship between neutron probe θ and EC_a has been independently re-created in South America (Sheets and Hendrickx, 1995), but extensive calibration was needed to establish the relationship as well. Calibration with capacitance probes has been performed (Tromp-van Meerveld and McDonnell, 2009), although with these methods involving field methods for θ, the issue in determining the spatial variation in AWC is not being addressed.

2.4.2.1. Gamma Radiometrics

Gamma radiation is emitted by the soil from the beta and alpha decay of soil constituents such as Potassium (K), Uranium (U) and Thorium (Th), the total count of radiation is also be measured (Bierworth, 1996). Potassium is a major component of the earth's crust and occurs predominantly in potassic feldspars and mica's. When these rocks weather the potassium remains in the soil and undergoes beta decay, releasing a gamma ray of 1.46 MeV (Grasty, 1997). Uranium and Thorium are rarer elements but still occur in low concentrations across the globe. They are concentrated in felsic rocks high in silica such as granite and rhyolite. When they are weathered out, Uranium and Thorium tend to concentrate in shales and sandstones. In each case, Uranium undergoes beta decay emitting a gamma ray of 1.76 MeV and Thorium 2.61 MeV (Grasty, 1997). Gamma radiation is measured by a spectrometer. A spectrometer consists of a detector (most commonly a sodium iodide crystal), a photomultiplier and a counting device (Cook et al., 1996). When a gamma ray hits the sodium iodide crystal it creates a flash of light proportionate to the energy of the radiation, this flash of light is amplified by the photomultiplier and counted by the counting device. In an airborne survey 256 channels of data are collected, however only four channels are commonly used, total count, potassium, uranium and thorium (Cook et al., 1996). Gamma radiation is often plotted by giving each channel a specific colour in a ternary plot (Figure 22), and then mapping this. Most common is for Potassium to be assigned red, Thorium green, and Uranium blue. Then from a map of a given area, it is possible to identify the relative concentrations in radiation. This is useful in identifying features such as granitic parent

material, weathering in the form of total potassium, and soil texture (Nelson and Odeh, 2009, Robinson et al., 2009).

Because gamma radiation is highly correlated to the rock material, it is often used in aerial surveys for detecting ore bodies in geology (Cook et al., 1996). However, it has been observed there are relations between gamma radiation and soil moisture (Grasty, 1997, Jones and Carroll, 1983), soil class (Nelson and Odeh, 2009, Schmugge et al., 1980), soil forming minerals such as clay (Cook et al., 1996), and crop yield (Robinson et al., 2009). Although it was established that gamma radiation is able to distinguish the spatial variability in θ (Cook et al., 1996, Jones and Carroll, 1983), it requires field calibration to determine the quantitative θ values relative to AWC. The main benefit that can be seen in using airborne gamma radiometrics is that it can be used to effectively delineate soil type at the district scale based on mineral composition for further investigation into its main properties.

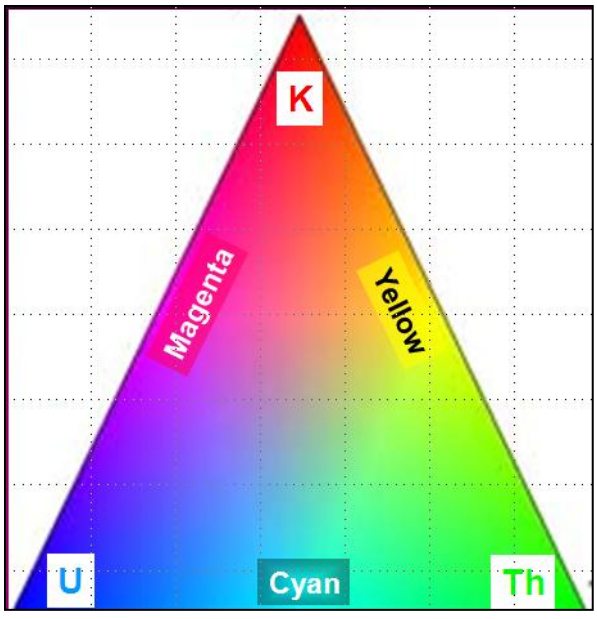

Figure 22: example of a ternary plot. (Triantafilis, 2009c)

2.4.2.2. Spectral Radiation

Spectral data in the form of optical, infra-red or microwave spectrums can be used to gain information on soil parameters such as vegetation cover (Haubrock et al., 2008, Wuthrich, 1996), soil texture (Haubrock et al., 2008, Triantafilis et al., 2009a), water use associated with vegetation type (Bindlish et al., 2006), and soil moisture content (Schmugge et al., 1980, Stafford, 1988, Wuthrich, 1996). EM radiation is emitted by the soil, water, and vegetation due to varying reflectance values. Spectral data is gathered by satellite or airborne surveys with specialised sensors for receiving the wavelength being investigated. Optical spectra gives values across the visible spectrum of light and can be interpreted by breaking it into its main components of red, blue and green (Triantafilis et al., 2009a). Through this, red and green values have been shown to relate to the organic matter contained within a soil and can aid in defining soil texture classes. Infra-Red spectra primarily relates to heat given off by the earth's surface (Wuthrich, 1996). This can be related to differences in land use, plant water stress, and moisture content in the topsoil. This is primarily because different land uses give off different heat signatures, and soil water affects the temperature of the soil and whether the plants growing in it are water stressed – hence giving off more heat. Wavelengths in the microwave spectrum provide information on soil moisture, vegetation, and surface roughness (Bindlish et al., 2006, Haubrock et al., 2008). Although Binlish et al. (2006) created an algorithm to predict soil moisture based on microwave spectra and mapped the spatial variation in soil moisture across their investigative district; they were unable to map the spatial variation in AWC across with

district without further ancillary data or precise measurement of the soil water characteristic.

As was seen in most of the case studies, spectral data relies on field calibrated data to be more robust in predictions, and more ancillary data than gamma radiometrics is required for more accurate estimates (Schmugge et al., 1980, Stafford, 1988). Of particular concern with spectral radiation is soil moisture impacts across optical, infra-red and microwave spectra (Haubrock et al., 2008), vegetation significantly interferes with moisture readings (Bindlish et al., 2006), and optical spectra only gives surface values (Wuthrich, 1996, Triantafilis et al., 2009a). In order to use spectral radiation data effectively, it must be combined with the relative ancillary data such as EMI determined EC_a or lab determined AWC, and even then the relationship may not be significant.

2.5 Statistical Analysis

Statistical analysis is the use of mathematical models to make more informed predictions about data. Statistical analysis is particularly important in soil science where it is the relationship between soil properties that is of particular importance. Through looking at EM and gamma radiometrics it is possible to see that there are relationships between gamma radiation and mineralogy (Cook et al., 1996), as well as EC_a and θ (Tromp-van Meerveld and McDonnell, 2009), amoung others. Typical studies use linear or multiple linear regression to establish statistical significant relationships. However there is an increasing trend in the use of artificial neural networks (ANN) to predict a single soil variable because they take into account the multiple other factors which influence them.

ANNs are a form of inductive machine learning (Gahegan, 2003) which relies on computers to effectively 'learn' the trends in a dataset and then produce a representative statistic based on the complex interactions within the dataset. They are mainly used because they are non-linear and can predict an output from known inputs using a hidden layer of data, as well as finding patterns in data. There are many adaptions of ANNs with different pathways and functions being implemented. They are also used in many fields of science as well as economics and gaming technology.

The two main uses of ANN in the soil science literature has been for the estimation and prediction of θ (Contador et al., 2006, Jiang and Cotton, 2004), and for mapping soil units (Behrens et al., 2005, Chang and Islam, 2000, Cockx et al., 2009, McBratney et al., 2003). The most commonly used ANN method has been a feed

forward, back propagation mechanism. Feed-forward ANNs operate by applying weights to each input as it is calculated in the hidden layer by regression as well as a bias, then applying weights to each hidden layer as it is calculated in the outputs with a bias (Figure 23). The weights are determined by an iterative process through training the ANN using a sub-sample of the dataset. The benefit of this method is that it makes no error distributions as a normal regression model does, in doing this they are potentially able to compute more complex relationship than a regression model can handle.

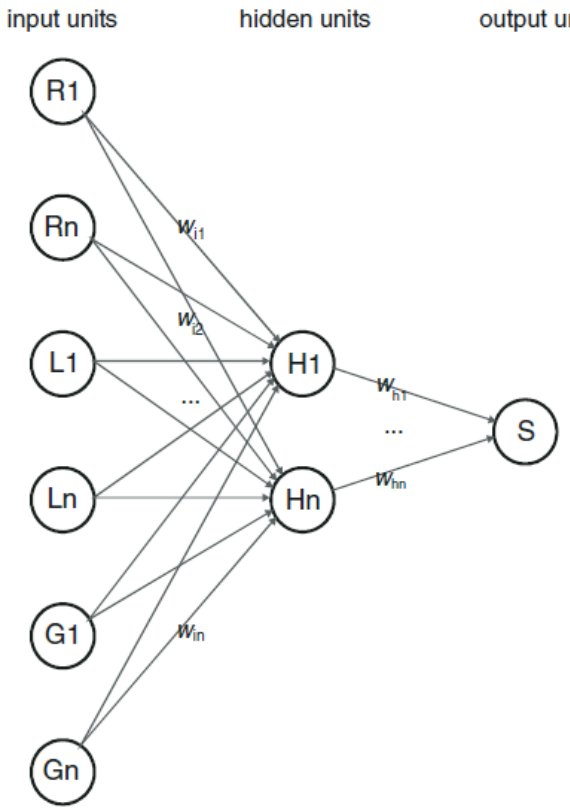

Figure 23: schematic of a feed-forward single layer ANN showing connections from input cells to output cells via the hidden cells with the learned relationships between inputs and outputs saved as weights. From (Behrens et al., 2005)

A feed-forward ANN was used by Behrens et al. (2005) to create a digital soil map covering 600 km^2 in Germany (Figure 24). They used 69 terrain attributes, 53 geologic-petrographic units, and three types of land use in training the ANN. The data was gathered by intense data-mining, but the trained ANN predicted 80% of the soil units with a training error less than 10%. Following validation of the model, a mean accuracy of 92% was achieved. In doing this they have shown that it is possible to use ANNs at the district scale to digital map soil properties given enough data.

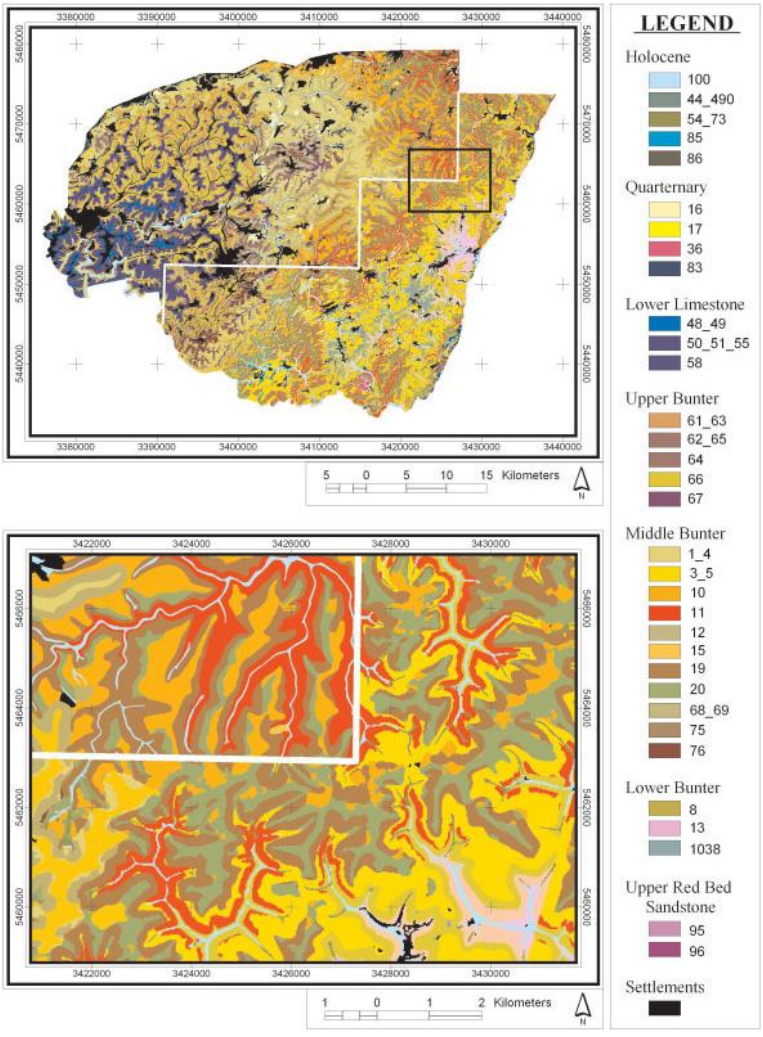

Figure 24: Top image showing existing soil units above the white line with predicted soil units below. Inset image showing surveyed soil units (upper left) and soil units predicted using the ANN. (Behrens et al., 2005)

Similar applications of ANNs have been to model percentage clay using inputs consisting of EC_a derived from an EMI as well as soil texture (Cockx et al., 2009), as well to estimate soil texture using remote sensed brightess, θ, and a known texture map as training data (Chang and Islam, 2000). Both these studies used ANNs with moderate success but met with the problems of not enough input data and sparse training data. In order to overcome this, the use of an ANN to predict any soil property requires a robust and diverse set of inputs as well a properly defined training set of data. Another issue with ANNs is that it is easy to over parameterise the inputs so the resulting analysis is only highly relevant to the exact data and location that was used. Overcoming this problem is an issue and as a result only a select number of datasets should be used. Linear Regression models have the benefit of being tested for bias using mean error and accuracy using root mean squared error (McBratney et al., 2003), in contrast to this ANNs do not function using error estimates so their bias and predictability are measured using jackknifing, comparison with other models, and random holdback.

As mentioned earlier, being able to predict the spatial variations of AWC at the district level is a major concern worldwide. ANN have the capacity to produce high resolution maps at the district scale (Behrens et al., 2005, McBratney et al., 2003), and they also have the benefit of being capable of modeling complex non-linear relationships, such as θ (Jiang and Cotton, 2004). Jiang and Cotton (2004) used the inputs of infra-red temperature, monthly accumulated rainfall, and vegetation index with a dataset from a previous season for training. The result from their ANN was an R^2 value of 0.99 in testing and a spatially representative map of the θ compared to the measured θ (Figure 25). Other possible inputs for determining θ in an ANN have been

found to be topography and vegetation cover (Contador et al., 2006), and remote data (Said et al., 2008, Wigneron et al., 2003).

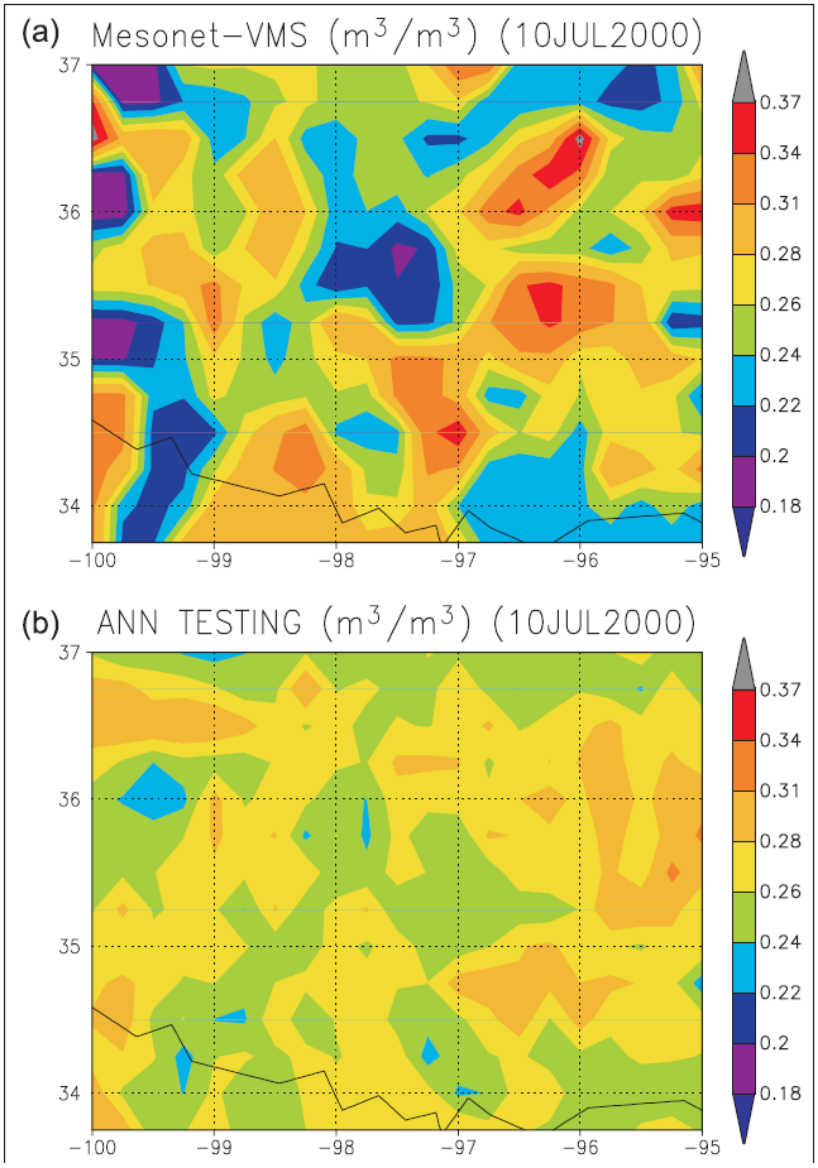

Figure 25: Spatial distribution of Mesonet θ (top) compared to ANN estimate (bottom) from testing results

3. Conclusion

Based on the current changing climate and stresses on the irrigation industry in the Murray Darling Basin, it is evident that improved practices of irrigation are needed. In order to increase irrigation efficiency it is essential to understand the dynamics of how the available water content of soils varies spatially with texture in a district. In order to achieve this, digital soil maps of showing the spatial variation of the available water content at the field scale is required. Given that it is too costly and time consuming to sample the entire district, it is more efficient to have a relatively small sample of soil sites within which to determine the available water content. Because the available water content is determined by the difference between field capacity and permanent wilting point, the pressure plate apparatus is the fastest and most effective laboratory method to use.

It has been shown that various EM and DCR instruments aim to measure the spatial variations in EC_a, and that this is directly related to the volumetric soil content. As well as this it is known that the volumetric is a function of more than one soil attribute and is best captured by the interrelationships of clay content, soil mineralogy, and conductivity. This is mirrored by the fact that EC_a is a function of the volumetric water content, clay content and texture. Other factors which influence EC_a are temperature, salinity, and bulk density. Other ancillary methods of gathering soil data such as gamma radiometrics have met with high success and it is now possible to map the variations in soil texture at the district scale using this readily available information.

In order to create a digital soil map of the available water content, it is important to recognise that there are multiple factors such as soil type, mineralogy and conductivity which are interrelated and must be combined to make an accurate estimate. In order to combine these different datasets, a powerful statistical tool which distinguishes these relationships is required. Artificial Neural Networks have proven to be effective in this capacity. This is due to their inductive learning and hidden pathways which enable them to make non-linear connections to the different variables that affect soil moisture.

Although it is important to understand the spatial dynamics of the volumetric water content over time, it is just as effective to map the spatial variability of the available water content across a district and irrigate according to how much water the soil can actually hold. This literature review has shown that it is possible to accurately measure the variety of inputs required for a statistical tool such as a feed-forward back-propagation artificial neural network to map a property such as the available water content, at the district scale with high resolution.

References

ACWORTH, R. I., YOUNG, R. R. & BERNADI, A. L. 2005. Monitoring soil moisture status in a Black Vertosol on the Liverpool Plains, NSW, using a combination of neutron scattering and electrical image methods. *Australian Journal of Soil Research,* 43, 105-117.

AL-AIN, F., ATTAR, J., HUSSEIN, F. & HENG, L. K. 2009. Comparison of nuclear and capacitance-based soil water measuring techniques in salt-affected soils. *Soil Use and Management,* 25, 362-367.

ALLRED, B. J., EHSANI, M. R. & SARASWAT, D. 2006. Comparison of electromagnetic induction, capacitively-coupled resistivity, and galvanic contact resistivity methods for soil electrical conductivity measurement. *Applied Engineering in Agriculture,* 22, 215-230.

BEHRENS, T., FORSTER, H., SCHOLTEN, T., STEINRUCKEN, U., SPIES, E. D. & GOLDSCHMITT, M. 2005. Digital soil mapping using artificial neural networks. *Journal of Plant Nutrition and Soil Science-Zeitschrift Fur Pflanzenernahrung Und Bodenkunde,* 168, 21-33.

BESSON, A., COUSIN, I., BOURENNANE, H., NICOULLAUD, B., PASQUIER, C., RICHARD, G., DORIGNY, A. & KING, D. 2010. The spatial and temporal organization of soil water at the field scale as described by electrical resistivity measurements. *European Journal of Soil Science,* 61, 120-132.

BETHUNE, M. 2004. Towards effective control of deep drainage under border-check irrigated pasture in the Murray-Darling Basin: a review. *Australian Journal of Agricultural Research,* 55, 485-494.

BIDDISCOMBE, E. F. 1963. A Vegetation Survey in the Macquarie Region, New South Wales.: CSIRO Division of Plantt Industry Tech. Paper No. 18.

BIERWORTH, P. 1996. Investigation of Airborne Gamma-Ray Images as a Rapid Mapping Tool for Soil and Water Degradation. Australian Geological Survey Organisation.

BINDLISH, R., JACKSON, T. J., GASIEWSKI, A. J., KLEIN, M. & NJOKU, E. G. 2006. Soil moisture mapping and AMSR-E validation using the PSR in SMEX02. *Remote Sensing of Environment,* 103, 127-139.

BITTELLI, M. & FLURY, M. 2009. Errors in Water Retention Curves Determined with Pressure Plates. *Soil Science Society of America Journal,* 73, 1453-1460.

BREWER, R., CROOK, K. A. W. & SPEIGHT, J. G. 1970. Proposal for Soil-Stratigraphic units in the Australian Stratigraphic code. *Australian Journal of Earth Sciences,* 17, 103-111.

CANCELA, J. J., DAFONTE, J., MARTINEZ, E. M., CUESTA, T. S. & NEIRA, X. X. 2006. Assessment of a water activity meter for rapid measurements of soil water potential. *Biosystems Engineering,* 94, 285-295.

CHANG, D. H. & ISLAM, S. 2000. Estimation of soil physical properties using remote sensing and artificial neural network. *Remote Sensing of Environment,* 74, 534-544.

CHANZY, A., CHADOEUF, J., GAUDU, J. C., MOHRATH, D., RICHARD, G. & BRUCKLER, L. 1998. Soil moisture monitoring at the field scale using

automatic capacitance probes. *European Journal of Soil Science,* 49, 637-648.
CHARMAN, P. E. V. & MURPHY, B. W. (eds.) 2003. *Soils: Their Properties and Management*: Oxford University Press.
COCKX, L., VAN MEIRVENNE, M., VITHARANA, U. W. A., VERBEKE, L. P. C., SIMPSON, D., SAEY, T. & VAN COILLIE, F. M. B. 2009. Extracting Topsoil Information from EM38DD Sensor Data using a Neural Network Approach. *Soil Sci Soc Am J,* 73, 2051-2058.
CONTADOR, J. F. L., MANETA, M. & SCHNABEL, S. 2006. Prediction of near-surface soil moisture at large scale by digital terrain modeling and neural networks. *Environmental Monitoring and Assessment,* 121, 213-232.
COOK, S. E., CORNER, R. J., GROVES, P. R. & GREALISH, G. J. 1996. Use of airborne gamma radiometric data for soil mapping. *Australian Journal of Soil Research,* 34, 183-194.
COVENTRY, R. J. & FETT, D. E. R. 1979. *A pipette and sieve method of particle size analysis and some observations on its efficacy*, CSIRO Australia Division of Soils, Divisional Report, No. 38. CSIRO, Australia.
CRESSWELL, H. P., GREEN, T. & MCKENZIE, N. J. 2008. The adequacy of pressure plate apparatus for determining soil water retention. *Soil Science Society of America Journal,* 72, 41-49.
CURTIS, M. J. & CLAASSEN, V. P. 2005. Compost incorporation increases plant available water in a drastically disturbed serpentine soil. *Soil Science,* 170, 939-953.
CURTIS, M. J. & CLAASSEN, V. P. 2008. An Alternative Method for Measuring Plant Available Water in Inorganic Amendments. *Crop Science,* 48, 2447-2452.
DA SILVA, A. P., NADLER, A. & KAY, B. D. 2001. Factors contributing to temporal stability in spatial patterns of water content in the tillage zone. *Soil and Tillage Research,* 58, 207-218.
DICKSON, B. L., FRASER, S. J. & KINSEYHENDERSON, A. 1996. Interpreting aerial gamma-ray surveys utilising geomorphological and weathering models. *Journal of Geochemical Exploration,* 57, 75-88.
DICKSON, B. L. & SCOTT, K. M. 1997. Interpretation of aerial gamma-ray surveys - adding the geochemical factors. *AGSO Journal of Australian Geology & Geophysics,* 17, 187-200.
DOMSCH, H. & GIEBEL, A. 2004. Estimation of Soil Textural Features from Soil Electrical Conductivity Recorded Using the EM38. *Precision Agriculture,* 5, 389-409.
DUNIWAY, M. C., HERRICK, J. E. & MONGER, H. C. 2007. The high water-holding capacity of petrocalcic horizons. *Soil Science Society of America Journal,* 71, 812-819.
FOTH, H. D. 1990. *Fundamentals of Soil Science. 8E*, John Wiley & Sons.
FRIEDMAN, S. P. 2005. Soil properties influencing apparent electrical conductivity: a review. *Computers and Electronics in Agriculture,* 46, 45-70.

GAHEGAN, M. 2003. Is inductive machine learning just another wild goose (or might it lay the golden egg)? *International Journal of Geographical Information Science,* 17, 69 - 92.

GAWNE, B., CRASE, L. & WATSON, A. S. 2010. Can a collaborative focus on solutions improve our capacity to achieve sustainable water management? *Marine and Freshwater Research,* 61, 814-820.

GEBBERS, R., LUCK, E., DABAS, M. & DOMSCH, H. 2009. Comparison of instruments for geoelectrical soil mapping at the field scale. *Near Surface Geophysics,* 7, 179-190.

GHEZZEHEI, T. A. 2008. Errors in determination of soil water content using time domain reflectometry caused by soil compaction around waveguides. *Water Resources Research,* 44.

GRASTY, R. L. 1997. Radon emanation and soil moisture effects on airborne gamma-ray measurements. *Geophysics,* 62, 1379-1385.

GREEN, S. R., KIRKHAM, M. B. & CLOTHIER, B. E. 2006. Root uptake and transpiration: From measurements and models to sustainable irrigation. *Agricultural Water Management,* 86, 165-176.

HAUBROCK, S. N., CHABRILLAT, S., KUHNERT, M., HOSTERT, P. & KAUFMANN, H. 2008. Surface soil moisture quantification and validation based on hyperspectral data and field measurements. *Journal of Applied Remote Sensing,* 2.

HEDLEY, C. B. & YULE, I. J. 2009. A method for spatial prediction of daily soil water status for precise irrigation scheduling. *Agricultural Water Management,* 96, 1737-1745.

HEDLEY, C. B., YULE, I. Y., EASTWOOD, C. R., SHEPHERD, T. G. & ARNOLD, G. 2004. Rapid identification of soil textural and management zones using electromagnetic induction sensing of soils. *Australian Journal of Soil Research,* 42, 389-400.

HEZARJARIBI, A. & SOURELL, H. 2007. Feasibility study of monitoring the total available water content using non-invasive electromagnetic induction-based and electrode-based soil electrical conductivity measurements. *Irrigation and Drainage,* 56, 53-65.

HULUGALLE, N. R., WEAVER, T. B. & FINLAY, L. A. 2010. Soil water storage and drainage under cotton-based cropping systems in a furrow-irrigated Vertisol. *Agricultural Water Management,* 97, 1703-U3.

JIANG, H. L. & COTTON, W. R. 2004. Soil moisture estimation using an artificial neural network: a feasibility study. *Canadian Journal of Remote Sensing,* 30, 827-839.

JIANG, P. P., ANDERSON, S. H., KITCHEN, N. R., SUDDUTH, K. A. & SADLER, E. J. 2007. Estimating plant-available water capacity for claypan landscapes using apparent electrical conductivity. *Soil Science Society of America Journal,* 71, 1902-1908.

JOHNSON, C. K., DORAN, J. W., DUKE, H. R., WIENHOLD, B. J., ESKRIDGE, K. M. & SHANAHAN, J. F. 2001. Field-scale electrical conductivity mapping for delineating soil condition. *Soil Science Society of America Journal,* 65, 1829-1837.

JONES, D. P. & GRAHAM, R. C. 1993. WATER-HOLDING CHARACTERISTICS OF WEATHERED GRANITIC ROCK IN CHAPARRAL AND FOREST ECOSYSTEMS. *Soil Science Society of America Journal,* 57, 256-261.

JONES, W. K. & CARROLL, T. R. 1983. ERROR ANALYSIS OF AIRBORNE GAMMA-RADIATION SOIL-MOISTURE MEASUREMENTS. *Agricultural Meteorology,* 28, 19-30.

KACHANOSKI, R. G., GREGORICH, E. G. & VANWESENBEECK, I. J. 1988. ESTIMATING SPATIAL VARIATIONS OF SOIL-WATER CONTENT USING NONCONTACTING ELECTROMAGNETIC INDUCTIVE METHODS. *Canadian Journal of Soil Science,* 68, 715-722.

KELLENERS, T. J., PAIGE, G. B. & GRAY, S. T. 2009. Measurement of the Dielectric Properties of Wyoming Soils Using Electromagnetic Sensors. *Soil Science Society of America Journal,* 73, 1626-1637.

KIM, Y., EVANS, R. G. & IVERSEN, W. M. 2008. Remote sensing and control of an irrigation system using a distributed wireless sensor network. *Ieee Transactions on Instrumentation and Measurement,* 57, 1379-1387.

KOTHAVALA, Z. 1999. The duration and severity of drought over eastern Australia simulated by a coupled ocean-atmosphere GCM with a transient increase in CO2. *Environmental Modelling & Software,* 14, 243-252.

KUHN, J., BRENNING, A., WEHRHAN, M., KOSZINSKI, S. & SOMMER, M. 2009. Interpretation of electrical conductivity patterns by soil properties and geological maps for precision agriculture. *Precision Agriculture,* 10, 490-507.

LAFFAN, S. W. & LEES, B. G. 2004. Predicting regolith properties using environmental correlation: a comparison of spatially global and spatially local approaches. *Geoderma,* 120, 241-258.

LEONG, E. C., HE, L. & RAHARDJO, H. 2002. Factors affecting the filter paper method for total and matric suction measurements. *Geotechnical Testing Journal,* 25, 322-333.

LESHER, C. M., BURNHAM, O. M., KEAYS, R. R., BARNES, S. J. & HULBERT, L. 2001. Trace-element geochemistry and petrogenesis of barren and ore-associated komatiites. *Canadian Mineralogist,* 39, 673-696.

LIU, W. D., BARET, F., GU, X. F., TONG, Q. X., ZHENG, L. F. & ZHANG, B. 2002. Relating soil surface moisture to reflectance. *Remote Sensing of Environment,* 81, 238-246.

LU, S., REN, T., GONG, Y. & HORTON, R. 2008. Evaluation of Three Models that Describe Soil Water Retention Curves from Saturation to Oven Dryness. *Soil Science Society of America Journal,* 72, 1542-1546.

MCBRATNEY, A. B., SANTOS, M. L. M. & MINASNY, B. 2003. On digital soil mapping. *Geoderma,* 117, 3-52.

MCCUTCHEON, M. C., FARAHANI, H. J., STEDNICK, J. D., BUCHLEITER, G. W. & GREEN, T. R. 2006. Effect of soil water on apparent soil electrical conductivity and texture relationships in a dryland field. *Biosystems Engineering,* 94, 19-32.

MCKENZIE, N. J. 1992. *Soils of the Lower Macquarie Valley, New South Wales*, CSIRO Division of Soils, Divisional Report No 117, Canberra, Australia.

MCNEILL, J. D. 1980a. Electrical Conductivity of Soils and Rocks. *Technical Note TN-5.* Geonics Ltd: Mississauga, ON, Canada.

MCNEILL, J. D. 1980b. Electromagnetic terrain conductivity measurement at low induction numbers. *Technical Note TN-6.* Geonics Ltd, Mississauga ON, Canada.

MCNEILL, J. D. 1990. Geonics EM38 Ground Conductivity Meter: EM38 Operating Manual. Geonics Ltd: Mississuaga, ON, Canada.

MERTENS, F. M., PAETZOLD, S. & WELP, G. 2008. Spatial heterogeneity of soil properties and its mapping with apparent electrical conductivity. *Journal of Plant Nutrition and Soil Science-Zeitschrift Fur Pflanzenernahrung Und Bodenkunde,* 171, 146-154.

MINASNY, B., MCBRATNEY, A. B. & WHELAN, B. M. 2005. VESPER version 1.62. *Australian Centre for Precision Agriculture, The University of Sydney*.

MINTY, B. R. S. 1997. Fundamentals of airborne gamma-ray spectrometry. *AGSO Journal of Australian Geology & Geophysics,* 17, 39-50.

MOHAMED, S. O., BERTUZZI, P., BRUAND, A., RAISON, L. & BRUCKLER, L. 1997. Field evaluation and error analysis of soil water content measurement using the capacitance probe method. *Soil Science Society of America Journal,* 61, 399-408.

MONTAGNE, C., RUDDELL, J. & FERGUSON, H. 1992. WATER-RETENTION OF SOFT SILTSTONE FRAGMENTS IN A USTIC TORRIORTHENT, CENTRAL MONTANA. *Soil Science Society of America Journal,* 56, 555-557.

NAM, S., GUTIERREZ, M., DIPLAS, P., PETRIE, J., WAYLLACE, A., LU, N. & MUNOZ, J. J. 2010. Comparison of testing techniques and models for establishing the SWCC of riverbank soils. *Engineering Geology,* 110, 1-10.

NELSON, M. A. & ODEH, I. O. A. 2009. Digital soil class mapping using legacy soil pro. le data: a comparison of a genetic algorithm and classification tree approach. *Australian Journal of Soil Research,* 47, 632-649.

ODEH, I. O. A. & MCBRATNEY, A. B. 2000. Using AVHRR images for spatial prediction of clay content in the lower Namoi Valley of eastern Australia. *Geoderma,* 97, 237-254.

PAIGE, G. B. & KEEFER, T. O. 2008. Comparison of field performance of multiple soil moisture sensors in a semi-arid rangeland. *Journal of the American Water Resources Association,* 44, 121-135.

PALTINEANU, I. C. & STARR, J. L. 1997. Real-time soil water dynamics using multisensor capacitance probes: Laboratory calibration. *Soil Science Society of America Journal,* 61, 1576-1585.

PEVERILL, K. I., SPARROW, L. A. & REUTER, D. J. (eds.) 1999. *Soil Analysis: an interpretation manual*: CSIRO publishing.

REEDY, R. C. & SCANLON, B. R. 2003. Soil water content monitoring using electromagnetic induction. *Journal of Geotechnical and Geoenvironmental Engineering,* 129, 1028-1039.

RICHARDS, L. A. 1948. POROUS PLATE APPARATUS FOR MEASURING MOISTURE RETENTION AND TRANSMISSION BY SOIL. *Soil Science,* 66, 105-110.

ROBINSON, D. A., JONES, S. B., WRAITH, J. M., OR, D. & FRIEDMAN, S. P. 2003. A Review of Advances in Dielectric and Electrical Conductivity Measurement in Soils Using Time Domain Reflectometry. *Vadose Zone Journal,* 2, 444-475.

ROBINSON, N. J., RAMPANT, P. C., CALLINAN, A. P. L., RAB, M. A. & FISHER, P. D. 2009. Advances in precision agriculture in south-eastern Australia. II. Spatio-temporal prediction of crop yield using terrain derivatives and proximally sensed data. *Crop & Pasture Science,* 60, 859-869.

ROSSEL, R. A. V., WALVOORT, D. J. J., MCBRATNEY, A. B., JANIK, L. J. & SKJEMSTAD, J. O. 2006. Visible, near infrared, mid infrared or combined diffuse reflectance spectroscopy for simultaneous assessment of various soil properties. *Geoderma,* 131, 59-75.

ROYLE, J. A. & BERLINER, L. M. 1999. A hierarchical approach to multivariate spatial modeling and prediction. *Journal of Agricultural Biological and Environmental Statistics,* 4, 29-56.

SAID, S., KOTHYARI, U. C. & ARORA, M. K. 2008. ANN-based soil moisture retrieval over bare and vegetated areas using ERS-2 SAR data. *Journal of Hydrologic Engineering,* 13, 461-475.

SAILHAC, P., BANO, M., BEHAEGEL, M., GIRARD, J.-F., PARA, E. F., LEDO, J., MARQUIS, G., MATTHEY, P.-D. & ORTEGA-RAMÍREZ, J. 2009. Characterizing the vadose zone and a perched aquifer near the Vosges ridge at the La Soutte experimental site, Obernai, France. *Comptes Rendus Geosciences,* 341, 818-830.

SANKARANARAYANAN, K., PRAHARAJ, C. S., NALAYINI, P., BANDYOPADHYAY, K. K. & GOPALAKRISHNAN, N. 2010. Climate change and its impact on cotton (Gossypium sp.). *Indian Journal of Agricultural Sciences,* 80, 561-575.

SANTOS, F. A. M., TRIANTAFILIS, J., BRUZGULIS, K. E. & ROE, J. A. E. 2010. Inversion of Multiconfiguration Electromagnetic (DUALEM-421) Profiling Data Using a One-Dimensional Laterally Constrained Algorithm. *Vadose Zone Journal,* 9, 117-125.

SCHMUGGE, T. J., JACKSON, T. J. & MCKIM, H. L. 1980. SURVEY OF METHODS FOR SOIL-MOISTURE DETERMINATION. *Water Resources Research,* 16, 961-979.

SHEETS, K. R. & HENDRICKX, J. M. H. 1995. NONINVASIVE SOIL-WATER CONTENT MEASUREMENT USING ELECTROMAGNETIC INDUCTION. *Water Resources Research,* 31, 2401-2409.

SHERWIN, L. 1996. *Narromine 1:250 000 Geological Sheet*. Geological Survey of New South Wales; Department of Mineral Resources.

STAFFORD, J. V. 1988. REMOTE, NON-CONTACT AND INSITU MEASUREMENT OF SOIL-MOISTURE CONTENT - A REVIEW. *Journal of Agricultural Engineering Research,* 41, 151-172.

SUDDUTH, K. A., KITCHEN, N. R., WIEBOLD, W. J., BATCHELOR, W. D., BOLLERO, G. A., BULLOCK, D. G., CLAY, D. E., PALM, H. L., PIERCE, F. J., SCHULER, R. T. & THELEN, K. D. 2005. Relating apparent electrical

conductivity to soil properties across the north-central USA. *Computers and Electronics in Agriculture,* 46, 263-283.

THOMPSON, R. B., GALLARDO, M., VALDEZ, L. C. & FERNÁNDEZ, M. D. 2007. Determination of lower limits for irrigation management using in situ assessments of apparent crop water uptake made with volumetric soil water content sensors. *Agricultural Water Management,* 92, 13-28.

TOPP, G. C. & DAVIS, J. L. 1985. MEASUREMENT OF SOIL-WATER CONTENT USING TIME-DOMAIN REFLECTROMETRY (TDR) - A FIELD-EVALUATION. *Soil Science Society of America Journal,* 49, 19-24.

TRIANTAFILIS, J. & BUCHANAN, S. M. 2010. Mapping the spatial distribution of subsurface saline material in the Darling River valley. *Journal of Applied Geophysics,* 70, 144-160.

TRIANTAFILIS, J., KERRIDGE, B. & BUCHANAN, S. M. 2009a. Digital Soil-Class Mapping from Proximal and Remotely Sensed Data at the Field Level. *Agronomy Journal,* 101, 841-853.

TRIANTAFILIS, J. & LESCH, S. M. 2005. Mapping clay content variation using electromagnetic induction techniques. *Computers and Electronics in Agriculture,* 46, 203-237.

TRIANTAFILIS, J., LESCH, S. M., LA LAU, K. & BUCHANAN, S. M. 2009b. Field level digital soil mapping of cation exchange capacity using electromagnetic induction and a hierarchical spatial regression model. *Australian Journal of Soil Research,* 47, 651-663.

TRIANTAFILIS, J., ODEH, I. O. A., JARMAN, A. L., SHORT, M. G. & KOKKORIS, E. 2004. Estimating and mapping deep drainage risk at the district level in the lower Gwydir and Macquarie valleys, Australia. *Australian Journal of Experimental Agriculture,* 44, 893-912.

TROMP-VAN MEERVELD, H. J. & MCDONNELL, J. J. 2009. Assessment of multi-frequency electromagnetic induction for determining soil moisture patterns at the hillslope scale. *Journal of Hydrology,* 368, 56-67.

TUCKER, B. M. 1974. *Laboratory procedure for cation exchange measurements in soils*, CSIRO Division of Soils, Technical Paper No. 23, CSIRO, Australia.

VERA, J., MOUNZER, O., RUIZ-SANCHEZ, M. C., ABRISQUETA, I., TAPIA, L. M. & ABRISQUETA, J. M. 2009. Soil water balance trial involving capacitance and neutron probe measurements. *Agricultural Water Management,* 96, 905-911.

VOLTZ, M. & WEBSTER, R. 1990. A COMPARISON OF KRIGING, CUBIC-SPLINES AND CLASSIFICATION FOR PREDICTING SOIL PROPERTIES FROM SAMPLE INFORMATION. *Journal of Soil Science,* 41, 473-490.

WATERS, P. 1980. COMPARISON OF THE CERAMIC PLATE AND THE PRESSURE MEMBRANE TO DETERMINE THE 15 BAR WATER-CONTENT OF SOILS. *Journal of Soil Science,* 31, 443-446.

WATKINS, J. J. & MEAKIN, N. S. 1996. *Nyngan 1:250 000 Geological Sheet*. Geological Survey of New South Wales; Department of Mineral Resources.

WESSOLEK, G., PLAGGE, R., LEIJ, F. J. & VAN GENUCHTEN, M. T. 1994. Analysing problems in describing field and laboratory measured soil hydraulic properties. *Geoderma,* 64, 93-110.

WIATRAK, P., KHALILIAN, A., MUELLER, J. & HENDERSON, W. 2009. Applications of Soil Electrical Conductivity in Production Agriculture. *Better Crops,* 93, 16-17.

WIGNERON, J. P., CALVET, J. C., PELLARIN, T., VAN DE GRIEND, A. A., BERGER, M. & FERRAZZOLI, P. 2003. Retrieving near-surface soil moisture from microwave radiometric observations: current status and future plans. *Remote Sensing of Environment,* 85, 489-506.

WRAITH, J. M. & OR, D. 2001. Soil water characteristic determination from concurrent water content measurements in reference porous media. *Soil Science Society of America Journal,* 65, 1659-1666.

WUTHRICH, M. 1996. Thermal infra-red underflights compared to ERS-1 C-band synthetic aperture radar focusing soil moisture distribution. *Theoretical and Applied Climatology,* 53, 69-78.